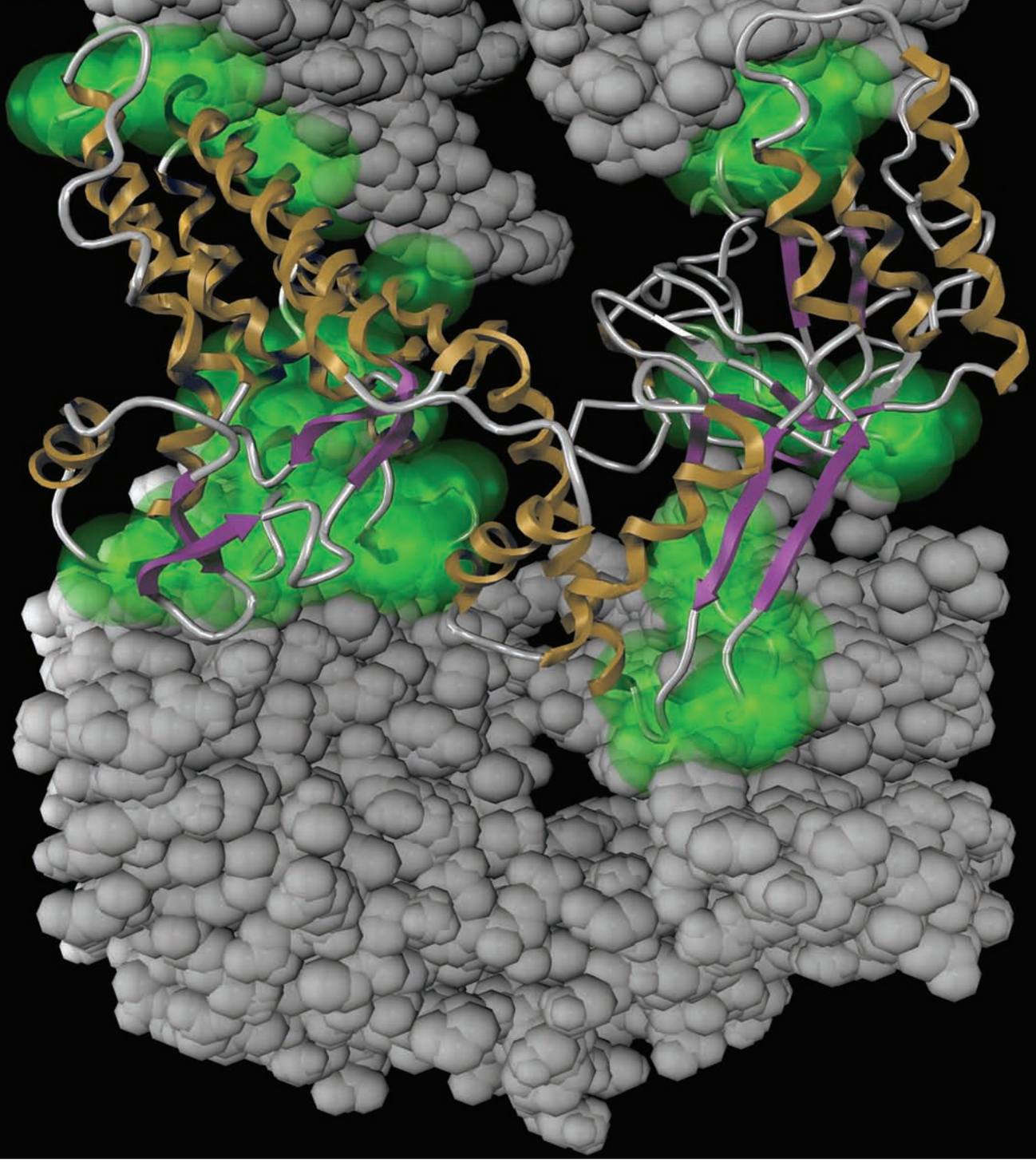
MICROSCOPY TODAY

JULY 2008 VOLUME 16 - NUMBER 4



MT Full Page Ad Master.indd 1 06/22/2008 8:42:35 PM

Explore and Identify
Your Partner for Material Analysis and Life Science

Come and See us at M&M 2008, Booth #804, Albuquerque, NM, August 3-7, 2008







For further information please visit us at www.smt.zeiss.com/nts

Carl Zeiss SMT Inc.

Enabling the Nano-Age World®

One Corporation Way
Peabody
MA 01960
USA

Tel. +1 978 / 826 7909
Fax +1 978 / 532 5696
info-usa@smt.zeiss.com
www.smt.zeiss.com/nts

ZEISS

We make it visible.

How Much Force Does it Take to Move an Atom on a Surface?

Stephen W. Carmichael[1] Mayo Clinic

It was demonstrated 18 years ago that atoms could be manipulated, one at a time, on a surface. Yet only recently has the force required to move an atom been determined. Markus Ternes, Christopher Lutz, Cyrus Hirjibehedin, Franz Giessibl, and Andreas Heinrich, in a technical *tour de force*, have engineered a microscope that incorporates features of the scanning tunneling microscope (STM) and atomic force microscope (AFM) to accurately quantitate the lateral and vertical forces needed to move a single atom on a surface.[2]

The STM was a breakthrough in the 1980's when it ushered in a new era of scanning probe microscopes. Of these new microscopes, the AFM is perhaps the most widely used these days. Each instrument has its advantages and limitations, but the best features of both have not previously been combined into a single instrument. At the "heart" of this new instrument is a small quartz tuning fork, with one fixed prong and the free end with a sharp tip. The free prong acts as a stiff cantilever in an AFM; variations in its longitudinal bending can be detected by measuring tiny piezoelectric currents that result when the quartz deforms. The stiff cantilever allows stable, small amplitude oscillation close to a surface. It was used in the frequency modulated mode with the oscillation amplitude constant. A force detected between the tip and surface produces a quantifiable variation in the resonant frequency of the cantilever. Under the conditions of these experiments, this variation approximates the force gradient between the tip and surface. To allow comparisons with STM manipulations, Ternes *et al.* also measured the tunneling conductance between the tip and the surface.

Ternes *et al.* derived the force to move an atom from the measurement of the vertical stiffness of the junction between the tip and sample. By computing this as a function of both vertical and lateral tip position, they could derive the force to move an atom in either direction. They found that moving a cobalt atom (Co) on a special surface of platinum [Pt(111)] requires a lateral force of 210 picoNewtons (pN) and this force is independent of the vertical force. Interestingly, the lateral force varied substantially with the underlying surface as it required only 17 pN to move a Co atom on a copper surface [Cu(111)].

Essentially, Ternes *et al.* measured the lateral force by pulling on a Co atom with the probe until it "hopped" from its initial binding site (a small depression in the surface) to the next binding site. This was reproducible and the force required was consistently in the same range (± 5%). The vertical force was determined by integrating the lateral force along the vertical axis in a series of line scans. They interpreted the vertical force as the sum of a background force (including van der Waals and other long range forces) and a short range force between the bound atom and the surface. The lateral force was determined by integrating the vertical force again along the vertical axis and differentiating the resulting potential laterally. The vertical force exerted on the moving atom was much larger than the lateral force, and could be varied within a wide range whereas the lateral moving force stayed constant. This suggested that the lateral force is the key for manipulation of metal atoms on flat metal surfaces.

The lateral force needed to move a symmetrical (spherical) Co atom was an order of magnitude less than that required to move an asymmetrical molecule (carbon monoxide). The spatial dependence of the forces was also found to be markedly different.

The methods developed by Ternes *et al.* provide important information about the manipulation process of individual atoms and molecules based on direct observations. This opens the way for exploration of atomic-scale friction and atom and molecule diffusion on surfaces. It will also lead to a deeper insight into controlled assembly mechanisms from the bottom up. The driving mechanism to create future nanoscale devices can now be explored in a quantitative manner.

1 The author gratefully acknowledges Dr. Markus Ternes for reviewing this article.

2 Ternes, M., C.P. Lutz, C.F. Hirjibehedin, F.J. Giessbl, and A.J. Heinrich, The force needed to move an atom on a surface, *Science* **319**:1066-1069, 2008. See also Perspectives article by O. Custance and S. Morita, How to move an atom, *Science* **319**:1051-1052, 2008

INDEX OF ARTICLES

How Much Force Does it Take to Move an Atom on a Surface? 3
Stephen W. Carmichael, Mayo Clinic

Beyond the Black Box: Interactive Global Docking of Protein Complexes 6
Jochen Heyd, Stefan Birmanns, University of Texas at Houston, School of Health Information Sciences, Houston, Texas

Comparing Binary Image Analysis Measurements – Euclidean Geometry, Centroids and Corners 10
Dennis W. Hetzner, Timken, Co. Canton, Ohio

Confocal Laser Microscopy on Biofilms: Successes and Limitations 18
Betsey Pitts and Philip Stewart, Center for Biofilm Engineering, Montana State University, Bozeman, Montana

Extreme High-Resolution SEM: A Paradigm Shift 24
R. Young, T. Templeton*, L. Roussel**, I. Gestmann**, G. van Veen**, T. Dingle** and S. Henstra** FEI, *Hillsboro, OR and **Eindhoven, The Netherlands*

Testing Parameters for Two-Dimensional Crystallization and Electron Crystallography on Eukaryotic Membrane Proteins with Liposomes as Controls 30
G. Zhao[a], V. Mutucumarana[b], D. Stafford[b], Y. Kanaoka[c], K. F. Austen[c] and I. Schmidt-Krey[a] ,[a]GA Inst. of Tech., Atlanta, [b]UNC, Chapel Hill, NC, [c]Harvard and Brigham and Women's Boston, MA

A New Perspective on Mechanical Testing: *In Situ* Compression in the TEM 36
*Julia Deneen Nowak, Zhiwei Shan and Oden L. Warren, *Hysitron Incorporated, Minneapolis, MN*

Confocal Micro X-Ray Fluorescence: A New Paradigm in Materials Characterization 38
Brian M. Patterson, George J. Havrilla, Kimberly A. DeFriend, *LANL, Los Alamos, NM*

Hardware and Techniques for Cross-Correlative TEM and Atom Probe Analysis 42
B.P. Gorman,[1] D. Diercks,[1] N. Salmon,[2] E. Stach,[2] G. Amador,[3] C. Hartfield,[3] [1]U. of North Texas, Denton, TX, [2]Hummingbird Scientific Instruments, Salem, OR, [3]Omniprobe, Inc., Dallas, TX

Imaging Skin Epidermal Stem Cells: A Review 48
Hilda Amalia Pasolli, The Rockefeller University New York, NY

Signature Analysis Applied to EDS Microanalysis 52
J.W. Colby & D. C. Ward, xk, Incorporated, Clackamas, OR

Cryo-Fracture or Freeze-Fracture, a Method to Expose Internal Tissue Surfaces and Cell Surfaces for Viewing in the Scanning Electron Microscope 56
Jeannette Taylor, Emory University, Atlanta, Georgia

SEM Remote Control with a 3D Option 60
F. Mighela, C. Perra, R. Pintus, S. Podda, M. Vanzi, Sardegna Ricerche, Pula, Italy and DIEE, U. of Cagliari, Cagliari, Italy

Coloring Pictures for Electron Microscopists .....62 or Elements of Digital Image Manipulation for Students
V.M.Dusevich, J.H.Purk, J.D.Eick, University of Missouri, Kansas City, MO

Industry News 64
NetNotes 66
Advertiser's Index 86

ABOUT THE COVER

The cover shows three subunits of the chaperonin GroEL, with favorable interactions highlighted by green spheres. All monomers were docked into an experimental 3D reconstruction of the chaperoning using Interactive Global Docking (see article on page 6).

AAPage 3_08n4.indd 1 06/24/2008 1:41:06 PM

COMING EVENTS

2008

- ✓ **College of Microscopy (Multiple Courses each month)**
  See ad in this issue for details
  www.collegeofmicroscopy.com
- ✓ **Microscopy and Microanalysis 2008**
  August 3-7, 2008, Albuquerque, NM
  www.msa.microscopy.org
- ✓ **American Chemical Society**
  August 17-21, 2008, Philadelphia, PA
  help@acs.org
- ✓ **EMC 2008 Symposium**
  August 18-22, 2008, Detroit, MI
  www.emc2008.org/
- ✓ **14th Electron Microscopy Congress, EMC 2008**
  September 1-5, 2008, Aachen, Germany
  www.eurmicsoc.org/emc2008.html
- ✓ **International Workshop on Electron Crystallography of Membrane Proteins**
  September 7-13, UC Davis, CA
  http://2dx.org/workshop/2008
- ✓ **Frontiers in Cell Migration: From Mechanism to Disease**
  September 16-18, 2008, NIH Bethesda, MD
  www.cellmigration2008.org/program
- ✓ **The 3d International workshop on Piezoresponse Force Micros.**
  September 23-25, 2008, ORNL, Oak Ridge, TN
  cnms.ornl.gov/workshops/2008/CNMS_PFM_Workshop_2008.pdf
- ✓ **Optical Microscopy and Imaging in the Biomedical Sciences**
  October 7-16, 2008, MBL Woods Hole, MA
  www.mbl.edu
- ✓ **9th Asia-Pacific Microscopy Conference (APMC9)**
  November 2-7, 2008, Jeju, Korea
  www.apmc9.or.kr
- ✓ **American Society for Human Genetics**
  November 12-15, 2008, Philadelphoa, PA
  Society@ashg.org
- ✓ **Neuroscience 2008**
  November 15-19, 2008, Washington, DC
  www.sfn.org
- ✓ **2008 MRS Fall Meeting**
  December 1-5, 2008, Boston, MA
  mrs.org
- ✓ **American Society for Cell Biology**
  December 13-17, 2008, San Francisco, CA
  www.ascb.org

2009

- ✓ **PITTCON 2009**
  March 8-13, 2009, Chicago, IL
  www.pittcon.org
- ✓ **The 4th International workshop on Piezoresponse Force Micros.**
  February 2009, Aviero, Portugal
  ftp.ua.pt/incoming/4th_PFM_workshop/4thWorkshop_Aveiro.pdf
- ✓ **Microscopy and Microanalysis 2009**
  July 26-30, 2009, Richmond, VA
  www.msa.microscopy.org

2010

- ✓ **Microscopy and Microanalysis 2010**
  August 3-7, 2009, Portland, OR
  www.msa.microscopy.org

Please check the "Calendar of Meetings and Courses" in the MSA journal "Microscopy and Microanalysis" for more details and a much larger listing of meetings and courses.

MICROSCOPY TODAY

The objective of this publication is to provide material of interest and value to working microscopists!

The publication is owned by the Microscopy Society of America (MSA) and is produced six times each year in odd months, alternating with MSA's peer-reviewed, scientific journal *Microscopy and Microanalysis*. We greatly appreciate article and material contributions from our readers—"users" as well as manufacturers/suppliers. The only criterion is that the subject matter be of interest to a reasonable number of working microscopists. *Microscopy Today* has authors from many disparate fields in both biological and materials sciences, each field with it's own standards. Therefore *MT* does not have a rigid set of style instructions and encourages authors to use their own style, asking only that the writing be clear, informative, and accurate. Length: typical article length is 1,500 to 2,000 words plus images, longer articles will be considered. Short notes are encouraged for our Microscopy 101 section. See our "Instructions to Authors" document on our website.

MICROSCOPY TODAY

ISSN 1551-9295

Ron Anderson, Editor
randerson20@tampabay.rr.com
Phil Oshel, Technical Editor
oshel1pe@cmich.edu
Thomas E. Phillips, Contributing Editor
PhillipsT@missouri.edu
Dale Anderson, Art Director
microscopytoday@tampabay.rr.com
Renée Stratmoen, Advertising Director
oshel1pe@cmich.edu
Regular Mail to:
Microscopy Today, P.O. Box 247, Largo, FL 33779
Courier Mail to:
1001 Starkey Road, Lot #374, Largo, FL 33771
Telephones:
1-(727)507–7101 • Fax: (727)507–7102 • Cell: (727) 631-1022
e-Mail:
microscopytoday@tampabay.rr.com
www Page:
http://www.microscopy–today.com

Colophon: Microscopy Today is created using components of Adobe Creative Suite CS3®

Total Circulation: 16,191

Disclaimer: By submitting a manuscript to Microscopy Today, the author warrants that the article is original (or that the author has the right to use any material copyrighted by others). The use of trade names, trademarks, *etc.*, does not imply that these names lack protection by relevant laws and regulations. Microscopy Today, the Microscopy Society of America, and any other societies stated, cannot be held responsible for opinions, errors, or for any consequences arising from the use of information contained in Microscopy Today. The appearance of advertising in Microscopy Today does not constitute an endorsement or approval by the Microscopy Society of America of the quality or value of the products advertised or any of the claims, data, conclusions, recommendations, procedures, results or any information found in the advertisements. While the contents of this magazine are believed to be accurate at press time, neither the Microscopy Society of America, the editors, nor the authors can accept legal responsibility for errors or omissions.

© Copyright, 2008, The Microscopy Society of America. All rights reserved.

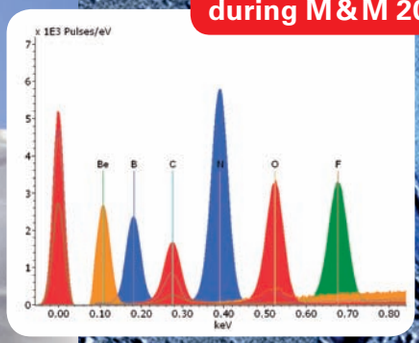
AAPage_4.indd 1 06/20/2008 10:35:29 AM

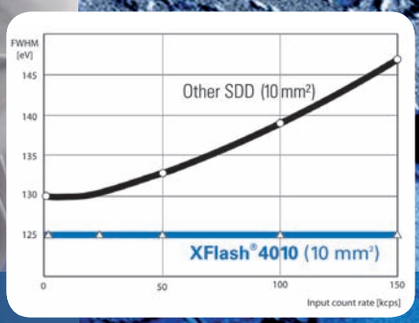
Bruker AXS Microanalysis

This is the badge…



Visit us at booth #1109 during M&M 2008!





…our XFlash® 4010 SDDs receive – guaranteeing 125 eV at 100,000 cps for Mn Kα on your SEM

The XFlash® silicon drift detectors are part of our QUANTAX EDS systems

- Superb performance in the low energy range (F Kα ≤ 57 eV, C Kα ≤ 48 eV)
- Detection from beryllium (4) to americium (95)
- Fastest SDD on the market
- LN_2, vibration and maintenance free
- Excellent element ID in combination with worldwide most comprehensive atomic data library
- XFlash® SDDs are available with 10, 30 and 40 mm^2 active area



www.bruker-axs-microanalysis.com

think forward

MICROANALYSIS

MT Full Page Ad Master.indd 1 06/20/2008 3:17:18 PM

Beyond the Black Box: Interactive Global Docking of Protein Complexes

Jochen Heyd, Stefan Birmanns
University of Texas at Houston, School of Health Information Sciences, Houston, Texas
Stefan.Birmanns@uth.tmc.edu

1. Introduction

A key to understanding the function of biological systems is the visualization of their natural state, ideally in a natural environment. At a molecular level, this is challenging. Traditional experimental techniques, like X-ray crystallography, can provide the atomic structure of proteins, but only by removing them from their native surroundings and forcing them into crystals. Over the past decade, microscopy techniques have emerged as alternatives to these traditional structure determination methods, with the advantage of visualizing molecules in a near-native state. Given the current focus of structural biology on interactions between proteins and better understanding of large protein complexes, cryo-electron microscopy (cryo-EM) has become a valuable tool [1]. Both image acquisition techniques and the computational synthesis of 3D volumetric models from micrographs have advanced considerably. 3D reconstructions of large protein complexes or even individual proteins can now be obtained (Figure 1). While cryo-EM thus offers numerous advantages (small sample size, no need to crystallize, no packing effects, *etc.*), its main drawback is its inability to attain atomic resolution. Other techniques, such as cryo-electron tomography (cryo-ET, [2]) or small-angle X-ray scattering (SAXS, [3]) also yield volumetric reconstructions of proteins in near-native states, but with even lower resolution than cryo-EM.

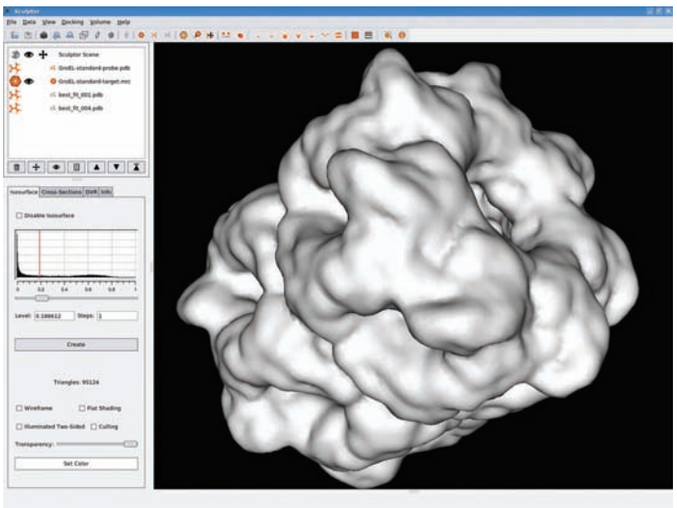


Figure 1: The interface of the Sculptor visualization package, showing a 3D volumetric reconstruction (from cryo-EM) of a GroEL chaperonin.

The failure to achieve atomic resolution with cryo-EM, cryo-ET or SAXS is not as big a stumbling block as one might expect. Often, crystal structures or good homology models are available for individual subunits. These known atomic structures can be docked into experimental volumetric reconstructions, yielding an atomic model of the whole complex. The present report first briefly discusses existing fitting methods and then describes our novel technique.

The current multi-resolution docking approaches generally fall into two categories: 1. Purely user-guided, interactive docking in a visualization program; 2. Exhaustive search based, non-interactive software packages. Each approach has different strengths and weaknesses. The existing user-guided techniques allow a biologist to directly apply his or her knowledge about the system under study. On the other hand, this interactive procedure is highly subjective and the software does not support the user in any way. Manipulating a protein in six dimensions (6D, three translations and three rotations) is non-trivial and the best docking solutions are not necessarily evident. The situation is reversed for exhaustive search based approaches. Here, the 6D search is handled in software, eliminating this tedious process for the user. However, all docking criteria need to be incorporated into a single scoring function, which is used during the exhaustive search. An ideal scoring function would include a large variety of indicators to distinguish correct docking solutions from the rest. In practice, only a single indicator is usually employed, with cross-correlation [4] and feature vector deviations [5] being the most widely used. Besides the scoring function itself, exhaustive search methods encounter a second problem: How are candidate solutions picked? Solely relying on high docking scores is only feasible at relatively high resolutions. At lower resolutions, many almost equivalent solutions exist and the user is then inundated by hundreds of solutions for a protein complex containing only a few proteins.

Our current research focuses on combining these two diametrically opposed docking techniques. Exhaustive search techniques generally only produce a set of candidate solutions but some approaches can easily yield a 3D field of fitting scores. Such a field is amicable to both visualization and further feature extraction. The present report details a first attempt to combine an exhaustive search based scoring field with monomer distance information to allow an intuitive and visual exploration of a given docking problem.

2. Interactive Global Docking

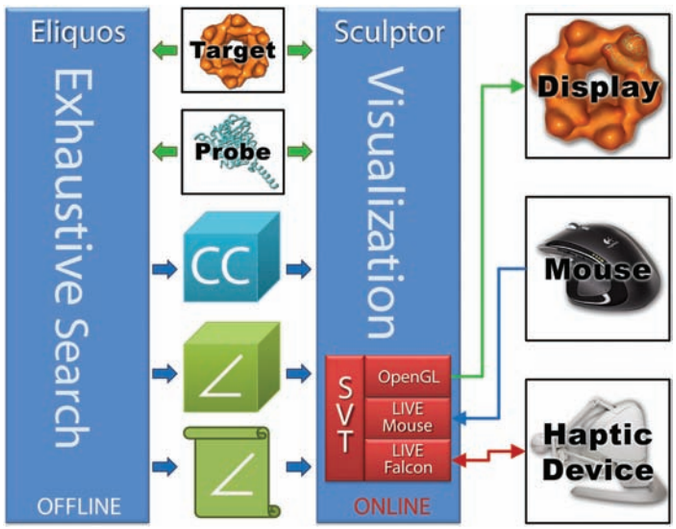


Figure 2: The overall software architecture of the interactive global docking system.

Interactive global docking (IGD) consists of two separate steps: First, an offline exhaustive search is performed in Eliquos, our cross-correlation based exhaustive search software. This typically takes from a few minutes to a few hours, depending on the

ABHeyd-Birmanns.indd 1 06/20/2008 3:47:10 PM

NEW

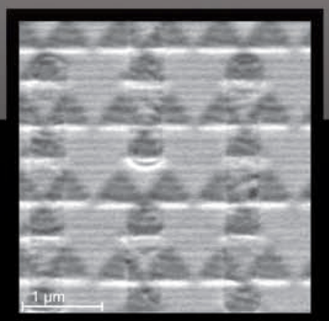
OmniGIS™

Multi-Source Gas Injection System for the FIB & SEM



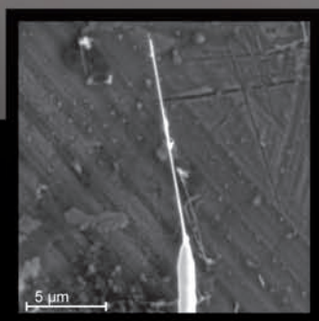
FEATURES:

- Programmable Process Flows
- Feedback Control
- Single Needle Delivery
- Fast & Easy Crucible Replacement
- Economical



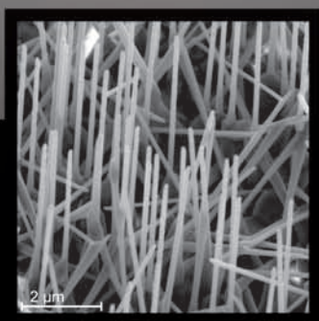
Make

FIB deposited plasmonic nanostructures



Move

Single nanowire analysis



Modify

Chemical surface alteration

For more information visit us at **http://www.omniprobe.com** or call us at **214.570.6800.**

omniprobe

www.omniprobe.com

MT Full Page Ad Master.indd 1 06/20/2008 3:54:01 PM

size of the system. The exhaustive search produces a vector field containing fitting scores and orientations of the probe structure, *i.e.* a scoring field. This field is read into our Sculptor visualization package and the user interactively explores both the scoring field and any additional docking information generated on-the-fly by Sculptor. Figure 2 shows an outline of the software architecture and the sections below discuss these two steps in more detail.

2.1 Exhaustive search

Eliquos, which performs the off-line exhaustive search, is a general, back box, multi-resolution docking application. It is geared towards fast and accurate docking of large data sets, using a scoring function based on cross-correlation. Several advanced filtering techniques are available to enable high-accuracy docking at both high and low resolutions. Like most exhaustive search docking programs, Eliquos is a black box in the sense that once the user specifies the input parameters, no further interaction occurs and the software will output a set of solutions guided solely by the chosen scoring function. For a detailed description, please see Ref. [4].

Eliquos performs a standard, FFT accelerated, exhaustive evaluation of the scoring function based on the user's choice of unfiltered or filtered (Laplacian or Hessian) cross-correlation. Traditionally, the top scoring candidate solutions are further refined and then written out. In the case of IGD, Eliquos instead generates several files containing the scoring field. These files consist of two volume data sets and one file with an index of sampled orientations. The first volume file contains the scalar component of the scoring field, *i.e.* the score of the best solution at each position. The second volume holds the corresponding orientation in the form of an index. Thus, the Sculptor visualization package can read in and use this scoring field as one of the docking criteria supporting the user's fitting decisions.

2.2 Interactive visualization

The interactive stage of IGD is performed in the Sculptor visualization package. Sculptor (Figure 1) is aimed primarily at working with volumetric data sets and docking of high resolution structures into these 3D reconstructions. It makes extensive use of hardware graphics acceleration to provide high performance visualization of large data sets. Some of the provided features are: volume manipulation tools, isosurface and direct volume rendering, feature-based multi-resolution docking using vector quantization, fast flexible fitting based on interpolation, haptic (force-feedback) rendering during docking, and cross-correlation based refinement of approximately fitted structures.

In addition to pure visual feedback during docking, Sculptor also supports haptic rendering, *i.e.* force-feedback to the user about the quality of the current docking position [6]. Until now, this force feedback was only based on a simplified cross-correlation score due to CPU time constraints. In order to provide smooth forces for the user, the forces need to be updated 1000 times per second. Thus, it is not possible to employ advanced filtering techniques during the cross-correlation calculation. By using a precomputed scoring field, scoring functions of arbitrary complexity can be used and the force calculation simplifies to a table lookup and trivial interpolation. In addition, the orientations contained in the field allow the software to rotate the probe structure into the best orientation at the current point in space. The user thus only has to translate the structure, which greatly simplifies his task. Limiting the interactive search space to 3D also has the advantage that inexpensive haptic devices can be used for the force feedback. Novint, for example, offers the Falcon 3D device priced below $200. While the Falcon was developed for immersive 3D gaming, it is ideally suited for our docking approach.

During the interactive stage of IGD, Sculptor not only uses the scoring field generated by Eliquos, but also generates additional, on-the-fly, docking information which the user can draw on to find ideal docking positions. This additional information is based on steric interactions between candidate solutions for different monomers in the protein complex. Whenever a new potential solution is found by the user, Sculptor calculates a distance map which contains the distance from any point in space to the closest existing solution. When the probe structure is moved, this map is consulted to quickly determine the existence of a steric clash or a good protein-protein contact.

3. IGD in practice

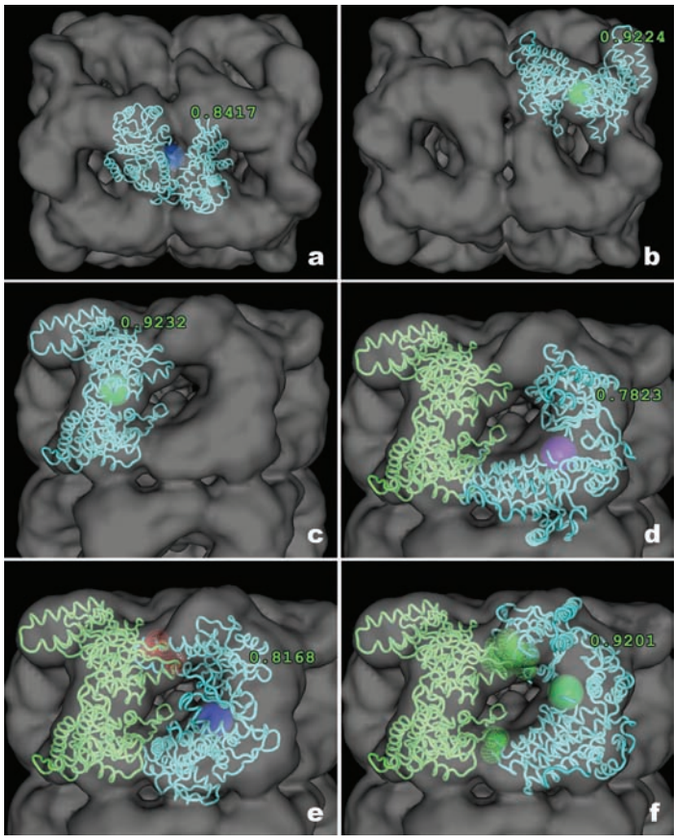


Figure 3: Stages of interactive global docking. The figure shows direct screen captures from the Sculptor visualization package. Please see text for details.

Let us now focus on a specific example and examine the steps performed by both the user and the software. As a test system, we chose the GroEL chaperonin (PDB entry 1GRL). This protein is a homo-14mer with a monomer weight of approximately 47 kDa and numerous experimental cryo-EM data sets are available. Here, we are using a 11.5 Å reconstruction [7]. First, an exhaustive search is performed in Eliquos and the scoring field is saved to a set of files. In the present case, the field was generated via standard cross-correlation, without the use of any filters. This scoring field is then loaded in Sculptor and the IGD is initialized. Figure 3a shows the initial display with the probe structure in the center of the experimental volume. The volume data set has been turned transparent

ABHeyd-Birmanns.indd 2 06/20/2008 3:47:11 PM

to make the probe structure visible. The user now activates IGD and starts moving the probe structure, using either the mouse or a haptic device (Figures 3b and 3c). The user is only responsible for translating the center of the monomer, the optimal orientation at the present position is determined by the scoring field. So, as the probe structure is moved around the experimental data set, it automatically rotates into the most favorable orientation. In addition, the (globally normalized) score at the present position is displayed graphically through color changes of the central sphere, as well as numerically. The user then locates a suitable candidate position for the first docked monomer, taking the global docking score and his or her knowledge of the system into account. This location is saved as a solution (Figure 3d, green structure) and the probe is moved in search for the next candidate location. At this stage, the additional steric information generated by Sculptor comes into play. The user can visualize steric clashes between the current probe structure and all previously docked solutions (Figure 3e) as well as good protein contacts (Figure 3f). Once all constituent proteins are approximately placed, their positions can be further adjusted by either manual or automatic refinement. For example, Figure 4 shows a closer view of the fit resulting from automatic Laplacian refinement of all subunits. No steric clashes are evident and the protein interfaces are highlighted by green spheres, signifying good contacts.

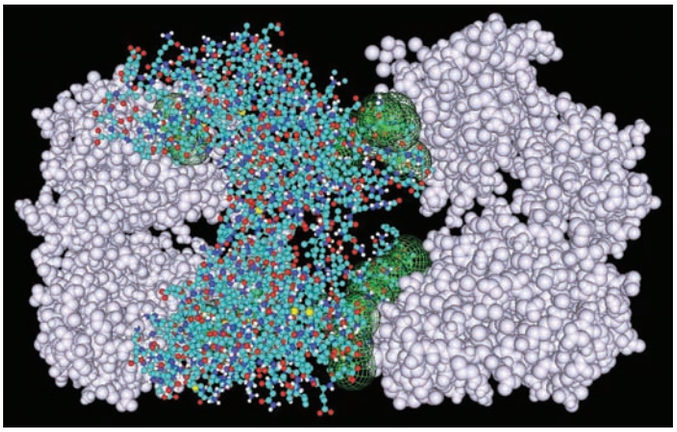


Figure 4: Results of automated refinement of the interactively docked structures. No steric clashes occur and the protein-protein interfaces are highlighted by green spheres.

4. Conclusions

The interactive global docking approach, presented here, combines the best features of non-interactive exhaustive search techniques and purely interactive visualization methods. It provides the user with visual feedback about global docking scores, steric clashes, and good protein-protein interfaces. In addition, haptic rendering can be employed to further enhance the interaction with the user. The additional information supplied during IGD allows biologists to not only rely on their personal knowledge of the system but also draw on objective, software-generated, fitting information. The currently available indicators represent only the first steps for incorporating more information into multi-resolution docking procedures. In the future, we plan on including contact information from mutation experiments, distances from NMR or FRET quenching measurements, as well as improving the existing scoring functions. ■

Availability

Both Eliquos and Sculptor are freely available on our website (http://www.biomachina.org).

Acknowledgments

This work was supported by NIH Grant R01-GM62968 as well as a training fellowship from the National Library of Medicine to the Keck Center for Interdisciplinary Bioscience Training of the Gulf Coast Consortia (NLM Grant No. 5T15LM-07093) to J. H.

References

[1] Frank, J. 2002. Single-particle imaging of macromolecules by cryo-electron microscopy. *Ann. Rev. Biophys. Biomol. Struct.* 31:303–319.

[2] Lučić, V., F. Förster, and W. Baumeister. 2005. Structural Studies by Electron Tomography: From Cells to Molecules. *Annu. Rev. Biochem.* 74:833–865.

[3] Petoukhov, M. V., and D. I. Svergun. 2007. Analysis of X-ray and neutron scattering from biomacromolecular solutions. *Curr. Op. Struct. Biol.* 17:562–571.

[4] Heyd, J., M. F. Schmid, W. Wriggers, and S. Birmanns. 2008. Hessian filtering for docking of atomic structures into 3D cryo-electron microscopy reconstructions. *J. Struct. Biol.* submitted.

[5] Birmanns, S., and W. Wriggers. 2007. Multi-resolution anchor-point registration of biomolecular assemblies and their components. *J. Struct. Biol.* 157:271–280.

[6] Birmanns, S., and W. Wriggers. 2003. Interactive fitting augmented by force-feedback and virtual reality. *J. Struct. Biol.* 144:123–131.

[7] Ludtke, S. J., J. Jakana, J. Song, D. T. Chuang, and W. Chiu. 2001. An 11.5 A Single Particle Reconstruction of GroEL Using EMAN. *J. Mol. Biol.* 314:241–250.

MANAGING ELECTRON MICROSCOPIST

The Materials Characterization Facility (MCF, www.ampac.ucf.edu/mcf) of the Advanced Materials Processing and Analysis Center (AMPAC, www.ampac.ucf.edu) at the University of Central Florida in Orlando is seeking to hire a scientist/engineer to manage and operate its electron microscopy facilities with an emphasis on transmission and scanning electron microscopy. The University of Central Florida is a major metropolitan research university with over 48,000 students. MCF is a multiuser facility with 2 TEMs, 2 SEMS, 2 SIMS, EPMA, FIB, AES, XPS, RBS, MicroRaman, AFM/STM, LSCM, and a complete specimen preparation laboratory. The SEM and TEM laboratory currently operates a JEOL 6400 FESEM, Hitach 3500N SEM, JEOL 1011B TEM, FEI Tecnai F30 TEM/STEM, and associated sample preparation equipment including an FEI 200TEM FIB. The MCF is a vibrant multiuser facility that provides microscopy and spectroscopy facilities to a wide range of users from academia, industry, and national laboratories around the world. In FY2007, 125 UCF internal users and 26 external users, including 20 private companies, worked at and with MCF for their materials characterization needs.

Applicants with an advanced degree in relevant sciences/engineering specialties with at least two years operation and/or maintenance experience are preferred. We are particularly interested in individuals who have a strong record in using TEM/STEM to solve scientific and engineering problems. The position will involve management and operation of instruments on a day-to-day basis, support, and training of users, instrument maintenance, and instrument development. The applicant should have strong interpersonal as well as oral and written communication skills.

Review of candidates will begin immediately, and will continue until the position is filled. Electronically submit *curriculum vitae*, containing a summary of expertise and accomplishments and contact information for references, should be sent to: Prof. Yongho Sohn, ysohn@mail.ucf.edu, Associate Director for MCF, University of Central Florida, AMPAC, PO Box 162455, Orlando, FL 32816

The University of Central Florida is an affirmative action/equal opportunity employer. As a member of the Florida State University System, all application materials and selection procedures are available for public review.

ABHeyd-Birmanns.indd 3 06/20/2008 3:47:12 PM

Comparing Binary Image Analysis Measurements - Euclidean Geometry, Centroids and Corners

Dennis W. Hetzner
Timken, Co. Canton, Ohio
dennis.hetzner@timken.com

Introduction

During the past several years, ASTM Subcommittee E04.14 on Quantitative Metallography has been developing an Image Analysis (I/A) methodology to determine the degree of circularity, roundness or sphericity of graphite nodules in ductile cast iron. In the as-polished condition, ideally the iron nodules should appear as dark circular objects in a light gray matrix, Figure 1. When performing Image Analysis measurements for these types of materials, complex gray image procedures should not be required to properly threshold the images to obtain an acceptable binary image on which to perform the measurements.

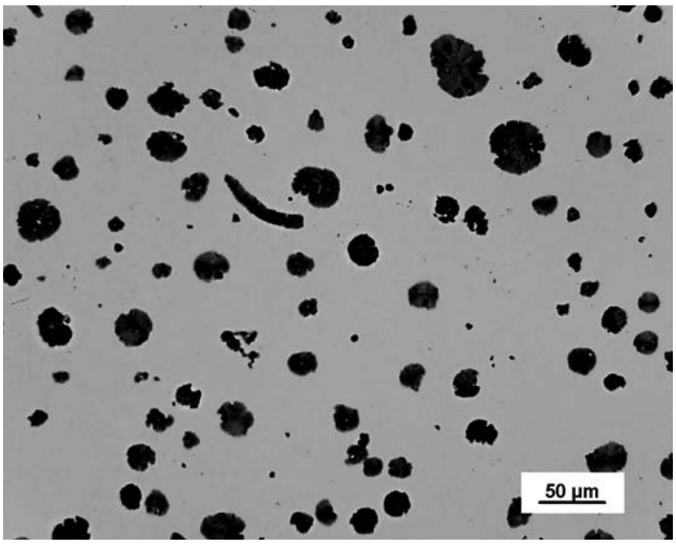


Figure 1. Gray image showing various morphologies of ductile iron particles.

During the development of the standard, it became evident that specific tolerances on the magnification used to perform the measurements or, more precisely, the number of pixels in the objects to be measured in the binary images, needed to be clearly specified. This was because during a preliminary test program, it was discovered that differences in the magnification used for the analysis could affect the results of the measurements.

As development of the standard progressed, not only was the magnification used for the analysis found to be important, but differences in the way I/A systems made measurements on binary images appeared to be of equal importance. Thus, some method of determining how different I/A systems made basic measurements was required.

Experimental Procedures

Initially, using a graphical interface, a preliminary test pattern consisting of a series of circles of known diameters was created. Members of Subcommittee E04.14 measured the circles with several different I/A systems, and it was discovered that there was a wide variation in the resulting measurements. This led to the creation of a second test image. The second test image consisted of the following series of filled objects:

1. Straight lines parallel to the x-axis of the I/A system having pixel lengths of 10, 20, 30, 40 and 50.
2. Rectangles having sides parallel to the principal axes of the I/A system and having dimensions of (3×4), (6×8), (9×12), (12×16) and (15×20) pixels.
3. Inscribed circles having pixel diameters of 4, 8, 16, 32 and 64.
4. A cosine rose having five leaves and a diameter of 200 pixels was included in the test pattern.

This test image was measured by four members of subcommittee E04.14 having different I/A systems. The same test pattern was later measured by several different manufacturers of I/A systems and software that attended the 2007 M&M show in Ft. Lauderdale, Florida. Eventually, software packages from the following vendors were used in the evaluation: Buehler Ltd., Carl Zeiss, Clemex, Leica, NIH Image J, Olympus, Smart Imaging and Struers.

The test results to be described were based on measurements made from exactly the same binary image. For simplicity, the calibration of the systems was set so that 1 pixel was equal to 1.0 µm, and the calibration was the same in both the horizontal and vertical directions; *i.e.* Cal *X* = Cal *Y*. For each object in the test pattern, the area, longest Feret's diameter ($F_{Max.}$), minimum Feret's diameter, perimeter and convex perimeter were measured.

Results and Discussion

Rectangles: The simplest object to consider first is the series of rectangles. As described, each of these rectangles is based on the ratio of sides having lengths of 3×4. Based on simple Euclidian geometry, the area of a 3×4 rectangle is 12, the perimeter is 14 and using the Pythagorean theorem, the diagonal, or maximum Feret's diameter, is 5. Similarly, for the 6×8 rectangle, the area would be 48, the perimeter would be 28 and $F_{Max.}$ would be 10, etc. When I/A measurements were performed by the various systems, the areas were exactly what would be calculated from simple Euclidean geometry. However, measurements of the other parameters showed considerable variations from the answers based on Euclidean geometry. For the 3×4 rectangle, the areas, maximum Feret's diameters and perimeters, as measured by the various systems, were as follows:

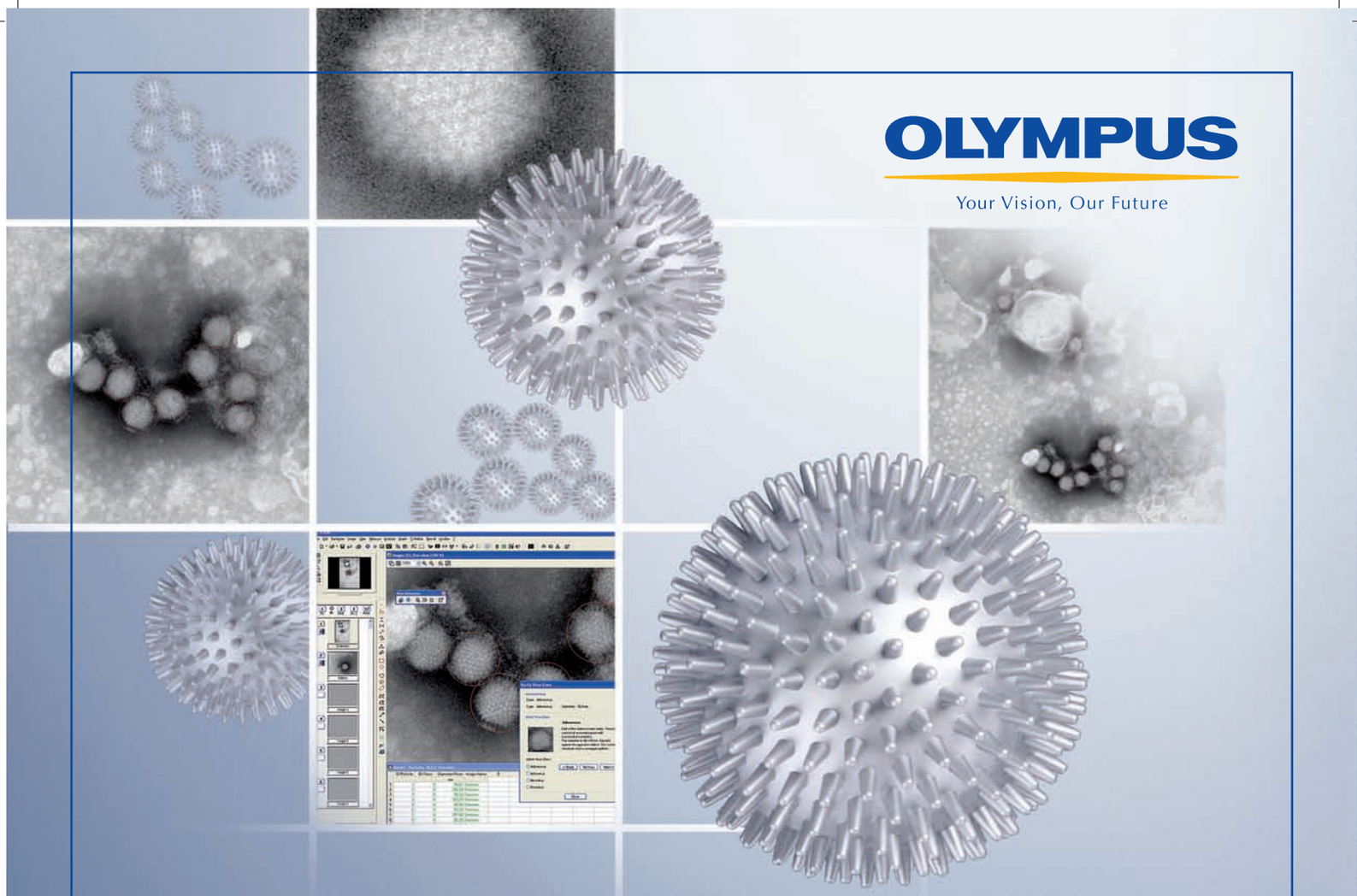
Table 1. Parameters for 3×4 rectangles measured by different I/A systems

	Area	Length	Perimeter
System			
A	12	4.50	10.00
B	12	4.61	14.00
C	12	3.61	10.00
D	12	5.00	12.83
E	12	5.00	11.66
F	12	4.00	14.00
G	12	4.95	12.17
H	12	5.00	12.83
Min	12	3.61	10.00
Max	12	5.00	14.00
Average	12	4.50	12.28
% Diff.	0	30.3	33.0

ABHetzner2.indd 1 06/20/2008 4:03:55 PM

OLYMPUS

Your Vision, Our Future



ELECTRON MICROSCOPY MADE SIMPLE
iTEM SOLUTION VIROLOGY
AUTOMATED VIRUS DETECTION AND IDENTIFICATION

Every year, gastroenteritis viruses cause epidemic outbreaks such as the graphically named ”winter vomiting disease”. Detecting and identifying these viruses have all become of critical interest globally. Common virus identification methods take several hours to provide results based on a specific and known virus and are problematic due to frequent mutation and similarity of symptoms. This problem can be avoided by visually identifying specific virus structures within TEM images. However, conventional TEM analysis is manual and heavily dependent on specialists of extensive experience to obtain diagnoses quickly and reliably.

Visit us at the
M&M
Booth #104

iTEM Solution Virology provides a new technological approach for automated detection and identification of the various gastroenteritis viruses in highly textured TEM images. This approach is based on internal and surface structure analysis. The analytical findings are presented in a report and can easily be confirmed by the virologist.



iTEM SOLUTION VIROLOGY

For detailed information please contact:

Olympus Soft Imaging Solutions
info.osis@olympus-sis.com
www.soft-imaging.net
North America: (888) FIND SIS, +1 (303) 234-9270
Europe: +49 (251) 79800-0
Asia / Pacific: +60 (3) 8313-1400

O L Y M P U S S O F T I M A G I N G S O L U T I O N S

MT Full Page Ad Master.indd 1 06/23/2008 12:01:35 PM

In the above table, the letters A through H represent the different I/A systems used for the analysis. The term percent difference is defined as:

$$\% \text{ Difference} = \frac{(Max - Min)}{Mean} \times 100 \qquad (1)$$

This term is referred to as difference rather than error. That is because while the results are not the same for each system, the operators made no errors in performing the tests or the analysis. The differences are only due to the differences among the algorithms used to make the measurements.

Similarly, the maximum Ferret's diameters and perimeters for the different sized rectangles were found to be as follows:

Table 2. Differences among I/A parameters measured for various size rectangles

	Rectangles				
$F_{Max.}$	**3:4**	**6:8**	**9:12**	**12:16**	**15:20**
Min.	3.6	8.6	13.6	18.6	23.6
Max	5.0	10.0	15.0	20.0	25.0
Mean	4.5	9.5	14.5	19.5	24.5
% Diff.	30.3	14.8	9.8	7.3	5.8
Perimeter					
Min.	10.0	24.0	38.0	52.0	66.0
Max	14.0	28.0	42.0	56.0	70.0
Mean	12.3	26.1	40.1	54.1	68.1
% Diff.	33.0	15.3	10.0	7.4	5.9

The data and associated graph, Figure 2, clearly indicate that as the number of pixels in the rectangles increases, the difference among the systems used to perform the measurements decreases.

In order to explain the differences among the various systems, it is necessary to understand how the pixels composing the image

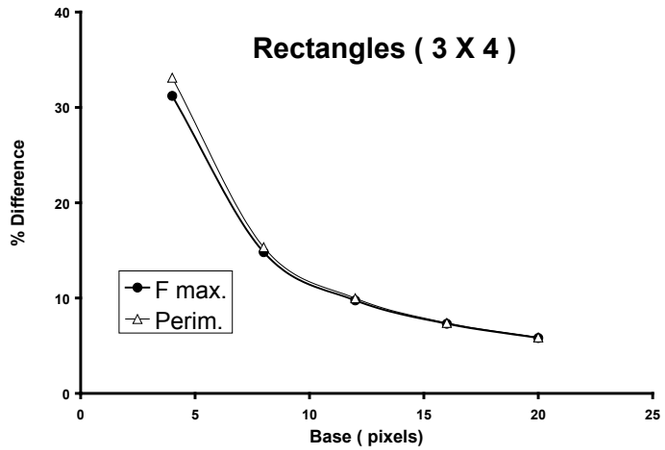


Figure 2. Difference among measured Image Analysis parameters with respect to rectangle size.

are manipulated. First, considering simple Euclidean geometry, a 3×4 rectangle, based on the Pythagorean theorem would have a diagonal equal to 5, Figure 3.

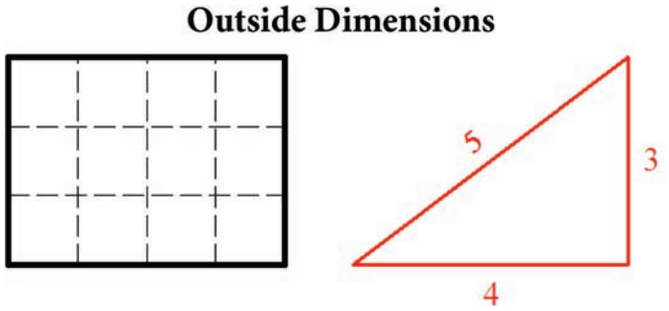


Figure 3. Euclidean Geometry: Dimensions of a 3 × 4 rectangle based on the outer dimensions.

However, as indicated by the dotted lines, each of the 12 pixels forming the rectangle contains a centroid, Figure 4. Thus, in the *X* direction, the distance between the centroids is 3 pixels. Similarly, the distance between the centroids in the *Y* direction is only 2 pixels. By using the centroids and the Pythagorean theorem, the diagonal of the rectangle is $D^2 = (F_{Max.})^2 = 3^2 + 2^2 = 13$; hence, $F_{Max.} = 3.61$. This explains the first difference among the various I/A systems.

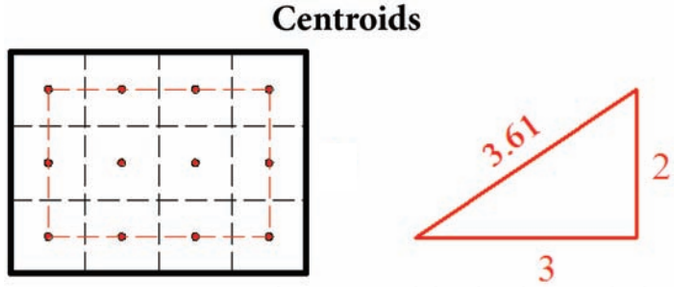


Figure 4. Dimensions of a 3 × 4 rectangle based on the centroids of the pixels forming the object.

Now, consider the perimeter of the 3×4 rectangle. Using simple Euclidean geometry, the lengths of each of the segments parallel to the *X*-axis are 4 pixels and the lengths of each of the segments parallel to the Y-axis are 3 pixels, Figure 3. Thus, the simple perimeter of the 3×4 rectangle is 4 + 3 + 4 + 3 = 14. However, now consider what can happen if the centroids are used for the measurement of perimeter. In this situation, again using simple Euclidean geometry, the lengths of the segments parallel to the *X*-axis are 3 pixels and the lengths of the segments parallel to the *Y*-axis are 2 pixels, Figure 4. Thus the perimeter of the 3×4 rectangle based on pixel centroids is 3 + 2 + 3 + 2 = 10.

These results account for the maximum and minimum values of the perimeter measurements; however, as indicated in Table 2, other intermediate values also exist. To show how these other measurements are derived, the geometries of the corner pixels must be considered. In these tests, it was found that there were four different ways to analyze the corner pixels, Figure 5.

As shown by the circled pixel, Figure 5a, the simplest method to account for the corner is to let it be equal to 2; that is, use the entire *X* and *Y* components of the corner pixel. The next level of refinement is to replace the two portions of the corner with a diagonal having a length of 1.41 pixels, Figure 5b. Finally, as was found in these tests, a shorter diagonal and a shorter portion of the corners can replace the corner pixel, Figures 5c and d. Thus, different systems

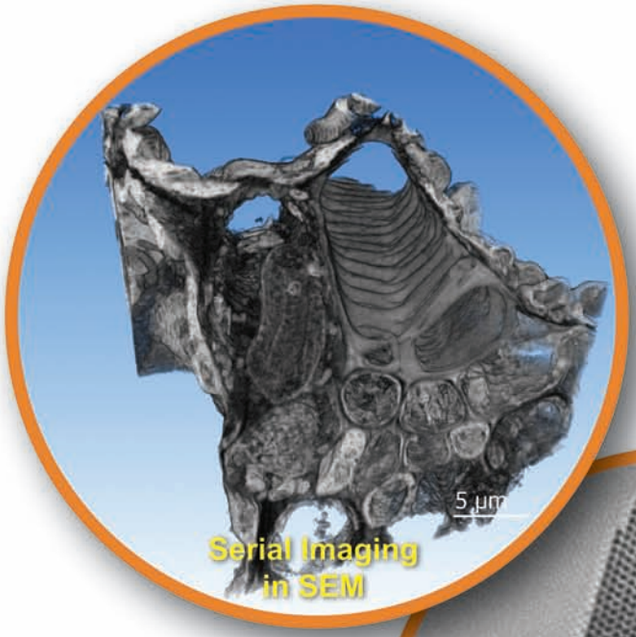
ABHetzner2.indd 2 06/20/2008 4:03:56 PM

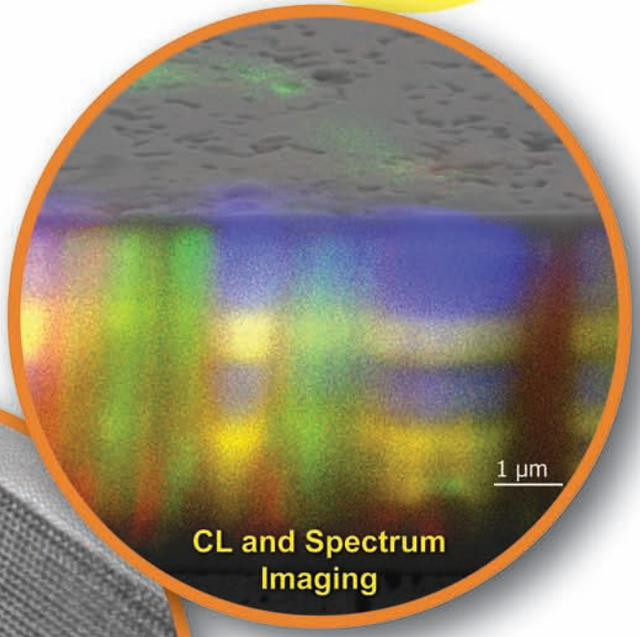
gatan gets it

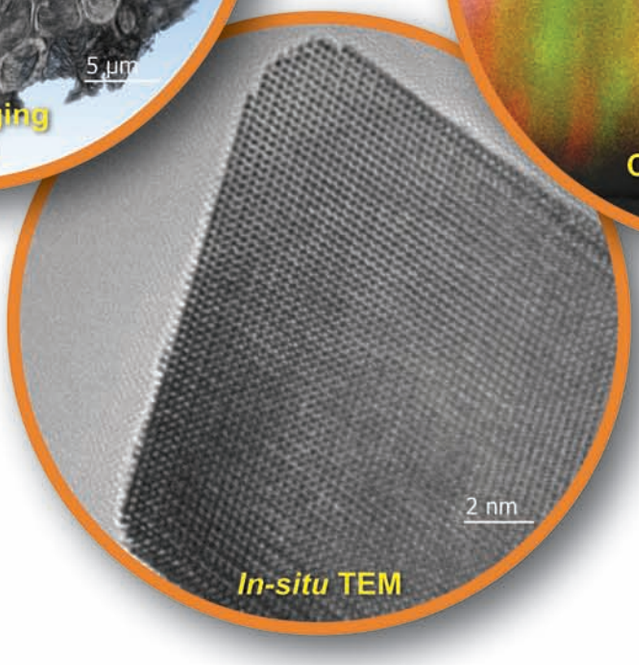
Do you want to improve the performance of your EM and your productivity?

To learn how, visit us at M&M in Booth 1130 or www.gatan.com

We design tools that enable and advance EM applications. We understand your application criteria and will provide you with the right solutions.







Images (from left to right): Serial Imaging in SEM: 600 individual images of maize leaf sample acquired with Gatan 3View™ to create a model with dimensions of 30 x 25 x 45µm; images were rendered using Gatan 3D Visualization Tool. Images courtesy of Dr. G. Wanner of Ludwig-Maximilian University, Munich, Germany. *In-situ* TEM: HREM image of active catalytic nanoparticle of ceria zirconia recorded with Gatan ORIUS™ SC600 CCD camera in environmental TEM operating at 200kV. Cerium atomic columns appear as black dots in the image. Image courtesy of Dr. Ruigang Wang and Dr. Peter Crozier, Center for Solid State Science, School of Materials, Arizona State University, USA. CL and Spectrum Imaging: Composite image showing defect distribution and compositional variations in a light-emitting material revealed by CL and spectrum imaging. Image acquired with Gatan MonoCL3+ CL imaging and spectroscopy system derived from 4 monochromatic CL images plus SE image. Results courtesy of Dr. Uwe Jahn of the Paul Drude Institute for Solid State Electronics, Berlin, Germany.

gatan

MT Full Page Ad Master.indd 1 06/20/2008 4:53:38 PM

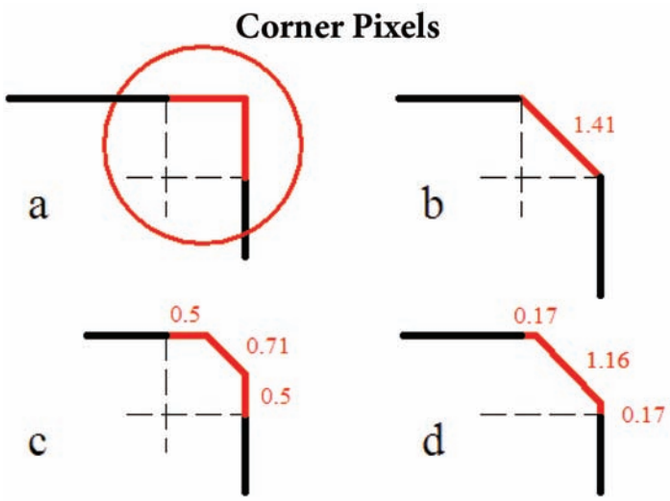


Figure 5. Geometrical methods for measuring the perimeter from corner pixels.

can obtain a variety of different perimeter measurements based on the algorithm used to account for the corner pixels.

Circles: The next level of complexity considered was a series of filled, inscribed, circles. Here again it is easiest to understand how the Image Analysis systems operate by using an inscribed circle having a diameter of four pixels, Figure 6. When the Euclidean and centroid analysis is used to calculate the maximum Feret's diameters, the results are found from equations 2 and 3.

$$\text{Euclidian Ferret Max} = \sqrt{4^2 + 2^2} = 4.47 \qquad (2)$$

$$\text{Centroid Ferret Max} = \sqrt{3^2 + 1^2} = 3.16 \qquad (3)$$

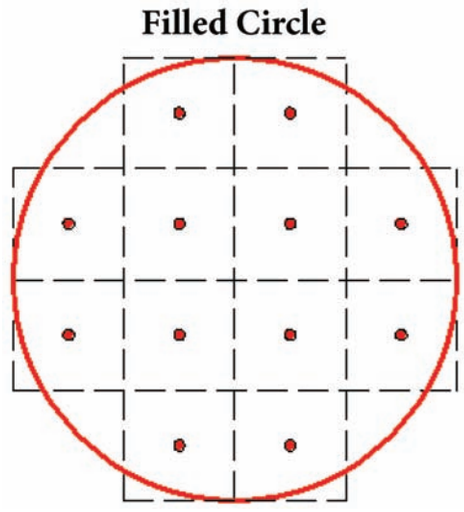


Figure 6. Pixels contained in a filled circle having a diameter of 4.

In all measurements, the object was found to have an area of 12 square pixels. However, as indicated by the above calculations and measurements, in some cases, the maximum Feret's diameter is larger than the diameter of the inscribed circle, while in the other cases, the maximum Feret's diameter is smaller than the diameter of the inscribed circle. Based on the number of corners in image, it is not surprising that the perimeter of the inscribed circle has even more variation than the maximum Feret's diameter. As for the rectangles, as the size of the inscribed circles increases, the difference among the parameters measured by the various I/A systems decreases, Figure 7.

For most applications, it is a rare occurrence when the objects to be evaluated are well-defined rectangles that have sides parallel to the principal axes. Generally, an object with curved sides similar to a circle is encountered.

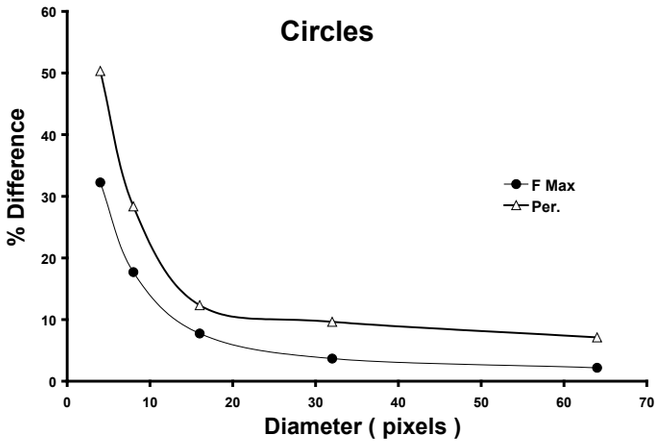


Figure 7. Difference among measured Image Analysis parameters with respect to inscribed circle diameter.

Thus, for practical applications, the results based on the analysis of circular objects best represents what sized objects should be measured if comparisons among different I/A systems are to be made. Hence to have an error of less than 5%, the minimum feret diameter of the measured objects should be at least 40 pixels. Furthermore, no matter what the size of the object, the differences in perimeter measurements are always greater than the differences in Feret's diameters.

Convex Perimeter: Another perimeter measurement is often discussed; *i.e.* convex perimeter. In simple terms, it is explained as the perimeter of a rubber band stretched around an object. In most applications for large objects, this may be true; however, this measurement is not quite that simple. In this study, several unusual things were discovered. As before, not all the systems make the measurement in the same manner. In some cases, the perimeter of the rectangles was smaller than the convex perimeter of the rectangles. While, in other cases, the perimeter of the rectangles was larger than the convex perimeter. A very strange occurrence was noted for one of the systems; when the convex perimeter of the rectangles was measured, the pixels at the corners were removed from the rectangle. Thus, the area of the rectangles decreased. This could be a significant problem for irregularly shaped or large features. One other problem was encountered; the freeware did not measure convex perimeter.

Crofton Perimeter: There is another perimeter measurement that was not used since most systems do not include it in the software packages - Crofton Perimeter. The Crofton perimeter is based on intercept counts made by using test lines with a known spacing between the lines. The Crofton perimeter is based on topological relationships that exist between objects and surfaces [2]. In general, the Crofton perimeter is more accurate than the simple perimeter measurements used by most I/A systems.

Shape Factors: With these observations in mind, it is now possible to consider the original problem of nodularity measurements from a more enlightened frame of mind. Through the years, several different shape factors have been proposed by various investigators, as well as manufacturers of I/A systems. Several of the initial shape factors proposed date back to one of the original QTM systems

ABHetzner2.indd 3 06/20/2008 4:03:56 PM

create by Cambridge Instruments in the late 1960's [3]. Roundness and shape factor were defined as follows:

$$\text{Roundness} = \frac{P^2}{4\pi A} \tag{4}$$

and

$$\text{S.F.} = \frac{4\pi A}{P^2} \tag{5}$$

For a circle, each of these parameters is equal to one. As the object becomes more elliptical, the roundness increases, while the shape factor decreases. In time, similar parameters based on convex perimeter were developed. The problem with each of these parameters is that perimeter to the second power is used in each of these formulas. Thus, in evaluation the sphericity of nodularity of a particular object, the square of one of the least accurate I/A parameters is utilized.

ASTM Committee E04 has proposed using a shape factor based on the area of a circumscribed circle as the measurement of the degree of nodularity. For any object that is measured, the objects area and its maximum Feret's diameter are measured. The degree of nodularity is then the area of the measured object divided by the area of the circle that circumscribes it, $\left(\pi F_{Max}^2\right)/4$. That is,

$$\text{ASTM Nodularity} = \frac{4\pi \cdot \text{Area}}{F_{Max}^2} \tag{6}$$

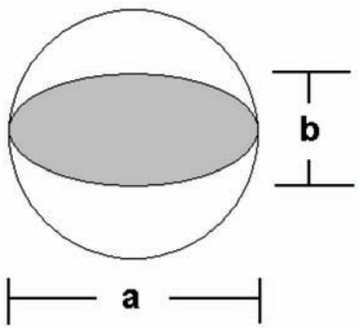


Figure 8. An ellipse, having major and minor axes of a and b respectively, and its circumscribed circle.

This parameter does not contain a perimeter measurement. In addition, it is more sensitive to departures from true circularity than the shape factor previously defined by equation 5. It is interesting to note that this parameter is referred to as Roundness in the CRC Image Processing Handbook [4]. Consider the relationship between an ellipse and its circumscribed circle, Figure 8.

The area of the circumscribed circle is $\pi \cdot a^2/4$ and the area of the ellipse is Area = $\pi a \cdot (b/4)$. The approximate perimeter of an ellipse, was first given by Euler [5] as,

$$\text{Ellipse Perimeter} \approx \pi \sqrt{\frac{a^2 + b^2}{2}} \tag{7}$$

As the minor diameter of the ellipse decreases, the area of the ellipse decreases in a linear manner as compared to the area of the circle circumscribing it, Figure 9. However, for the term Shape Factor, a significant change in the minor axis of the ellipse must occur before the shape factor begins to correspondingly start to decrease. Thus, the proposed ASTM descriptor of nodularity is a more accurate measuring parameter than the factors including perimeters for two reasons. First, the ASTM parameter is more sensitive to departures from circularity than the shape factor. Second, the linear relationship between the area of the objects means differences in the shape factor at high values are similar to differences in the shape parameter at other values.

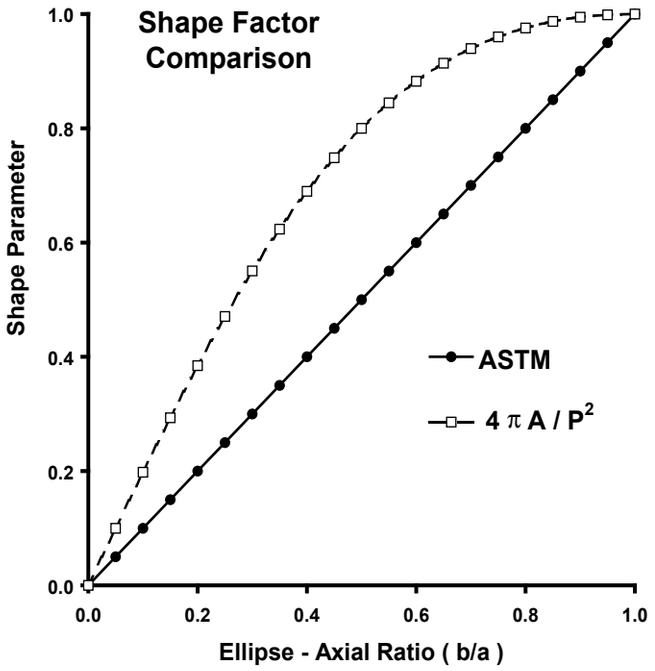


Figure 9. Shape factor comparison.

Conclusions

Differences among how various I/A systems perform measurements on simple geometric features were clearly established and rationalized. When feature area is measured, all the systems performed the same. However, discrepancies in other parameters such as Feret's diameter and especially perimeter differ quite a lot among the systems evaluated. Convex perimeter was found to be a more complicated parameter than generally perceived, and very system sensitive. For these reasons, shape parameters using any type of perimeter are subject to greater differences among I/A systems than other types of shape parameters. The shape factor proposed by ASTM committee appears to be quite good in describing the degree of roundness of features. For all the parameters considered, the minimum dimension of the objects being measured should be at least 40 pixels to maintain a difference among various systems of 5% or less. ■

Acknowledgements

The assistance of Albert Brandemarte, Gabriel Lucas and Steven Glancy from ASTM Subcommittee E04.14 in performing various tests on the binary images was most helpful. The assistance provided by the various I/A manufacturers at the 2007 M&M Conference is appreciated.

References

1. H. E. Exner, 'Analysis of Grain and Particle Size Distributions in Metallic Materials,' *Int. Met. Reviews*, 1972, Review 159, Vol. 17, pp 25-42.
2. M. P. do Carmo, 'Differential Geometry of Curves and Surfaces,' 1976, Prentice Hall, Englewood Cliffs, NJ, pp 41-46.
3. Cambridge Instruments Q720 Instruction Manual, 1969.
4. *The Image Processing Handbook*, CRC, 2002, Chapter 9.
5. Leonhard Euler, Circa 1773.

ABHetzner2.indd 4 06/20/2008 4:03:57 PM

Hitachi High Technologies America

Achieving Global Excellence Through Strength in Advanced Technologies









Hitachi High Technologies America – Centers of Excellence
Pleasanton, CA (top); Dallas, TX (bottom)



NEW! SU-1500 Scanning Electron Microscope



NEW! SU8000 Ultra-High Resolution Field Emission Scanning Electron Microscope



Visit us at M&M 2008 in Albuquerque, NM Booth # 1329

Hitachi High Technologies America, Inc. ✹ Nanotechnology Systems Division ✹
5100 Franklin Drive ✹ Pleasanton, CA 94588 925.218.2800 ✹ www.hitachi-hta.com

MT Full Page Ad Master.indd 1 06/20/2008 6:07:28 PM



NEW! NB5000 Focused Ion and Electron Beam System



TM-1000 Tabletop Microscope
(SwiftEd version)



S-3400N Variable Pressure Scanning Electron Microscope



NEW! SU6600 Schottky Emission Variable Pressure Field Emission Scanning Electron Microscope

Hitachi will continue to provide the best equipment solutions for our customers and for society by carrying through on our mission. Our corporate statement – Inspire the Next – symbolizes Hitachi's determination and commitment to take on the new challenges of the coming nano era.

HITACHI
Inspire the Next

MT Full Page Ad Master.indd 1 06/20/2008 6:04:05 PM

Confocal Laser Microscopy on Biofilms: Successes and Limitations

Betsey Pitts and Philip Stewart
Center for Biofilm Engineering, Montana State University, Bozeman, Montana
betsey_p@erc.montana.edu

Introduction

Biofilms are communities of microbial cells and extracellular polymeric substances (EPS) attached to a surface. Bacteria exist preferentially in the biofilm state in nature and in many engineered systems. In this state, microbes tolerate antibiotics and disinfectants. Bacterial biofilms are now implicated in a wide range of human diseases and infections including cystic fibrosis, otitis media, chronic wounds, artificial joint and prosthesis infection, and many nosocomial infections. Biofilm-related infections and industrial fouling problems cost billions of dollars each year.

Imaging of bacterial biofilms with microscopes has been an essential and transformative method in biofilm research. Fluorescence microscopy can elucidate specific biofilm components and cellular activities that cannot be separated otherwise. In particular, confocal fluorescence microscopy extends that examination through the thickness of a fully hydrated, *in-situ* biofilm, affording the potential for 3D, non-invasive, time-lapse imaging.

This article discusses some striking examples of the insight provided by confocal fluorescence microscopy into biofilm structure, composition, and heterogeneity, and will enumerate some limitations of this imaging process.

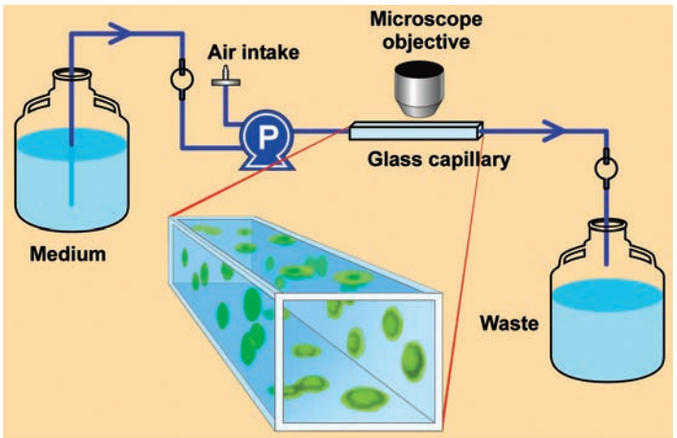


Figure 1 Illustration of a 1mm square glass capillary flow-cell. Biofilm microcolonies are imaged through the glass ceiling of the capillary. Drawing by J.Meyer, MSU-CBE.

Biofilm Growth Methods

Bacteria

Bacteria used in this work were *Staphylococcus epidermidis* ATCC 35984; *Pseudomonas aeruginosa* PA01, and a number of PA01 fluorescent protein constructs: pMF230-*gfp* (constitutively expressed green fluorescent protein), PA01 pMF230-*cfp*, or -*yfp* or PA01 pAB1 (inducible *gfp* expression) (Werner *et al.*, 2004); or a dental biofilm consortium: *Streptococcus oralis* ATCC 10557, *Streptococcus gordonii* ATCC 10558 and *Actinomyces naeslundii* ATCC 19039.

Growth Reactors

Biofilms were grown in either the CDC reactor (Goeres *et al.*, 2005) or a 1mm square glass capillary flow cell (Werner *et al.*, 2004). In both reactor systems, a no-flow inoculation or attachment period was followed by the continuous flow biofilm growth period until the desired cell density was reached.

The CDC reactor consists of a stirred 1L beaker fitted with a stopper from which hang 8 rods. Each rod holds 3 glass biofilm growth surfaces or coupons, 1.27 cm^2 in area. The reactor is operated as a continuously stirred tank reactor, using parameters detailed in ASTM Method E2562-07 with the addition that, for the organisms used in these studies, the reactors were incubated at 37°C. After 18 hours of stirred inoculation and 48 hours of growth in continuous flow conditions, coupons were aseptically removed from the reactor, stained, rinsed, and imaged while submerged in water.

The capillary flow cell reactor uses a 1mm square glass tube (Friedrich and Dimmock), roughly 4 inches long, as the biofilm growth surface. The tubing walls are 0.17 mm +/- 0.1mm thick. The reactor is plumbed on either end so that nutrients are pumped in and effluent is pushed out and is operated under continuous flow conditions for 24 hours at 37°C. Capillary flow cell biofilms are usually imaged through the ceiling of the reactor, as shown in Fig. 1.

Imaging

A Leica TSC-SP2 AOBS confocal microscope was used for all imaging, with a laser excitation source of 488, 561, or 633 nm. In some cases, a Spectra Physics MaiTai 2-photon attachment was used instead of, or in addition to, those single photon excitation sources.

All biofilms were stained prior to imaging with stains specific to total bacterial cells, EPS and matrix components, or to a particular aspect of bacterial activity. Flow cell biofilms were stained *in situ*; that is, stain was pumped into the reactor to fill the volume, then the flow was stopped. The biofilm was stained statically for the desired time, then rinsed and immediately imaged. Flow cell biofilms were imaged with an N PLAN 20X 0.4NA dry objective or for very thick biofilms, a 40X W 0.8NA U-V-I 3.3mmWD dipping objective. CDC reactor coupons were removed from the reactor and placed in a 35mm diameter petri dish. 200µL of stain was gently pipetted onto the coupon surface, and allowed to remain for the necessary staining period. When staining was complete, filtered water was gently added to the 200 µL of liquid on the coupon surface to rinse until clear, then water was added to the dish to cover the coupon by roughly 2mm. Biofilm on the coupon surface was imaged immediately in this state with either a 40X W 0.8NA U-V-I 3.3mmWD or a 63X W 0.9 NA U-V-I 2.2mmWD dipping objective. Images were processed in either Imaris software for qualitative presentation (Bitplane Inc.) or MetaMorph software (Molecular Devices) for quantitative analysis.

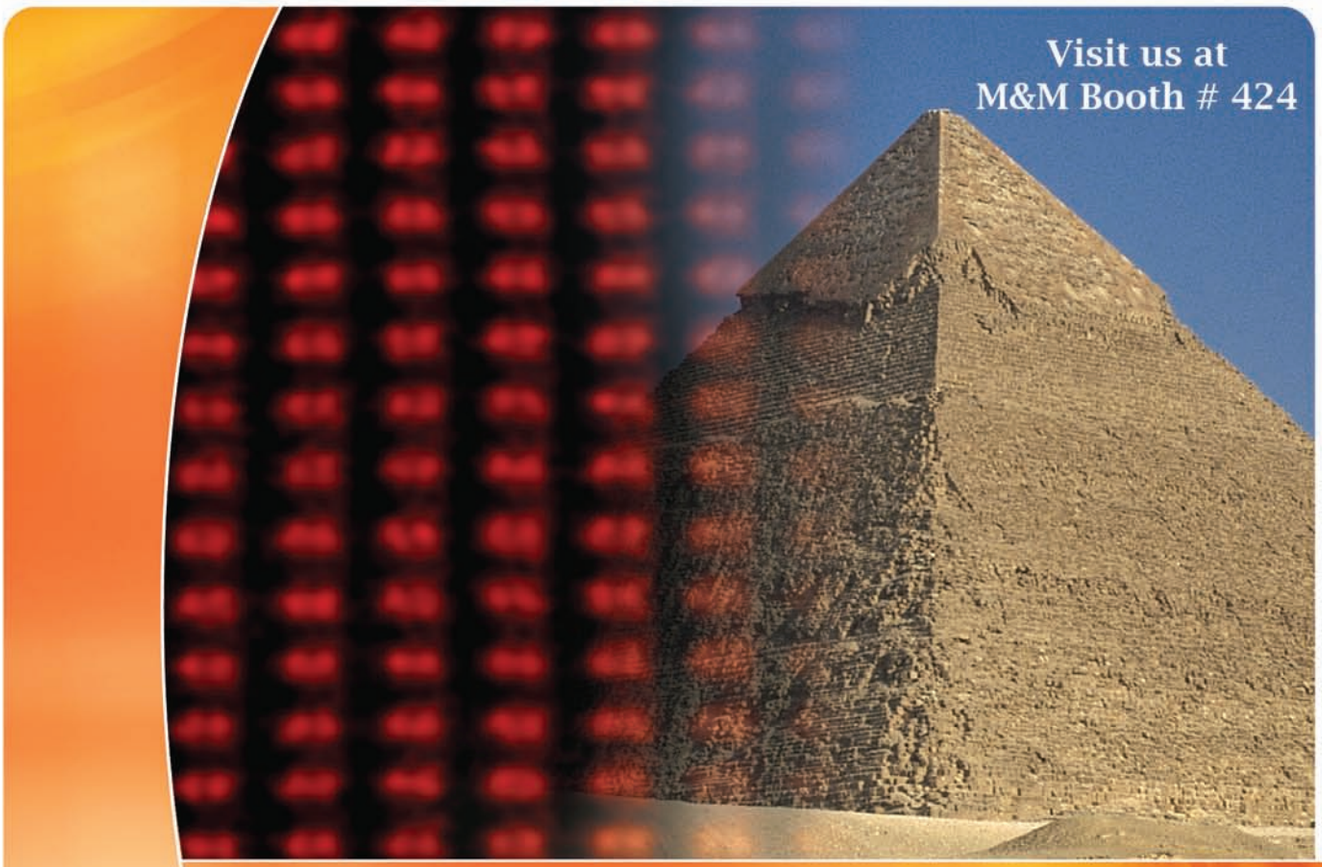
Imaging Results

Strengths of confocal scanning laser microscopy for imaging microbial aggregates include:

3D structural imaging with the potential to discriminate individual cells

A single fluorescent stain for either total or active cells applied to an untreated biofilm can produce the 3D images shown in Figures 2a and 2b respectively. Figure 2a is a shadow projection of a confocal stack of images taken of a *P. aeruginosa* (ATCC 15442) CDC biofilm stained with FM®1-43 (Molecular Probes/Invitrogen). FM ®1-43 has not been used extensively to stain biofilms, so it is not yet well understood as a biofilm probe. It is a lipophilic styryl dye, and it appears to bind only to cell membranes. Our data indicate that FM ®1-43 binds to all bacterial cells in a biofilm—dead or live—with very high specificity.

ABPitts.indd 1 06/20/2008 6:27:33 PM



Discovering Tomorrow's Wonders

Nanotechnology promises new generations of wonders for our world, impacting virtually every aspect of our lives.

Since 1966, Fischione Instruments has served the microscopy community with:

- **TEM/SEM specimen preparation instrumentation**
- **Imaging technology**
- **TEM specimen holders**

Whether you work in life sciences, physical sciences, or in nanotechnology, our products enable atomic-scale imaging and analysis for genuine insights into the properties and behavior of materials.

Customers worldwide depend on Fischione for innovation, quality, service, and flexibility. Our products support your creativity and give you a clear picture of how materials interact at the most fundamental level — the atomic level.

About the image: Sub-Angstrom image of rows of dumbbell-shaped Si atoms. The specimen was prepared with the Fischione Model 1010 Ion Mill. Information is present down to 0.6 Angstrom. Image courtesy of the Oak Ridge National Laboratory.

The Great Pyramid of Giza, Egypt, one of the wonders of the ancient world.

FISCHIONE INSTRUMENTS

9003 Corporate Circle, Export, PA 15632 USA • Tel: 1.724.325.5444 • www.fischione.com

EXCELLENCE...MAGNIFIED

MT Full Page Ad Master.indd 1 06/21/2008 9:35:00 AM

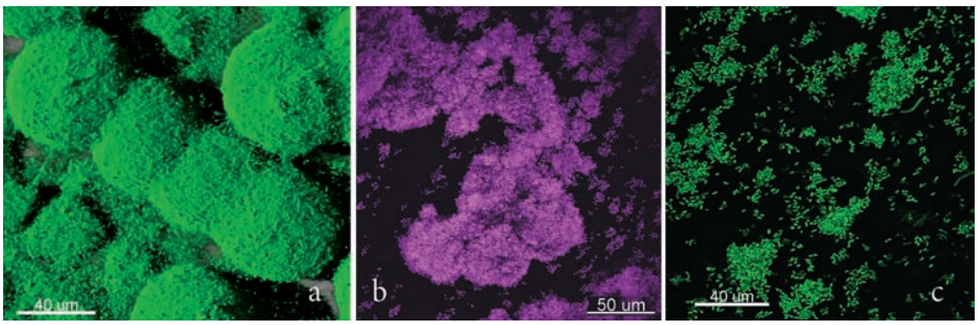


Figure 2 3-D structural imaging with the potential to discriminate individual cells. a) P. aeruginosa biofilm stained with FM ®1-43; b) S. epidermidis biofilm stained with Calcein violet AM; c) individual cells of an FM ®1-43-stained P. aeruginosa biofilm.

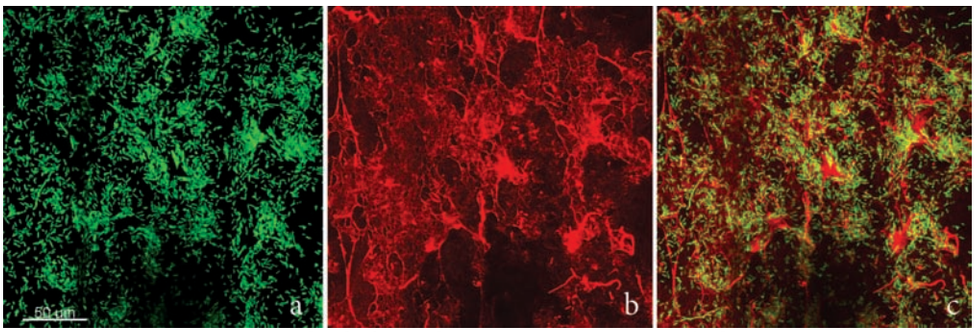


Figure 3 Discrimination of multiple specific constituents or activities. a) gfp-expressing P. aeruginosa cells; b) the biofilm matrix stained with Bodipy ®630/650-X, SE; c) the overlay of cell and matrix images.

Figure 2b is a shadow projection of an *S. epidermidis* CDC biofilm stained with Calcein violet AM (Molecular Probes/Invitrogen). CAM violet is a fluorogenic esterase substrate that passively diffuses into bacterial cells, is hydrolyzed by cellular esterase present in live cells, and is trapped in its fluorescent form inside the cell. The CAMs (available in green, red, violet or blue form) are often used as bacterial activity probes. CAM violet was imaged using the 2-photon confocal, with excitation at 785nm. This biofilm was not treated with an antimicrobial, so one would expect the majority of cells in the biofilm to be "live," as the staining indicates. Comparison of Figures 2a and b shows clear differences in morphology of pseudomonas biofilms compared to staph. The pseudomonas biofilm has a "haystack" cluster morphology characteristic of that strain, whereas the staph biofilm has a much denser structure, composed of tightly packed cells.

Figure 2c is a close-up of an FM® 1-43 stained *P. aeruginosa* biofilm showing individual cells. These images illustrate the range in visual scale possible with confocal microscopy of biofilms. Images 2a and b are on the scale of community assessment, where larger-scale effects such as disinfection and removal or the effect of fluid shear on biofilm structure can be monitored. In contrast, the ability to visualize single cells allows us the opportunity to monitor the state of individuals in the community. We can observe protein expression in individual cells or watch cells toggle between two physiological states as indicated by different fluorescence emission colors (Vlamakis et al, 2008).

Discrimination of multiple specific constituents or activities

For imaging purposes, biofilm biomass is often divided into three simplified categories: total bacterial cells, active cells, and EPS or matrix. A major challenge of research-relevant biofilm microscopy is to find fluorescent stains that can bind specifically to one of the three biofilm biomass components *and* also be used in concert with other specifically binding stains.

Two examples of dual staining are shown in Figures 3 and 4. Figure 3 is a confocal image of a *P. aeruginosa* PAO1 pMF230 capillary flow cell biofilm. The green and red channels are shown separately in panels 3a and 3b, and the overlay is shown in panel 3c. The *gfp*-expressing bacteria are green fluorescent, and the biofilm has been stained with red fluorescent Bodipy®630/650-X SE, which has bound to the matrix. Bodipy ®630/650-X SE is an amine-reactive dye that may adhere to the matrix or to the lipopolysaccharide capsule of different bacteria depending upon the state, the age of the biofilm, the species, or growth conditions. The biofilm matrix is notoriously difficult to stain. Because of this, panel a of Figure 3 might be considered a typical, straightforward image of a biofilm, and it is what we see in transmitted light images. It is the addition of the previously invisible structural components shown in panel b that hints at the complexity of biofilms.

Figure 4 is also a flow cell biofilm, but this time the bacterial strain is the inducible *gfp* pseudomonas construct PAO1 pAB1. In this experiment, the biofilm was treated with 20 mg/L chlorine for 1 hour, before inducer was added. The green fluorescence reveals biofilm bacteria that were still able to produce *gfp* after the chlorine treatment. Finally, the biofilm was counterstained with rhodamine B (red fluorescent), which should stain all cells, regardless of state. The layer of red fluorescence shows that cells on the periphery of the biofilm cluster were unable to produce *gfp* after chlorine exposure, or were dead, whereas the cells in the more protected center of the cluster were still able to produce protein, and would be considered live on the basis of this activity.

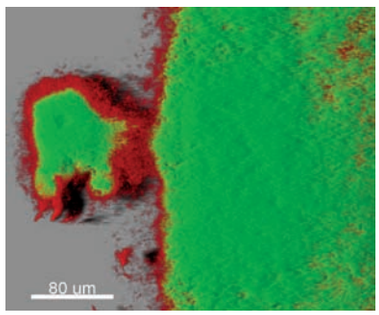


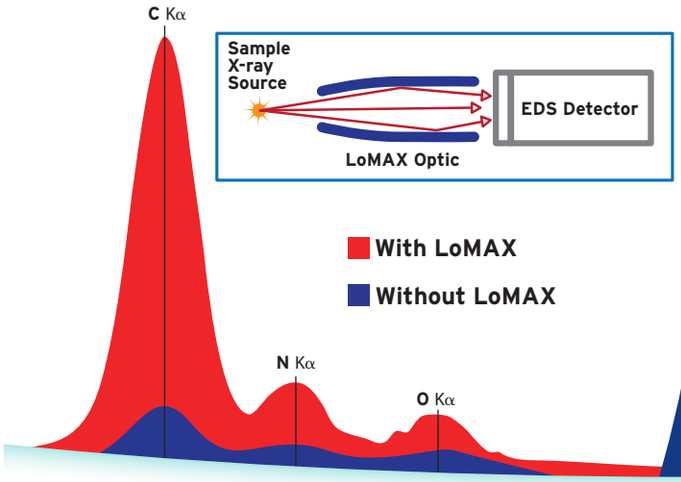
Figure 4 Imaging of antimicrobial efficacy. A P. aeruginosa biofilm, imaged after chlorine treatment, gfp induction, and counterstaining with rhodamine B (red). Green cells are still able to produce gfp, while the red cells are not.

Non-invasive time-lapse imaging

Using time-lapse confocal imaging, the action of an antimicrobial against a biofilm can be visualized in real time and then analyzed quantitatively. CAM green is a fluorogenic esterase substrate, like CAM violet discussed above, that is excited with a 488 nm laser and is viewed with a typical FITC emission bandwidth. CAM is trapped inside intact bacterial cells once it is hydrolyzed. If, however, the cell membrane is compromised by an antimicrobial agent such as chlorine or a quaternary ammonium compound, the fluorescent CAM will leak out. In this context, CAM becomes a probe for intact cells, or a means of separating live (green) and compromised or dead (not green) cells. We can record this entire process using time lapse imaging on the confocal: cell loading with CAM, application of the antimicrobial and loss of fluorescence.

ABPitts.indd 2 06/20/2008 6:27:34 PM

Let There Be Light (elements!)



Discover LoMAX™
Attachable low energy x-ray EDS optic

- Fast easy installation - detector safety guaranteed
- Adapts to most detector sizes
- Boosts sensitivity up to 15X for energies < 1000eV
- Quantitative analysis of Be, B, C, N, O, F
- Analyze heavier elements using x-ray lines below 1000ev

The new patented LoMAX low-energy x-ray optic enables your EDS to see and analyze both light and heavy elements with x-ray lines below 1000eV. LoMAX is both easy and safe to install and remove – it simply slides onto your EDS detector. It won't interfere with high-energy x-rays. With LoMAX you will 'See the Light' – x-rays that is.

LoMAX. See the Light.
Call 866.581-XRAY for more information.
www.parallaxray.com

US Patent #6,442,231 B1

Parallax™ RESEARCH



MT_Half over 2 qtr pg ads.indd 1 06/20/2008 6:57:31 PM

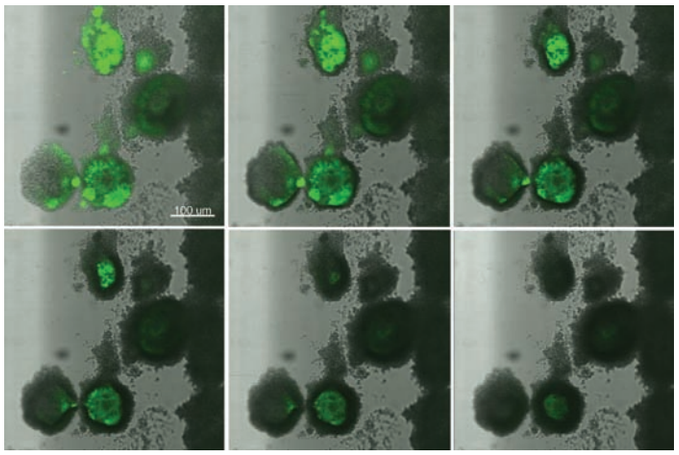


Figure 5 Non-invasive time-lapse imaging. The images in this panel are a series of overlays of transmission and fluorescence channels, beginning at the upper left, and ending at lower right. Biofilm clusters are stained with green fluorescent CAM, which leaks out of live cells during a 15 minute treatment with the mouthwash additive CPC.

Using image analysis we can measure the fluorescence intensity in a region in the biofilm throughout the time stack, calculate parameters such as penetration time and depth, and gain insight into differing modes of action for antimicrobial agents, as well as protective mechanisms exhibited by biofilms. A series of still images taken from such a time stack is shown in Figure 5a - f. Dental biofilm clusters attached to the ceiling of a capillary tube were imaged. The series shows an overlay of transmitted and fluorescence channels. It begins with the cells already loaded with CAM, and follows a 15 minute-long treatment under flow conditions with 0.05% cetylpyridinium chloride (CPC), a quaternary ammonium compound which is added to mouthwash and toothpaste. Over the 15 minute treatment time, CPC can be seen to work in through the outer layers of the biofilm, and a front of permeabilized, non-fluorescent cells moves in towards the center of the clusters. The region of more protected, still-fluorescent cells in the center of each cluster becomes progressively smaller as the CPC works its way in. It is important to note that this advancing edge of permeabilized cells is not a typical *spatio*-temporal pattern: not all treatments "chew" their way in to the center of a biofilm cluster. Some other antimicrobial agents tested affect cells throughout the entire cluster nearly simultaneously.

Evolution of 3D structures in time

The final example of a successful application of fluorescent confocal microscopy to biofilms is that of utilizing *xyz* scans over time. In this research, *P. aeruginosa* PAO1 pMF230*cfp* and PAO1 pMF230*yfp* were grown together in a capillary flow cell. The two-color system allowed microcolonies of the same strain to be identified and imaged early on, then followed through the development process to a mature biofilm. Figure 6 shows a series of *xyz* confocal stacks collected over a period of 72 hours, as a cyan cluster grows and expands in a predominantly yellow fluorescent field. This kind of imaging provides unique insight into community organization and development.

Limitations of confocal laser microscopy for imaging microbial biofilms

While confocal laser microscopy holds great potential for revealing the complexities of biofilm structure and behavior, there are also a number of limitations that we have encountered. These are listed briefly below.

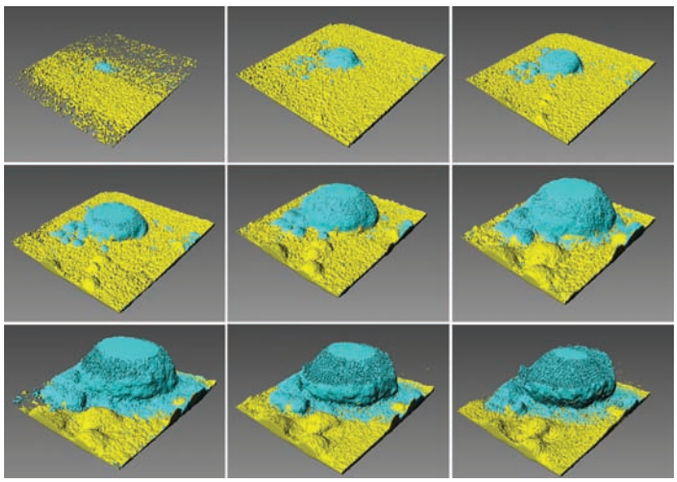


Figure 6 Evolution of 3-D structures in time. Time-lapse series showing xyz scans of a two-color P. aeruginosa biofilm (cfp and yfp) as it develops over 72 hours.

- Light is attenuated by the biofilm, limiting the depth of imaging to approximately 50 to 100 microns, depending upon the opacity of the biofilm.
- Individual cells are often only discernable at the surface of the biofilm or in areas where the biofilm is sparse. Within dense cell clusters, it usually becomes impossible to resolve individual cells.
- Tapping the potential to measure specific chemical and biological properties depends upon the availability of appropriate fluorescent probes (*i.e.*, component-specific probes) and the ability to cleanly separate emission signals.

Conclusions

Confocal imaging has become a critical aspect of biofilm research. Fluorescent stains, probes and reporter genes, used with a system designed for imaging provide the opportunity for creative and relevant research to elucidate biofilms. The information obtainable by these techniques has been valuable for discovering fundamental characteristics of biofilms, and has also provided useful insights for industry, such as visualizing in real time, and the action of specific antimicrobials. There is plenty of room and tremendous need for further exploration of fluorescent stains and combinations of stains that have not previously been applied to biofilm imaging. ■

Acknowledgements

In addition to the authors, the following people contributed research and images: Audrey Corbin, Ben Klayman, Amber Harrer and Ellen Swogger. Thank you to them and to Diane Gray at Molecular Probes/Invitrogen and to Peg Dirckx for their assistance and collaboration.

References

ASTM E2562-07 Standard Test Method for Quantification of *Pseudomonas aeruginosa* Biofilm Grown with High Shear and Continuous Flow using CDC Biofilm Reactor

Goeres, D.M., Loetterle, L.R., Hamilton, M.A., Murga, R., Kirby, D.W., and Donlan, R.M. 2005. *Statistical assessment of a laboratory method for growing biofilms*. Microbiology. 151: 757-762.

Werner, E., F. Roe, A. Bugnicourt, M.J. Franklin, A. Heydorn, S. Molin, B. Pitts, and P.S. Stewart, "*Stratified Growth in* Pseudomonas aeruginosa *Biofilms*," Appl. Environ. Microbiol., 70(10):6188-6196 (2004)

Vlamakis H., Aguilar C., Losick R., Kolter R., "*Control of cell fate by the formation of an architecturally complex bacterial community,*" Genes Dev. 2008 Apr 1;22(7):945-53.

ABPitts.indd 3 06/20/2008 6:27:35 PM

MIRA\\ Schottky FE-SEM

Value and Excellence in SEMs



www.tescan.com

- Wide Field Optics™
- In-Flight Beam Tracing™
- In-Beam Detector
- Active Vibration Isolation

All as Tescan standard for the highest-quality imaging

Find out more at M&M 2008
Booth 330

TESCAN
PERFORMANCE IN NANOSPACE

Tescan USA Inc.
Web: www.tescan-usa.com
Email: info@tescan-usa.com
Tel: 724-772-7433

MT Full Page Ad Master.indd 1 06/21/2008 9:53:51 AM

Extreme High-Resolution SEM: A Paradigm Shift

Richard Young*, Todd Templeton*, Laurent Roussel**, Ingo Gestmann**, Gerard van Veen**, Trevor Dingle** and Sander Henstra**

*FEI Company, *Hillsboro, OR and **Eindhoven, The Netherlands*

Richard.young@fei.com

"Extreme high-resolution" (XHR) scanning electron microscopy (SEM) has the potential to change the way we look at SEM. Anyone in the SEM world knows that you don't do high-resolution SEM at low accelerating voltages because of chromatic aberration limitations. The XHR design offers a new way to deal with chromatic aberration and realize the huge benefit of reduced beam penetration.

The new Magellan 400 SEM family is the first to offer sub-nanometer resolution over the entire electron energy range from 1 keV to 30 keV, effectively establishing a new performance category known as XHR SEM (Figure 1). To achieve this unprecedented performance, the Magellan combines novel electron optical design elements with technologies developed for the industry-leading Titan (scanning) transmission electron microscope (S/TEM) and DualBeam (focused ion /SEM) platforms.

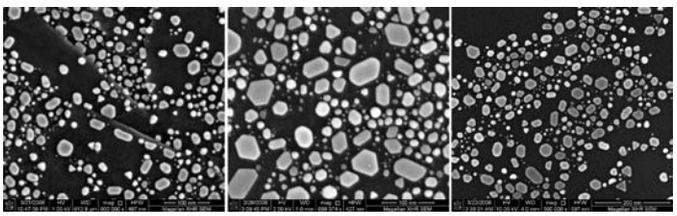


Figure1: Gold on carbon, the original images were analyzed for resolution confirming <0.9 nm @1 kV (a), <0.8 nm@2 kV (b), <0.8 nm@ 10 kV (c). Horizontal field widths (HFW): 500, 430, 600 nm respectively.

Unique Capability

The system's extraordinary low-voltage performance provides high-resolution, surface-specific information that is simply unavailable from other techniques. Although SEM is considered a surface imaging technique, it would be more accurately called near-surface since the signals it uses may originate as much as a micrometer below the surface, depending upon the beam energy used. S/TEM images, in contrast, are projections presenting information generated as the 200-300 kV electrons travel through a thin section. They can reveal detailed internal structure at atomic resolution, and in some cases, using advanced three-dimensional (3D) tomography reconstruction techniques, some detail about internal surfaces and interfaces. The XHR SEM's low-voltage capabilities allow it to provide exquisitely-detailed images of complex 3D surfaces that are difficult or impossible to obtain any other way.

XHR Applications

A key driver for the development of the XHR SEM came from the semiconductor market. Whether for research, process development, process control, or for failure analysis, semiconductor device manufacturers have made heavy use of SEMs throughout the history of their industry. With new processes being introduced at design rules of 45 nm and below, the drive for high-resolution information of their ever smaller layers and structures pushes them in two main directions – lower beam energies in the SEM (to allow for more surface sensitive imaging) and to more S/TEM analysis. Each technique has its own benefits – SEM generally has simpler sample preparation, and lends itself to high-throughput imaging of cleaved sections and of complex 3D surfaces, while S/TEM offers atomic level imaging and chemical analysis, unmatched by SEM, but requires much more sample preparation and is not well suited to inspecting 3D surface features. Therefore, it is to be expected that both XHR SEM and S/TEM will become more prevalent and critical with the progression to each new, smaller technology node.

Figure 2 shows an XHR SEM application, where a deprocessed sample has been stripped back to the poly-silicon level. Here the benefits of using XHR SEM to inspect the complex 3D surfaces created are apparent – the sample can be navigated around at lower magnification (Fig. 2a) and then areas of interest can be zoomed into (Fig. 2b and c) to observe the intersection of various layers. The flexibility of the XHR SEM to tilt and rotate enables multiple viewpoints to be used. With the advent of FIN-FET and similar 3D gate structures in future nodes, these kinds of needs will only increase. Similarly, SEMs have historically been used to inspect multiple cleaved samples in cross-section, or image samples top down (Fig. 3). To achieve the throughput needed for these applications, it is important to be able to mount multiple samples into the system and to avoid having to perform excessive sample preparation just to make the sample small enough to fit onto the stage.

Just as semiconductor and data storage manufacturers are well into the nanotechnology realm, the research community is also driven by a need for new ways to investigate nanoscale materials, such as nanoparticles (Fig. 4), nanowires and nanotubes, interfaces between materials, and details of surface processes. XHR SEM offers new and different information that is often complementary to that obtained by S/TEM, atomic force microscopy (AFM), atom probes and other high-resolution analytical techniques.

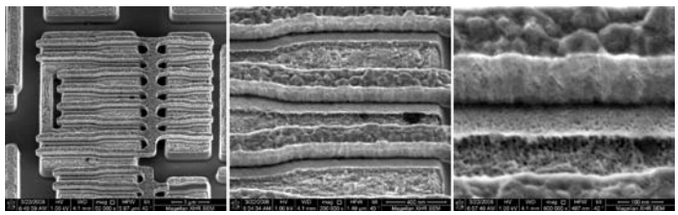


Figure 2: This series of images at increasing magnification demonstrates the Magellan's ability to capture detailed information from complex 3D surfaces at longer, analytical working distances. Smallest HFW: 500 nm.

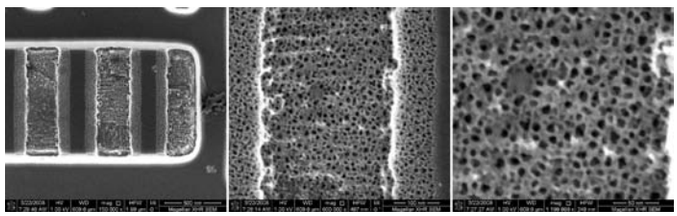


Figure 3: This magnification series, taken from a top down perspective, demonstrates excellent resolution at 1 kV at magnifications impossible on current SEMs. Smallest HFW: 250 nm.

Low Voltage Performance

Resolution in an SEM is controlled ultimately by the size of the excitation volume from which the imaged signal originates. This, in turn, is determined by the size of the spot formed where the beam intersects the sample surface, and the distance beam electrons penetrate into the sample as they spend their energy in signal-generating interactions with local atoms. Beam penetration is easily reduced by decreasing beam energy (Fig. 5), but in a conventional SEM, the

ABYoung.indd 1 06/21/2008 10:01:00 AM

FEI COMPANY™
TOOLS FOR NANOTECH

Explore Further.

In 1989, FEI introduced the world's first ESEM™ Environmental SEM.

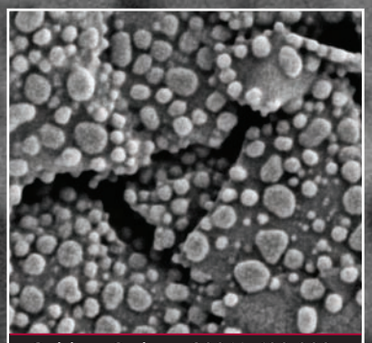
In 1993, FEI introduced the world's first DualBeam™ FIB/SEM.

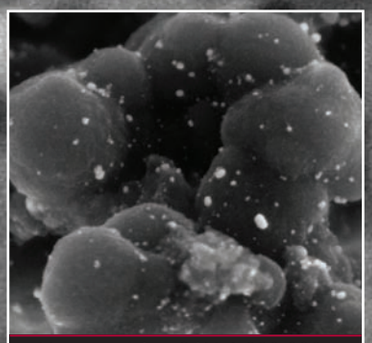
In 2005, FEI introduced the Titan™ TEM, the world's most powerful commercially-available electron microscope.

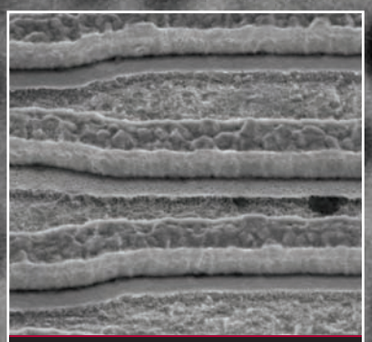
Now, FEI introduces the Magellan™ family, the world's first Extreme High Resolution SEMs.

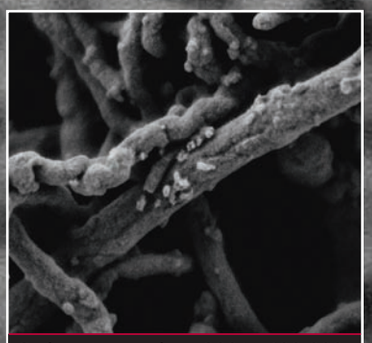
Prepare to see things you've never seen before. Visit FEI Company at Microscopy and Microanalysis and learn how you can explore further with this new class of XHR SEM.

See more at fei.com/magellan


Gold on Carbon: 200 V; 600,000x

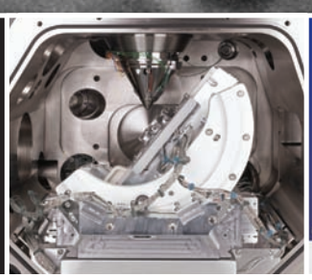

Nanoparticles: 2 kV, 1,000,000x


Logic Device: 1 kV, 200,000x


Carbon Nanotubes: 200 V, 600,000x

Background image: logic device, 1 kV, 1,200,000x. Logic device images courtesy of ST Microelectronics, Malta/Grenoble. Carbon nanotube image courtesy of Professor Raynald Gauvin and Camille Probst, Ph.D. student, McGill University.

©2008 FEI Company. All trademarks are the property of their respective owners.





FEI Company
Booth 528
Microscopy and Microanalysis
Albuquerque, NM

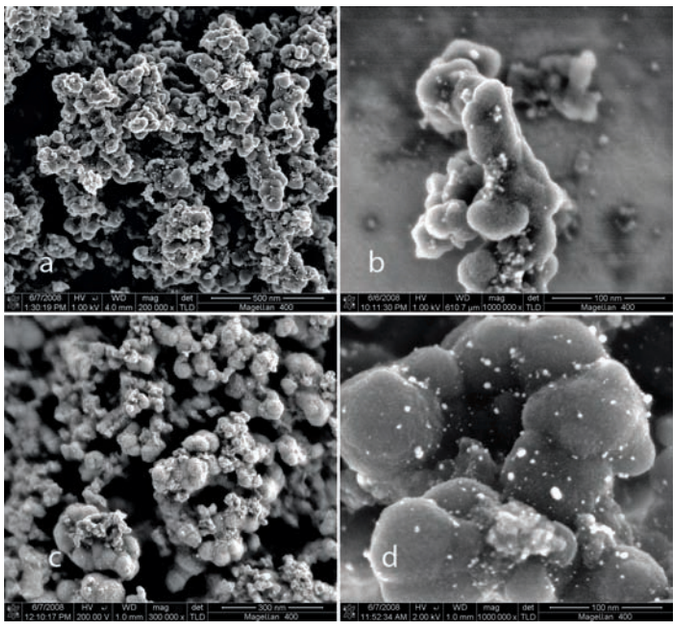


Figure 4: This series of images illustrate the XHR SEM capabilities of the Magellan on Pt catalyst nanoparticles. Magellan allows the jump from traditional UHR magnifications (a) to a million plus magnification (b) at 1kV, where individual nanoparticles are nicely visible. Highly-resolved images are obtained both at very low energies for highly sensitive surface information (c), and very balanced material and topographic information (d).

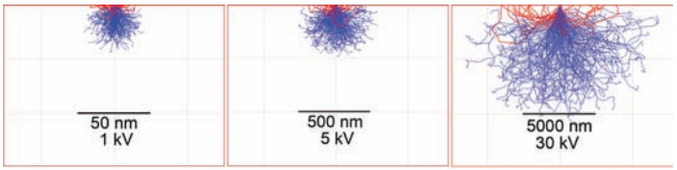


Figure 5: Monte Carlo simulations of electron scattering illustrate the effect of beam energy on interaction volume (the primary electrons are shown in blue, with back-scattered electrons in red)[1]. The effect of interaction volume on resolution depends on many factors, such as the signal chosen for imaging. For example, although the secondary electron signal usually selected for high-resolution imaging originates primarily from within the beam spot, its resolution is degraded by contributions from type II secondary electrons that are created when backscattered beam electrons exit the specimen surface and may originate from a much larger region roughly corresponding to the size of the interaction volume.

gain from reduced penetration is negated by increased spot size at beam energies below a few keV.

The deterioration in spot size at low energy results from chromatic aberration in the lenses used to focus the electron beam [2]. It causes electrons of different energies to focus at different distances—entirely reasonable since the focusing force exerted on the electron by the magnetic field of the lens is directly proportional to the electron's velocity. The effect of chromatic aberration on spot size is determined by the fractional energy spread—a measure of the variability among individual electron energies relative to overall beam energy. Even a few eV of variability has relatively little effect on the trajectories followed by 30 keV electrons through the magnetic field of the focusing lens. But the same level of variability becomes increasingly significant as beam energy decreases, eventually limiting the minimum size of the spot into which the electrons can be focused when balanced against the beam diameter resulting from diffraction through the beam limiting aperture.

The tremendous potential for improved performance over a broad range of SEM applications that would accrue from a breakthrough in low-voltage resolution became a primary driver in the Magellan development program, and is a cornerstone in the definition of the new XHR performance category the system has established.

The system's low-voltage solution begins with fundamental choices about the lens configuration and electron source. The adverse effects of chromatic aberration can be reduced by decreasing the focal length of the lens (for an electromagnetic lens that means increasing the lens current / field strength / optical power). In a typical, conically shaped SEM objective lens, the focusing field lies enclosed within the lens and the minimum usable focal length corresponds to the minimum distance from the pointed tip of the lens to the specimen. This distance defines the minimum focal length at which the lens can operate (*i.e.* the closest the specimen can come to the field) SEM objective lens performance is physically limited by the construction of the lens. An SEM optimized for low voltage performance needs to be able to operate at the shortest possible focal length. Generally, this requires a type of lens known as an immersion lens: the sample is immersed in the lens field, which is external to the lens structure. A variety of lens designs are in use, some of which can be operated in either conventional or immersion mode. It is important that the lens assembly does not restrict the flexibility and broad applicability that are fundamental to SEM's enduring value and popularity. The XHR SEM combines immersion capability with a highly flexible lens and chamber configuration that still allows for large or multiple samples, and a wide range of sample tilt angles.

The choice of electron source also affects low-voltage performance. For example, a Schottky field emission source provides a fivefold reduction in energy spread (0.6 – 1.0 eV) compared to a tungsten filament, as well as an immediate and commensurate reduction in the minimum useful accelerating voltage (where chromatic aberration begins to limit performance) to a few hundred volts. Cold-field emitters have an even narrower energy distribution (0.25-0.35 eV) but that benefit is offset by their instability, limited current capacity, high-vacuum requirements, vulnerability to contamination, and need for frequent "flashing" to restore the condition of the emitter tip.

The most innovative aspect of the electron column is its patented UniColore (UC) technology. In UC mode the beam is energy dispersed and focused through a small aperture that eliminates the most extreme components of the energy distribution, resulting in a beam with an energy spread of less than 0.2 eV. Figure 6 shows a schematic representation of how an improved energy spread in UC mode is balanced against diffrac-

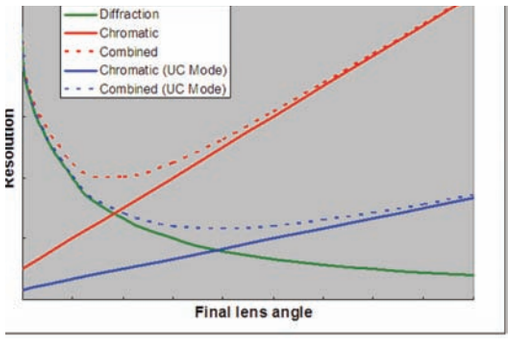


Figure 6: Low voltage spot size is limited primarily by diffraction and chromatic aberration. This schematic figure illustrates the effect on this balance of reducing the energy spread by using UC mode. The minimum spot size is reduced and occurs at a larger lens angle (larger aperture/more beam current). Note: the scales of both axes are linear, with arbitrary units.

ABYoung.indd 2 06/21/2008 10:01:01 AM

COLLEGE OF MICROSCOPY

Learn from experience... learn from the experts.



Raman Microspectroscopy Course

COM610

October 7-9, 2008

Infrared Microscopy Course

COM600

November 4-6, 2008

Learn from McCrone scientists with over 50 years of combined experience.

The College of Microscopy courses in Infrared and Raman Microscopy are designed to provide practical instruction in "real world" use of the FTIR and Raman microscopes. The classes utilize demonstrations and laboratory exercises supplemented with lectures. Students are strongly encouraged to bring their own samples for analysis.



Gretchen—Senior Research Chemist with McCrone Associates since 1995, Ph.D. in Archaeological Chemistry from the University of London, with a fellowship at the Metropolitan Museum of Art, she is responsible for chemical analysis using infrared spectroscopy, Raman microspectroscopy, gas and liquid chromatography, polarized light microscopy and microchemical techniques. She has problem-solving experience in a wide variety of industries including pharmaceutical, paints and coatings, electronics, forensics, polymers and metals.

Kate—Ph.D. in Physical Chemistry from Loyola University of Chicago, with McCrone Associates since 2004, employs infrared and Raman spectroscopy, gas and liquid chromatography, light microscopy and wet chemical methods in the course of analytical problem-solving for a wide variety of clients. At Unilever/Helene Curtis, Inc. she used spectroscopic techniques to support product claims, conduct ex-vivo and in-vivo performance testing; and assist manufacturing facilities in the development and production aspects of a variety of personal care products.





Kristie—Research Microscopist with McCrone Associates since 1998, at Rush University Medical Center in Chicago she gained microscopy experience in a cancer research laboratory and was certified as a Medical Technologist in Immunology. Current work involves microscopical analysis of particles in micrometer and sub-micrometer size ranges including: manipulation, characterization and preparation for instrumental ultramicroanalysis. Current research interests have focused on glass delamination in pharmaceutical products.

Mary—M.S., Analytical Chemistry, Loyola University, Chicago, 20 years of consulting and analytical service experience with particular specialization in plastic and polymer analysis, and currently a Senior Research Chemist at McCrone Associates. Served as VP of Analytical Services for Bodycote Broutman, Inc., a consulting company specializing in contract testing and R&D for the plastics industry.



Register today—www.collegeofmicroscopy.com *College of Microscopy, 850 Pasquinelli Drive, Westmont, IL 60559, 630-887-7100*

MT Full Page Ad Master.indd 1 06/21/2008 10:14:42 AM

tion to produce improved beam resolution. In addition to enabling reductions in spot size, UC mode also reduces the intensity of the beam "tails", further enhancing contrast and image quality. The abundant current delivered by the Schottky emitter and the efficient design of the gun ensure ample current in UC mode for the high resolution imaging applications it is intended to support. Ultimately, UC mode results in a beam that has an energy spread less than that of a cold field emitter but still retains the robust stability and other benefits of the Schottky source. In addition, UC mode is implemented as a simple push button operation and so its benefits are gained without the complexity of aberration correctors or similar approaches to performance improvement [3]. In high-current applications, UC mode is automatically switched off, instantly restoring the gun to its normal operating capability.

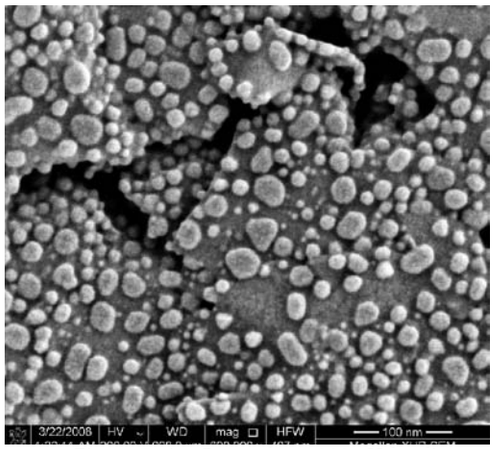


Figure 7: Au-C sample at 200 eV landing energy using 1 kV of beam deceleration. Under these conditions the Au and C contrast levels are similar to each other, quite different from the result normally seen at 1 kV accelerating voltages and above (see text for more details).

Traditional SEM Capability

While extending SEM imaging capability into the XHR realm, the Magellan sacrifices none of the traditional advantages of SEM in speed, flexibility, ease-of-use, minimal sample preparation, analytical capability, prototyping and much more. Its large specimen chamber easily accommodates a fully-automated 5-axis stage offering 0.5 µm precision over 100 mm of *x/y* travel. The accuracy of the stage's piezoceramic drives is a critical component of the eucentric tilt capability, allowing users to explore different viewing perspectives quickly without losing sight of the object. Its electrostatic scanning is fast and accurate at all beam currents and accelerating voltages and eliminates the hysteresis inherent in scanning coils. Provision for a beam blanker at a fixed cross over position enables fast blanking without tailing or streaking for lithographic and nanoprototyping applications.

A variety of detectors is available to support complex imaging operations. Secondary detection for topographic contrast and high-resolution applications is provided by an in-chamber Everhart-Thornley detector and a highly efficient in-lens detector. An in-lens backscatter mode and a solid state backscattered electron detector mounted under the pole piece provide compositional (*z*-contrast) imaging. A unique low voltage, high contrast detector (vCD) designed to increase detection efficiency for the low-energy backscattered electron generated by low-voltage microscopy is particularly useful in conjunction with beam deceleration to tune image contrast for specific applications.

Beam deceleration, which applies a negative bias to the specimen, permits imaging with beam landing energies (accelerating voltage minus decelerating voltage) as low as 50 eV. The deceleration field acts as an additional electrostatic lens, reducing spot size further – with the improvement in spot performance becoming greater as the landing energy is reduced [4]. The decelerating bias can also be used to enhance and manipulate image contrast by accelerating secondary and backscattered electrons toward the vCD detector.

Figure 7 shows an Au-on-C image taken using UC mode at a beam landing energy of 200 eV (1 kV of beam deceleration). It is observed that at 200 eV the gold and carbon contrast levels are much more similar to each other than is the case at 1 keV and above (compare to Fig. 1, where the gold signal is much greater than the carbon one). This change in contrast hints at the valuable image information that can be obtained by observing the same sample under a variety of beam energy conditions at high resolution.

The best optical design in the world cannot deliver its promised performance unless the supporting platform provides sufficient internal stability and resistance to external interferences. As the maker of Titan TEMs, the world's most powerful commercially-available microscopes, FEI probably understands these platform requirements better than most. In fact, the Magellan uses the same constant power lens technology developed for the Titan TEM, which permits changes in the electron optical power of the lens without changing the power dissipation of the lens, a change that might otherwise bring work to a halt while the system came to a new thermal equilibrium. Electron microscopes can be exquisitely sensitive vibration detectors and the most solid column in the world is worth little if the stage and sample are dancing around beneath it. The system's 5-axis piezoceramic stage combines rock solid stability with 0.5 micrometer positioning precision over 100 mm of travel. The column is also double shielded to reduce the effects of external sources of electromagnetic radiation on the electron beam.

The new XHR SEM is designed for optimal throughput and productivity with an optional automated loadlock. The large stage and flexible sample holders can accommodate up to 40 cleaved cross section samples at a time. An integrated plasma cleaner and liquid nitrogen cold trap maintain pristine conditions in the sample chamber and reduce the effects of sample generated contamination on image quality.

Conclusion

XHR SEM takes current high-resolution SEM applications and pushes them into a new regime of sub-nm resolution at low beam energies. For semiconductor and data storage manufacturers, this means continuing to use SEM for more node shrinks than was previous thought possible. For the researcher, it opens up exciting imaging possibilities for nanoscale structures, providing new and complementary information to that obtained by S/TEM, AFM and similar techniques. ■

References

[1] Casino Software: http://www.gel.usherbrooke.ca/casino/
[2] See for example: J. Goldstein et al, Scanning Electron Microscopy and X-Ray Microanalysis.,Third Edition. 2003, New York: Plenum.
[3] A. Braun, Semiconductor International (December 2007)
[4] I. Müllerová et al, *Surface Science* 601 (2007) 4768

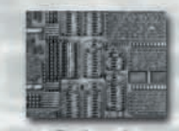
Acknowledgements

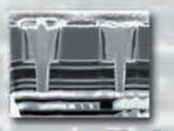
The authors gratefully acknowledge the support of the Smart Mix Programme of the Netherlands Ministry of Economic Affairs and the Netherlands Ministry of Education, Culture and Science. Samples shown in Figs. 2 and 3 are courtesy of STMicroelectronics Malta/Grenoble.

ABYoung.indd 3 06/21/2008 10:01:02 AM

Polishing Matters!

Flat Lapping & Polishing


De-layering


Cross-section FIB-edit



- Optical alignment makes flatness set-up fast & accurate
- Wide range of sample holders
- All polishing methods

ULTRAPOL Advance



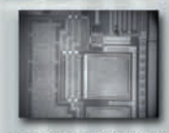
SEM & FIB STUB HOLDERS
Available for most microscopes



Selected Area Preparation

- Cavity milling - leaves outside circuits & structures intact
- Optical alignment
- Decap, grind, lap, & polish with one machine

ASAP-I


Backside Polishing


Decapsulation


Thin Films
(Courtesy of FIBICS, Inc.)

ULTRA TEC
MANUFACTURING, INC

Toll Free (US) 1-877-542-0609
Tel: 1-714-542-0608 Fax: 1-714-542-0627
E-mail: info@ultratecusa.com
www.ultratecusa.com

Need EM Equipment?

Come to the Experts.

Alicona
Micro-Materials
Hitachi High-Tech
Gatan Omniprobe Xenos EBS
Left Coast Instruments
Imago Millbrook
XEI Scientific, Inc.

Angstrom Scientific has partnered with leading manufacturers to deliver the right EM equipment solution for your application.

- Represents leading manufacturers
- Supports the Eastern US and Canada
- Offers over 40 years of experience and market knowledge

Need east coast representation?
Have Angstrom Scientific grow your business.

Angstrom Scientific Inc.

Angstrom Scientific, Inc.
(201)-760-2524
Info@angstrom.us
www.angstrom.us

Need Used EM Equipment?

Come to the Experts.

SEM
Dual Beam FIB
STEM FESEM
Single Beam FIB
TEM

Whether you're looking to buy used EM equipment or have used equipment to sell, Angstrom Scientific is your source.

- Turnkey installation that is guaranteed operational
- All major SEM, TEM, STEM and FIB brands
- 40 years of experience and market knowledge

See our current inventory of used EM equipment at
www.angstrom.us

Angstrom Scientific Inc.

Angstrom Scientific, Inc.
(201)-760-2524
Info@angstrom.us
www.angstrom.us

MT_Half over 2 qtr pg ads.indd 1 06/21/2008 10:40:41 AM

Testing Parameters for Two-Dimensional Crystallization and Electron Crystallography on Eukaryotic Membrane Proteins with Liposomes as Controls

Gengxiang Zhao[a], Vasantha Mutucumarana[b], Darrel W. Stafford[b], Yoshihide Kanaoka[c], K. Frank Austen[c] and Ingeborg Schmidt-Krey[a]

[a]*Georgia Institute of Technology, School of Biology, School of Chemistry and Biochemistry, Atlanta, GA*

[b] *The University of North Carolina, Dept. of Biology and Center for Thrombosis and Hemostasis, Chapel Hill, North Carolina*

[c]*Dept. of Medicine, Harvard Medical School and Division of Rheumatology, Immunology and Allergy, Brigham and Women's Boston, MA*

Ingeborg.Schmidt-Krey@biology.gatech.edu

Membrane proteins comprise the majority of known and potential drug targets, yet have been immensely difficult to analyze at the structural level due to their location in the membrane bilayer. Removal from the membrane necessitates replacement of the phospholipid bilayer by detergents in order to maintain protein solubility. However, the absence of lipids and the presence of detergents can render non-physiological conformational changes of the membrane protein (Tate, 2006). Electron crystallography is an important method for studying membrane proteins that usually takes advantage of reconstituting the protein in a phospholipid bilayer and removal of the detergent. Richard Henderson and Nigel Unwin used this technique to elucidate the three-dimensional (3D) arrangement of the transmembrane α-helices of bacteriorhodopsin, which was the first 3D structural information on a membrane protein (Henderson and Unwin, 1975). In recent years, electron crystallography was used to study a significant number of proteins at the atomic level (Henderson *et al.*, 1990; Kühlbrandt *et al.*, 1994; Nogales *et al.*, 1998; Murata *et al.*, 2000; Ren *et al.*, 2001; Löwe *et al.*, 2001; Miyazawa *et al.*, 2003; Gonen *et al.*, 2005; Hiroaki *et al.*, 2006; Holm *et al.*, 2006).

Electron crystallography of membrane proteins involves electron cryo-microscopy (cryo-EM) and image processing techniques (Amos *et al.*, 1982) that can now fairly routinely yield high quality structural information. The main limiting factors in using this method to study membrane protein structures are two-fold: (1) the production of large, highly ordered two-dimensional (2D) crystals and (2) screening for these 2D crystals (Kühlbrandt, 1992; Schmidt-Krey, 2007). Two-dimensional crystallization of membrane proteins by dialysis is comparable to reconstitution of solubilized membrane proteins for biochemical experiments (Fig. 1), except for the objective in 2D crystallization of having the largest possible amount of protein in the phospholipid bilayer. The protein-detergent mixture is combined with a lipid-detergent mixture, which is then dialysed against detergent-free buffer. Under ideal conditions, the membrane proteins form 2D crystals in each or most of the proteoliposomes.

Screening for crystals requires careful evaluation of the specimen so as not to miss the crystals, which can initially be small, sometimes only several unit cells, and few in number. Efforts in a number of laboratories are beginning to contribute major advances towards high-throughput screening (Cheng *et al.*, 2007; Nakamura *et al.*, 2003; Vink *et al.*, 2007) and equipment for controlled, large-scale crystallization (Engel *et al.*, 1988) as well as image processing (Gipson *et al.*, 2007). Little, however, is known about the parameters that influence crystal formation. This type of information could greatly reduce the required time and effort in this crucial step towards not only obtaining structural data on membrane proteins, but would also provide invaluable information for the design of automated and large-scale trials. Yet general conclusions on 2D crystallization conditions will require the accumulation of information from a large number of individual crystallization trials. Engel and coworkers have provided a particularly sizable and helpful contribution in documenting their findings over the years (Stahlberg *et al.*, 2001; Werten *et al.*, 2002).

Crystallization conditions for two eukaryotic membrane proteins with known crystallization conditions were further tested with the long-term aim of providing additional data for generalizing 2D crystallization screening. These proteins, human vitamin K-dependent γ-glutamyl carboxylase (Schmidt-Krey *et al.*, 2007) and human leukotriene C_4 synthase (LTC_4S), represent different hydrophobicities and detergents necessary for reconstitution. The carboxylase is predicted to have a large hydrophilic domain and is solublized in CHAPS (3-[(3-Cholamidopropyl) dimethylammonio]-1-propanesulfonate), while LTC_4S is mainly hydrophobic and purified in Triton X-100. The detergents are subsequently removed by dialysis and substituted by dimyristoyl phosphatidylcholine (DMPC) to form 2D crystals under controlled conditions. Parameters such as temperature, salt, glycerol, length of dialysis, lipid-to-protein ratio (LPR) and detergent concentration have been tested. Now identical buffer conditions with and without protein were used to examine the influence of the presence of proteins on the membrane size and morphology and whether

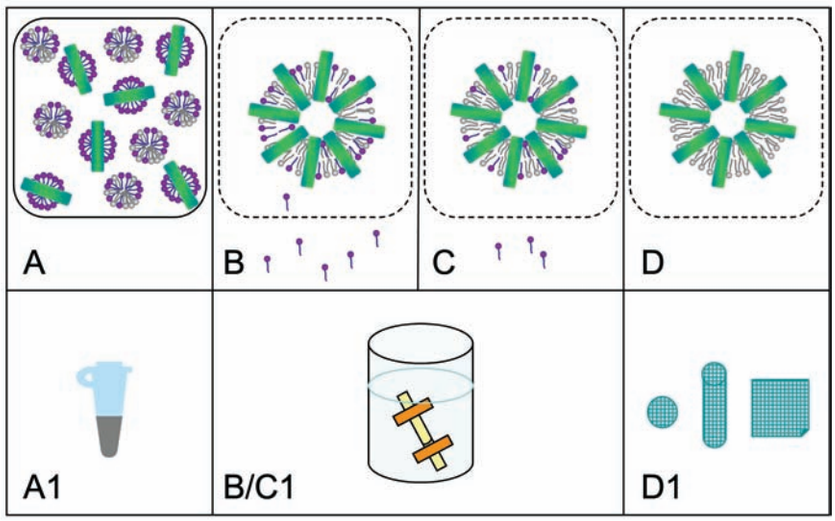


Figure 1. Schematic representation of 2D crystallization of membrane proteins by dialysis. In Figures A and A1 the purified and detergent-solubilized membrane protein is mixed with lipid-detergent micelles. The protein is depicted in green, the detergent in purple, and the lipid in grey. Figures B, C and B/C1 illustrate the detergent removal by dialysis against detergent-free buffer. After dialysis, the protein is reconstituted (D). Under the optimal conditions, 2D crystals form. These usually have a distinctive membrane morphology such as vesicles, planar-tubular, or sheet-like (D1, left to right). Mixtures of the morphologies are also frequently observed.

ABZhao.indd 1 06/21/2008 11:02:14 AM

Let 4pi take you beyond the capability of any SEM/STEM on the market with

RevolutionEDX™

X-ray Microanalysis Systems

Save time and production costs with 4pi's unique features

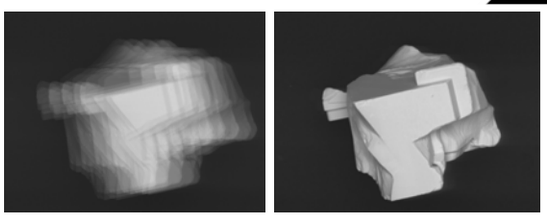
Features available exclusively from 4pi:

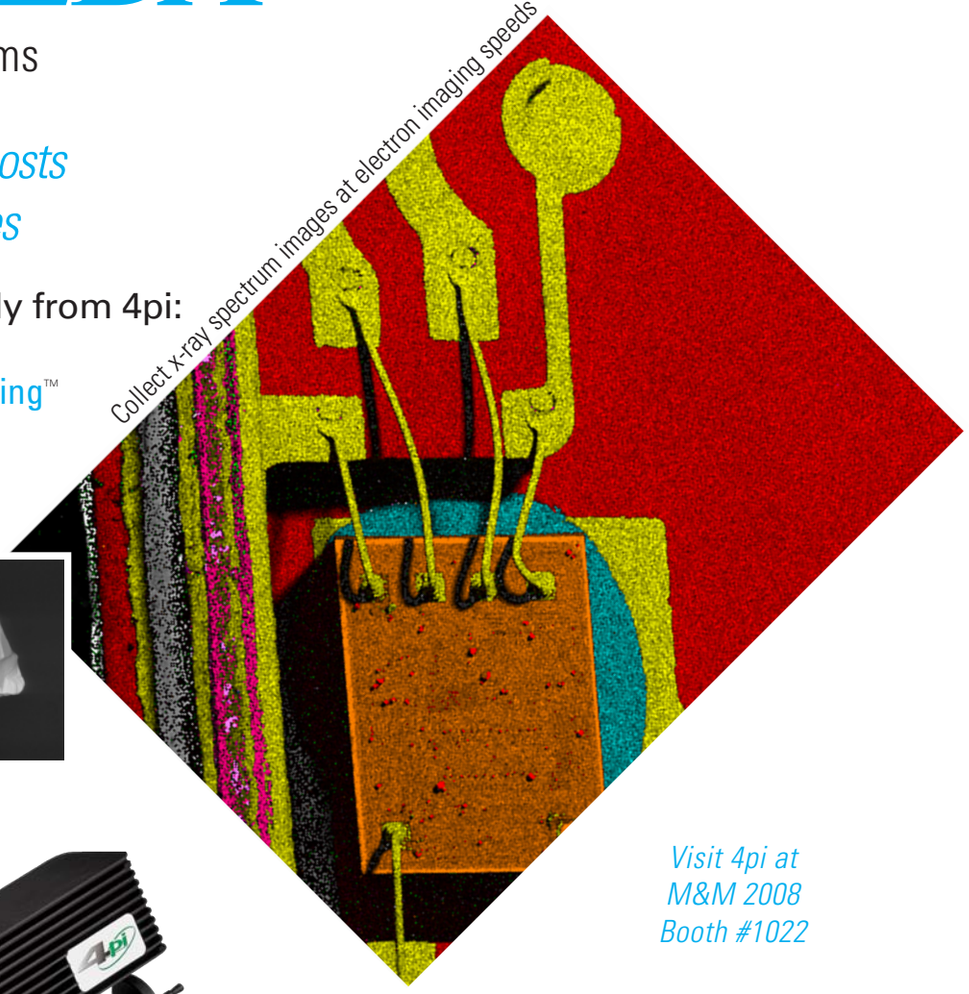
Event-Streamed Spectrum Imaging™

and

Spatial Frame Lock™

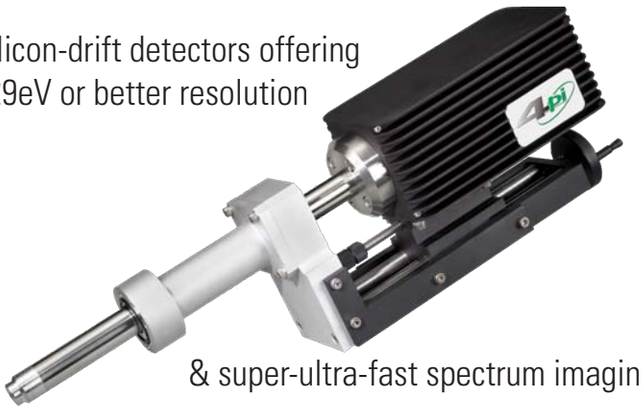
Real-time electron-beam drift correction





Visit 4pi at M&M 2008 Booth #1022

Silicon-drift detectors offering 129eV or better resolution



& super-ultra-fast spectrum imaging

- Work over a network via Gigabit Ethernet
- Easy to use: one-click acquisition for spectra, images, maps, spot probes and line scans
- Dynamic Dwell Modulation™– spend maximum time on areas of interest while continuing to obtain x-ray data from the entire area
- Robust auto peak-ID based on real-time full deconvolution of acquired x-ray spectra

TODAY only from

4pi

www.4pi.com • sales@4pi.com
4pi Analysis, Inc. 919.489.1757

MT Full Page Ad Master.indd 1 06/21/2008 11:18:36 AM

these lipid-detergent dialysis tests can be used as controls.

Screening for 2D crystals is performed on negatively stained grids, as these provide a rapid means of preparing a large number of samples (Kühlbrandt, 1992). While the negatively stained specimens have good contrast, they only provide lower resolution information. This is in most cases not beyond 15Å resolution, yet is more than sufficient to identify the two main criteria for success of 2D crystallization experiments: (1) crystal order and (2) size. While electron cryo-microscopy and image processing are essential for evaluating the achievable resolution of the crystals (Fujiyoshi, 1998), negative stain is the quickest means of optimizing crystals for order and size as well as possibly a reduction in mosaicity. Initially it is established that a satisfactory number of membranes are present on most grid squares, which will be necessary to allow for proper assessment of the sample based on an adequate number of proteoliposomes. The first successful step towards obtaining 2D crystals is in fact reconstitution of the membrane protein. Freeze-fracture is a very valuable tool in not only determining reconstitution, but also in giving a good indication of the relative amount of protein compared to lipid under the given conditions. Next, an overall impression of the membrane morphology is noted, which can be subdivided into vesicles, planar-tubular membranes or sheets (Fig. 2a – c). The specimens can be composed of either a single morphology or a mixture. Both types of samples will contain a range of membrane sizes. The most important point to note about the membrane dimension is that a sufficient number of membranes of a certain size is available for imaging.

Large numbers of membranes need to be inspected for crystallinity either with the help of a CCD camera and Fourier transform or on film, allowing for easier assessment of large crystals for size and mosaicity, as initial steps of 2D crystallization at suboptimal LPRs can result in less than 10% of proteoliposomes containing crystals (Zhao, Kanaoka, Irikura, Lam, Austen and Schmidt-Krey, in preparation). A similar observation was also made for vitamin K-dependent γ-glutamyl carboxylase (Schmidt-Krey *et al.*,2007), where the first crystals were few and limited in location to 1 or 2 grid squares. This was not caused by uneven grid preparation as the grids were otherwise uniform in appearance (not shown), but can be attributed to a low number of crystals.

In addition to testing the standard protein preparations for different crystallization parameters, it was found that dialysis of lipid-detergent mixtures under identical conditions, yet without protein, proved to be a valuable tool and control for assessing buffer conditions for at least two eukaryotic membrane proteins. This can be particularly helpful if only small amounts of protein are available, as well as for assessing buffers for their value in membrane formation. To test the feasibility of obtaining useful data from lipid-only dialysis experiments, buffers and lipid-detergent mixtures were used that reproducibly resulted in well-ordered 2D crystals in the presence of protein, namely human vitamin K-dependent γ-glutamyl carboxylase (Schmidt-Krey *et al.*, 2007) and human leukotriene C_4 synthase (LTC_4S) dialysis buffers (Zhao, Kanaoka, Irikura, Lam, Austen and Schmidt-Krey, in preparation).

Human carboxylase forms the largest continuous ordered arrays when it is induced to form planar-tubular crystals (Fig. 2b), while the most well-ordered LTC_4S 2D crystals are sheets that are on average at least 2μm in size (Fig. 2c). Both proteins crystallize in different morphologies and symmetries under controlled conditions, with the largest number of crystal forms observed for LTC_4S, namely, p2, p3, p312, and two different unit cell sizes of p321. In both cases it was found that the protein crystallizes before complete detergent removal, yet, as expected, the crystals proved far more stable, usually for at least several months, after elongated dialysis time. This stability could be extended much further by storing the 2D crystals at -80°C with the added advantage to prevent occurrence of effects observed in regular storage such as stacking (Schmidt-Krey, 2007).

By testing a lipid-detergent mixture without protein dialysed against detergent free buffer, liposomes in the micron-range of ~2-4μm and over 10μm in size could be obtained with characteristics typical of a particular buffer used. In the case of a DMPC-detergent mixture dialysis against vitamin K-dependent γ-glutamyl carboxylase buffer (25 mM Tris-HCl at pH 7.2, 20% glycerol, 250 mM NaCl, 10 mM β-mercaptoethanol) this resulted in planar-tubular liposomes (Fig. 3a and b) under similar conditions as the 2D crystallization conditions, as had also previously been observed for both the 2D crystals as well as DMPC planar-tubular membranes grown at 20°C. With the LTC_4S buffer (50 mM HEPES, pH 7.6, 1 mM EDTA, 10 mM 2-mercaptoethanol, 20% glycerol, 10 mM GSH, and 50 mM KCl), similar membrane sizes, morphologies and breakage could be observed as for the 2D crystals of the protein (Fig. 3c and d). The main differences with the carboxylase buffer appear to be the cleaner background in the lipid/detergent-only dialysis as well as the larger membrane size. The difference in membrane size can possibly be explained by additional curvature of the planar-tubular carboxylase crystals imposed by the protein

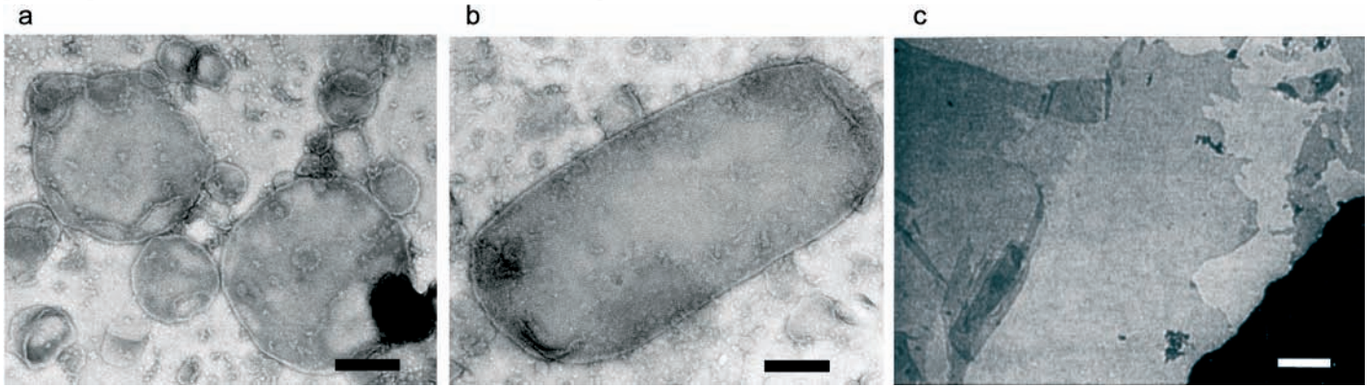


Figure 2. Images of typical two-dimensional crystals used for structural studies of (a) and (b) human vitamin K-dependent γ-glutamyl carboxylase and (c) human leukotriene C_4 synthase with (a) vesicle, (b) planar-tubular and (c) sheet morphology, respectively. The scale bars are (a) and (b) 200nm and (c) 1μm, respectively.

ABZhao.indd 2 06/21/2008 11:02:14 AM

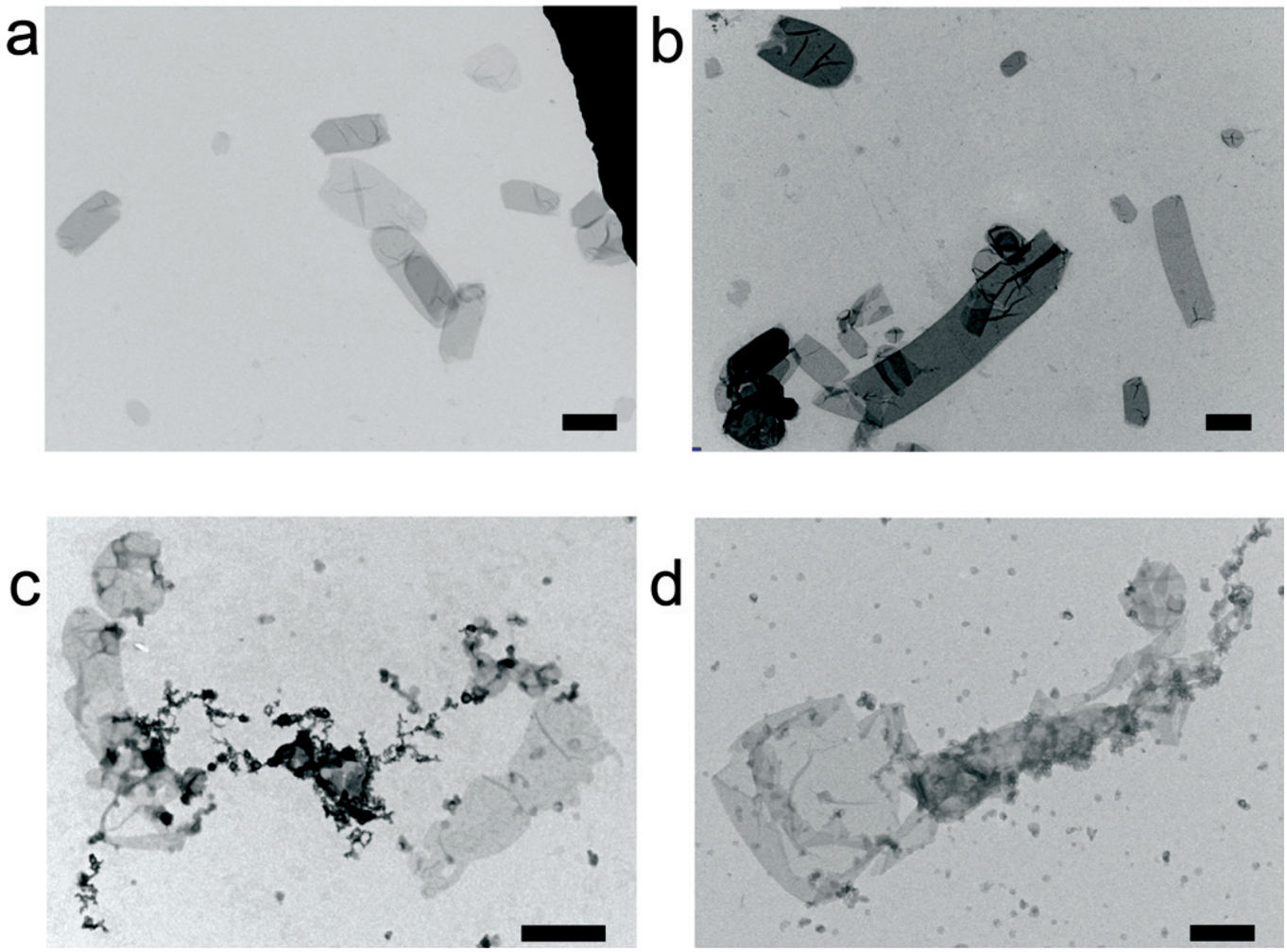


Figure 3. Images of a lipid-detergent mixture without protein after dialysis. (a) and (b) show planar-tubular membranes of DMPC-CHAPS dialysed against the carboxylase buffer. (c) and (d) are micrographs of a DMPC-Triton X-100 mixture dialysed against LTC_4S buffer. The scale bars are 1μm.

geometry, which is highly packed within the 2D crystals.

It was found that dialysis of detergent-solubilized lipid is a valuable indicator of membrane formation when optimizing buffer and lipid conditions. These tests without protein present could be particularly useful in cases where protein is difficult to produce or obtain. Consequently preliminary testing with the buffer can be done on lipid-detergent mixtures as well as used for controls of membrane formation under a given buffer condition. Similar tests will now have to be undertaken on other crystallizable membrane proteins to observe if this trend is general or can only be used in the screening of the LTC_4S and carboxylase crystallizations. ■

Acknowledgements

We thank our colleagues in the field of electron cryo-microscopy for open and generous discussions and Ben Bolaji and Jennifer Leavey for critical reading of the manuscript.

References

Amos, L.A., Henderson, R. & Unwin, P.N.T. (1982) *Prog. Biophys. Molec. Biol.* 39, 183 – 231.

Cheng, A., Leung, A., Fellmann, D., Quispe, J., Suloway, C., Pulokas, J., Abeyrathne, P.D., Lam, J.S., Carragher, B. & Potter, C.S. (2007) *J. Struct. Biol.* 160, 324 – 331.

Engel, A., Holzenburg, A., Stauffer, K., Rosenbusch, J. & Aebi, U. in: Bailey, G.W. (Ed.) *Proceedings of the 46th Annual Meeting of the Electron Microscopical Society of America*, San Francisco Press, San Francisco, 1988, pp. 152 – 153.

Fujiyoshi, Y. (1998) *Adv. Biophys,* 35, 25 – 80.

Gipson, B. , Zeng, X. & Stahlberg, H. (2007) *J. Struct. Biol.* 160, 375 – 384.

Gonen, T., Cheng, Y., Sliz, P., Hiroaki, Y., Fujiyoshi, Y., Harrison, S.C. & Walz, T. (2005) *Nature* 438 633 – 638.

Henderson, R., Baldwin, J.M., Ceska, T.A., Zemlin, F., Beckman, E. & Downing, K.H. (1990) *J. Mol. Biol.* 213, 899 – 929.

Hiroaki, Y., Tani, K., Kamegawa, A., Gyobu, N., Nishikawa, K, Suzuki, H., Walz, T., Sasaki, S., Mitsuoka, K., Kimura, K., Mizoguchi, A. & Fujiyoshi, Y. (2006) *J. Mol. Biol.* 355, 628 – 639.

Holm, P.J., Bhakat, P., Jegerschold, C., Gyobu, N., Mitsuoka., K., Fujiyoshi, Y., Morgenstern, R. & Hebert, H. (2006) *J. Mol. Biol.* 360, 934-945.

Kühlbrandt, W. (1992) *Q. Rev. Biophys.* 25, 1 – 49.

Kühlbrandt, W., Wang, D.N. & Fujiyoshi, Y. (1994) *Nature* 367, 614 – 621.

Löwe, J., Li, H., Downing, K.H. & Nogales, E. (2001) *J. Mol. Biol.* 313, 1045 – 1057.

Miyazawa, A., Fujiyoshi, Y. & Unwin, N. (2003) *Nature* 423, 949 – 955.

Murata, K., Mitsuoka, K., Hirai, T., Walz, T., Agre, P., Heymann, J.B., Engel, A. & Fujiyoshi, Y. (2000) Nature 407, 599 – 605.

Nakamura, N., Fujiyoshi, Y., Mitsuoka, K., Murata, K. & Shinkawa, T. (2003) *Microsc. Microanal.* 9 (suppl. 2) 1038 – 1039.

Nogales, E., Wolf, S.G. & Downing, K.H. (1998) *Nature* 391 199 – 203.

Ren, G., Reddy, V.S., Cheng, A., Melnyk, P. & Mitra, A.K. (2001) *Proc. Natl. Acad. Sci. U.S.A.* 98, 1398 – 1403.

Schmidt-Krey, I. (2007) *Methods* 41, 417 – 426.

Schmidt-Krey, I., Mutucumarana, V., Haase, W., Stafford, D.W. & Kühlbrandt, W. (2007) (2007) *J. Struct. Biol.* 157, 437 – 442.

Stahlberg, H., Fotiadis, D., Scheuring, S., Remigy, H., Braun, T., Mitsuoka, K., Fujiyoshi, Y. & Engel, A. (2001) *FEBS Letters* 504, 166 – 72.

Tate, C. (2006) *Curr. Opin. Struct. Biol.* 16, 457 – 464.

Vink, M., Derr, K.D., Love, J., Stokes, D.L. & Ubarretxena-Belandia, I. (2007) *J. Struct. Biol.* 160, 295 – 304.

Werten, P. J. L., Remigy, H.-W., de Groot, B. L., Fotiadis, D., Philippsen, A., Stahlberg, H., Grubmueller, H. & Engel, A. (2002) *FEBS Letters* 529, 65 – 72.

ABZhao.indd 3 06/21/2008 11:02:15 AM

A New Perspective on Mechanical Testing: *In Situ* Compression in the TEM

Julia Deneen Nowak, Zhiwei Shan and Oden L. Warren*
Hysitron Incorporated, Minneapolis, MN
**email: owarren@hysitron.com*

Testing the mechanical properties of nanoscale materials faces a number of inherent challenges. As the size of the "target" decreases, the inability to actually *see* what occurs during testing can be troublesome. While a number of studies have attempted to characterize the mechanical response of nanoscale materials using traditional nanoindentation techniques, certain lingering questions have always remained. For example, the nature and sequence of failure events in the case of multilayer films has long been the subject of scientific debate. Similarly, in the case of individual nanoparticles, it is often difficult to ascertain that contact was both made and maintained throughout the test. Further, the crystallographic orientation of the sample and/or the presence of preexisting defects, which can have a significant influence on mechanical properties at the nanoscale, typically remain unknown.

The transmission electron microscope (TEM) is an ideal tool for determining these unknowns. In particular, with careful attention to sample preparation, the TEM can be used to characterize samples after mechanical testing. With the TEM it is fairly straightforward to determine the sample orientation and to examine residual plastic deformation. However, these "*post mortem*" studies suffer from their own unknowns, in many ways complimentary to those faced by nanomechanical testing. For example, it is impossible to characterize any purely elastic deformation that occurred during testing. In addition, determining at what point during testing certain defects were formed is out of the question. A simultaneous combination of the two techniques has some clear advantages over a sequential approach. Here we present a discussion of the development of the *in situ* nanoindentation holder and of its application to characterizing the mechanical behavior of nanoscale materials.

The evolution of the *in situ* nanoindenter for the TEM has a long and varied history. In one of its early incarnations, developed in the 1960s, the *in situ* indenter was a piezo-driven indentation stage capable of loads on the order of 10^{-2} to 10^{-6} N [1]. Sample holders capable of indentation did not emerge until a few decades later, most notably from Lawrence Berkeley National Laboratory [2-4]. These holders employed a piezoelectric actuator for indentation, but lacked a force sensor. As such, they were essentially qualitative in nature, though quantitative displacement information could be extracted from the TEM images. This type of holder resulted in a number of fundamental studies characterizing deformation of nanoscale materials such as thin films and nanoparticles [5-8]. Until quite recently however, the major aspect of *in situ* indentation that had been lacking was the capability of determining both load and displacement *quantitatively* during a test. We have developed a system capable of both: the TEM PicoIndenter™ [9].

With the PicoIndenter it is possible to acquire quantitative mechanical data while simultaneously monitoring the microstructural evolution of the sample with the TEM. In the PicoIndenter, the sample is mounted directly opposite a boron-doped diamond indentation tip, such that the indentation direction is along the length of the holder and perpendicular to the electron beam (Figure 1). Using the relative foci of the tip and the sample, the tip can be brought into the same plane as the sample using the coarse (manual) and fine (piezoelectric actuator) controls. In addition, the PicoIndenter incorporates a patent-pending miniature transducer for electrostatic actuation and capacitive displacement sensing [10]. The transducer is the heart of the PicoIndenter, making it capable of producing quantitative load–displacement curves with load or displacement controlled as a function of time. The PicoIndenter, in its earliest form, has been used to characterize the onset of plasticity during the deformation of Al [11], to study dislocation–grain boundary interactions and dislocation motion in Mg-Al alloys [12, 13], and to quantify the mechanical behavior of nanoporous Au films [14].

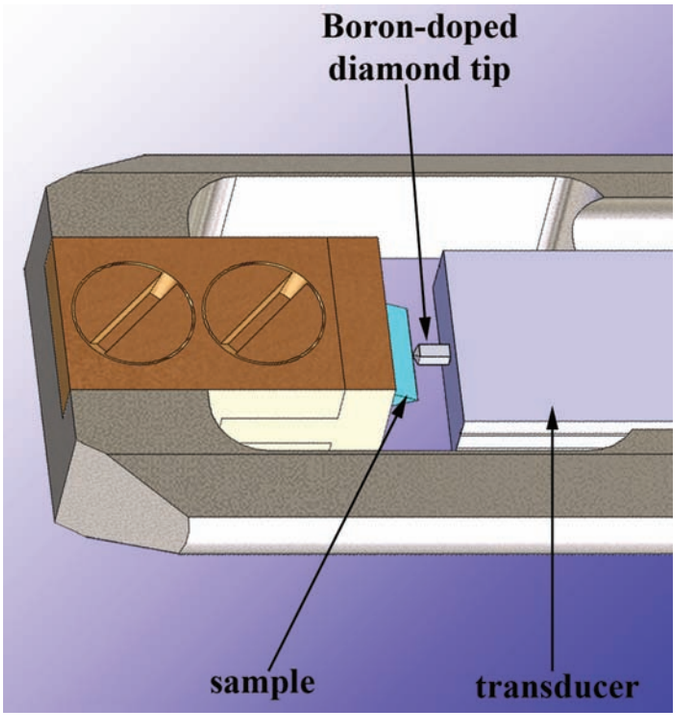


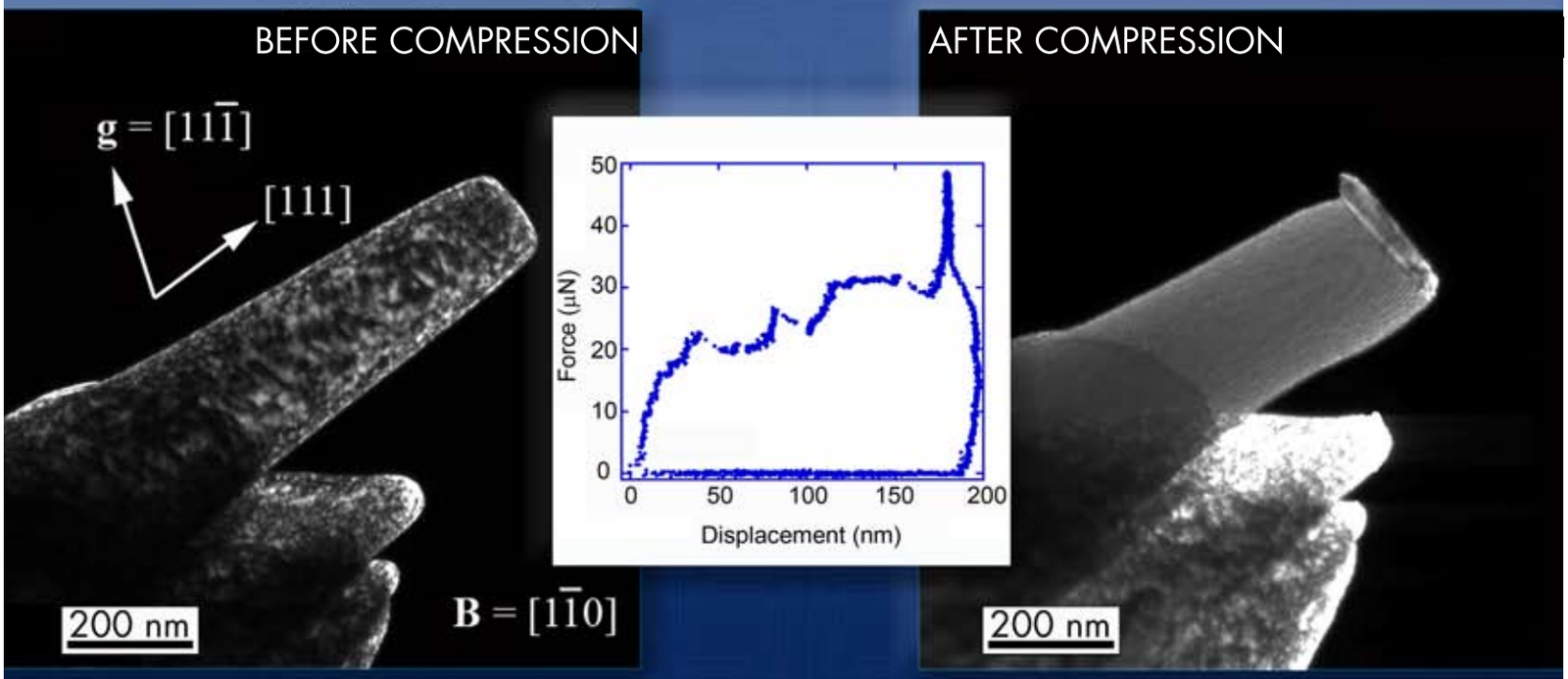
Figure 1: Schematic illustrating the geometry at the tip of the holder. The electron beam is perpendicular to the plane formed by the sample and the diamond tip.

More recently, the PicoIndenter has been used to study the mechanical response of individual Ni pillars, with astounding results [15-17]. The Ni pillars were fabricated from a bulk single crystal using a focused-ion beam (FIB) such that their long axis was oriented along a [111] direction. Prior to *in situ* testing the pillars had free-end diameters ranging from 150–290 nm with a sidewall taper angle of ~4°. The prepared sample was then mounted in the PicoIndenter for examination in the TEM. This PicoIndenter was equipped with a diamond flat-punch tip, doped with boron for conductivity in the electron microscope. With this system it is possible to align the tip with the area of interest and begin the test without making contact with the sample prior to testing—an important consideration as dislocation bursts have been observed in metals at near noise-level loads [11, 18]. Individual pillars were first oriented with respect to the electron beam and then compressed

ABNowak.indd 1 06/23/2008 12:36:27 PM

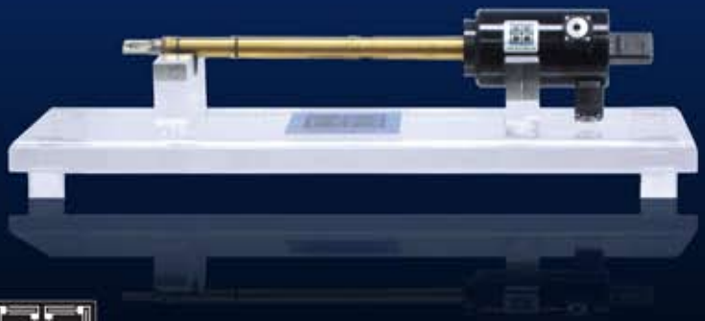
SEEING IS BELIEVING™

Quantitative, direct-observation nanomechanical testing interfaced to the TEM



Introducing the PI 95 TEM PicoIndenter™

Hysitron, Inc. is proud to announce the launch of this exciting new addition to its established range of nanomechanical testing products



- Quantitative load and displacement measurements
- Multiple test types and control modes
- Conductive diamond probes
- Time-synchronized TEM imaging and load-displacement data

HYSITRON™ For more information, please visit our website **www.hysitron.com/meet-pi-95**

MT Full Page Ad Master.indd 1 06/21/2008 12:43:14 PM

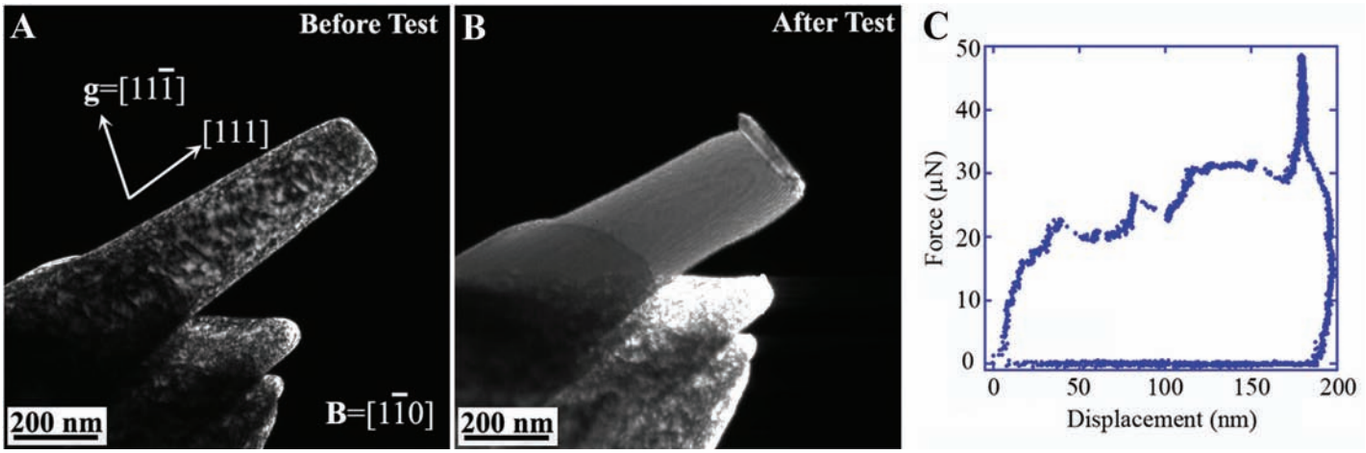


Figure 2: Dark-field TEM images of a Ni nanopillar before compression (A) and after compression (B), and the associated force vs. *displacement curve (C).*

with the diamond probe. During compression, both TEM video and load–displacement curves were acquired simultaneously. While we commonly refer to the holder as an "indentation holder", in this case it is more accurate to describe the test as a compression test due to the relative sizes of the sample and probe.

Prior to compression the Ni pillars were observed to contain a large number of dislocations (Figure 2A), but upon contact with the diamond probe the pillars yielded and upon further compression these pre-existing defects disappeared. The resulting structure was essentially a dislocation-free single-crystal pillar (Figure 2B), as determined by dark-field imaging under a number of two-beam conditions. This phenomenon, dubbed "mechanical annealing," is consistent with a dislocation starvation mechanism. The initially high dislocation density drops to zero and further deformation is controlled by the activation of new dislocation sources, taking place at higher stresses. The sharp load increase to nearly 50 μN shown in the load-displacement plot (Figure 2C) coincided with primarily elastic behavior. By measuring the instantaneous contact area from still frames of the recorded video, one of the advantages of performing the test in the TEM, it was possible to calculate the instantaneous contact stresses throughout the test. For this pillar, stresses as high as 1.3 GPa were sustained at peak load.

This *in situ* study represents the first direct observation of the dislocation starvation mechanism responsible for the strengthening of these nanopillars and gives new insight into the phenomena involved in the atypical mechanical properties associated with nanoscale structures. However, this work is really only the tip of the iceberg. The origins of the enhanced properties of materials in their nanoscale form are still poorly understood. Clearly, this technique could be extended to materials of different chemistries and morphologies. For example, it has already been used to explore the properties of metallic-glass pillars [19]. In the future, *in situ* TEM studies will undoubtedly benefit from the coupling of nanomechanical testing with other techniques. Sample holders which can test electrical or thermal properties in conjunction with quantitative nanomechanical testing will certainly contribute to a better understanding of how certain properties are coupled. The capability of investigating these phenomena *in situ* presents truly amazing possibilities. ■

Acknowledgments

This research and development was funded in part by a US DOE SBIR grant (No. DE-FG02-04ER83979) awarded to Hysitron, Inc, which does not constitute an endorsement by the DOE of our views. We also gratefully acknowledge our collaborators at the National Center for Electron Microscopy, Lawrence Berkeley National Laboratory.

References

1. Gane, N., *The direct measurement of the strength of metals on a sub-micrometer scale.* Proc. R. Soc. London, Ser. A, 1970. **317**: p. 367-391.
2. Wall, M.A., T.W. Barber, and U. Dahmen, *Techniques for in situ HVEM mechanical deformation of nanostructured materials.* 53rd Annual MSA Meeting, 1995: p. 240-241.
3. Wall, M.A. and U. Dahmen, *Development of an in-situ nanoindentation specimen holder for the high voltage electron microscope.* Microsc. Microanal., 1997. **3**(suppl. 2): p. 593-594.
4. Stach, E.A., et al., *Development of a nanoindenter for in situ transmission electron microscopy.* Microsc. Microanal., 2001. **7**: p. 507-517.
5. Deneen, J., et al., *In situ deformation of silicon nanospheres.* J. Mater. Sci., 2006. **41**: p. 4477-4483.
6. Deneen Nowak, J., et al., *Fracturing a nanoparticle.* Philos. Mag., 2007. **87**(1): p. 29-37.
7. Jin, M., et al., *Study of deformation behavior of ultrafine-grained materials through in situ nanoindentation in a transmission electron microscope.* J. Mater. Res., 2005. **20**(7): p. 1735-1740.
8. Minor, A.M., et al., *In-situ transmission electron microscopy study of the nano-indentation behavior of Al.* J. Electron. Mater., 2002. **31**(10): p. 958-964.
9. www.hysitron.com.
10. US Patent Application No. 20070180924.
11. Minor, A.M., et al., *A new view of the onset of plasticity during the nanoindentation of aluminium.* Nature Materials, 2006. **5**(9): p. 697-702.
12. De Hosson, J.T.M., et al., *In situ TEM nanoindentation and dislocation-grain boundary interactions: a tribute to David Brandon.* J. Mater. Sci., 2006. **41**: p. 7704-7719.
13. Soer, W.A., et al., *Incipient plasticity in metallic thin films.* Appl. Phys. Lett., 2007. **90**(18): p. 181924-3.
14. Sun, Y., et al., *The mechanical behavior of nanoporous gold thin films.* JOM, 2007. **59**(9): p. 54-58.
15. Shan, Z.W., et al., *Mechanical annealing and source-limited deformation in submicrometre-diameter Ni crystals.* Nature Materials, 2008. **7**(2): p. 115-119.
16. Shan, Z.W., et al., *Exploring the mechanical properties of nanostructures and nanomaterials inside a TEM.* Microsc. Microanal., 2008. **14**(Suppl. 2): p. in press.
17. Hemker, K.J. and W.D. Nix, *Nanoscale deformation: Seeing is believing.* Nature Materials, 2008. **7**(2): p. 97-98.
18. Warren, O.L., et al., *In situ nanoindentation in the TEM.* Materials Today, 2007. **10**(4): p. 59-60.
19. Shan, Z.W., et al., *Plastic flow and resistance of metallic glass: Insight from in situ compression of nanopillars.* Phys. Rev. B, 2008. **77**: p. 155419.

ABNowak.indd 2 06/23/2008 12:36:28 PM

EMS offers the breakthrough solutions of QuantomiX's proprietary WETSEM® Technology

now available at half price for a limited time



The biggest breakthrough is here in a nano-package.

WETSEM® TECHNOLOGY

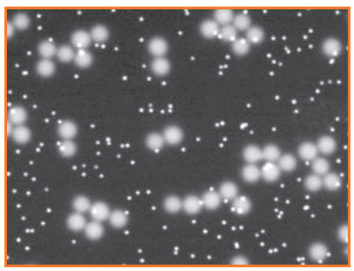
- Attain EM-level imaging of wet samples
- Reduce artifacts & time-consuming sample preparation
- Safe and simple to use
- Achieve reliable, reproducible & quantifiable results

Applications

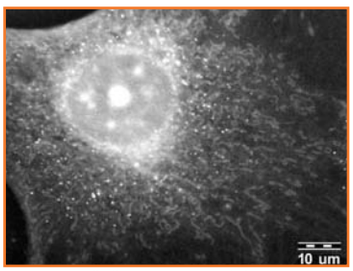
- Industrial research: food, oils, dyes, emulsions, pharmaceuticals, suspensions, personal care goods, cosmetics, inks.
- Quality control and quality assurance.
- Life sciences and medicine: cultured and primary cells, histology, nerve cells and myelin imaging, microbiology, plants.
- Tissue implants and prostheses.
- Environmental and toxicological applications.
- Clinical diagnosis: histopathology, cytology, oncology.

Capabilities

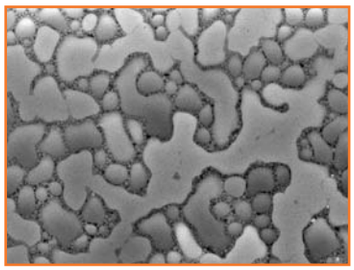
- Analyze size distribution, aggregation and homogeneity of particle suspensions.
- Perform EDS of fully hydrated samples.
- SEM imaging of oils, greases, volatile substances, emulsions and creams.
- Enables tissue morphology and analysis.
- Characterize cellular and subcellular organelles, cell contacts and receptors, cytoskeleton and other detail.
- Characterize and quantify lipids in fully-wet cells and tissues.



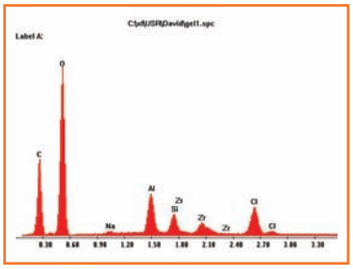
Silica (500nm) and gold (40nm) particles



NIH-3T3 cell, osmium tetroxide



Volatile deodorant showing phase separation



EDS graph showing deodorant material composition

Please contact us for more details.

Electron Microscopy Sciences

In PA: (215) 412-8400 • Toll-Free (800) 523-5874
Fax (215) 412-8450 or 8452
email: sgkcck@aol.com or stacie@ems-secure.com

www.emsdiasum.com

MT Full Page Ad Master.indd 1 06/21/2008 12:52:44 PM

Confocal Micro X-Ray Fluorescence: A New Paradigm in Materials Characterization

Brian M. Patterson, George J. Havrilla, Kimberly A. DeFriend
Los Alamos National Laboratory, Los Alamos, NM
bpatterson@lanl.gov

Introduction:

Micro x-ray fluorescence (MXRF) is a microscopic analysis and imaging technique that is used to characterize the elements in a material non-destructively. Micro XRF instruments use an x-ray source to shine x-rays on a sample, and a detector to detect the characteristic x-rays given off. These fluorescent x-rays have very specific energies corresponding to specific electron energy transitions. Therefore, it is possible to detect and identify all of the elements present in a sample (typically above sodium) as well as measure their concentrations. This technique is widely used for the characterization of materials including polymer[1] and metallic foams, powder samples, forensics applications, geological samples, works of art and nuclear fuels[2]. Commercial MXRF instruments use a fused silica optic (mono or polycapillary) to focus the x-rays on the sample with no optic on the detector (Figure 1a). In this geometry, it is possible to raster the sample in two dimensions to collect the x-ray fluorescent signal as a function of position and generate a 2D map, identifying the elements present, their locations, and their relative and absolute abundances. While very useful, this geometry provides *x-y* mapping of the sample only, it does not provide signal discrimination versus depth.

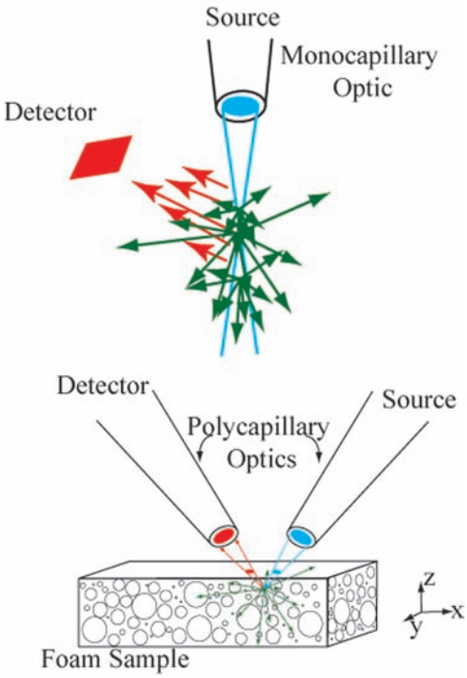


Figure 1: Top cartoon is the layout of a typical MXRF instrument showing an optic on the source but none on the detector. Fluorescent x-rays are detected even from the out of focus regions. The lower cartoon shows the optical geometry of a confocal MXRF instrument with an additional optic on the detector. Only fluorescent and scattered x-rays from the overlapping foci are detected.

As an improvement upon this design, confocal micro x-ray fluorescence (confocal MXRF) adds a new 'dimension' to this materials characterization technique by adding an optic on the detector. The foci of the two optics overlap in 3D space (Figure 1b), which can be useful for two purposes. The first is that any natural x-ray emission from a radioactive sample emitted off axis from the detector optic is rejected, reducing the background and improving the signal-to-noise when characterizing these samples. The second is that only the x-rays emitted from within the overlapping foci are measured, therefore a true 3D measurement is possible. By moving the sample through the confocal x-ray beam in the *x, y* and *z* directions, a 3D elemental map of the sample is possible, nondestructively providing elemental distribution and concentration. As an additional capability, the amount of x-ray scatter from low-density materials is proportional to the mass of material within the confocal volume, since this volume is measureable; the amount of scatter is proportional to the density of the material at that specific location. Confocal MXRF is useful for measuring the density of the material in 3D.

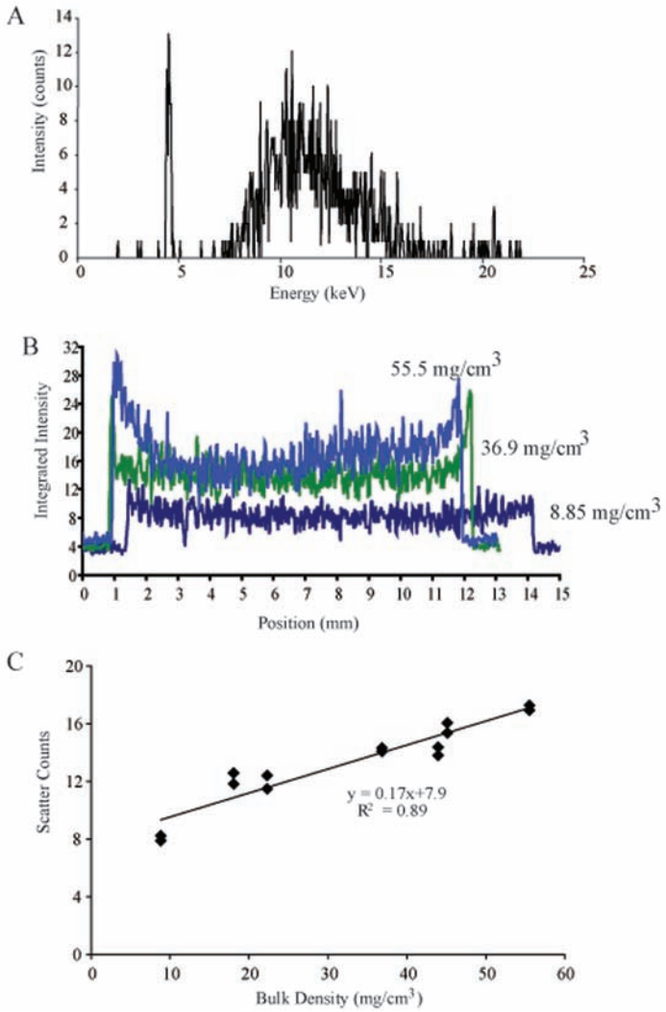


Figure 2: A) X-ray scatter spectrum indicating region of interest for the following figures. B) Line profiles of 8 (bottom), 37 (middle) and 55 (top) mg/cm^3 cast aerogels showing higher density gradients at the surfaces. C) Correlation of measured bulk density versus x-ray scatter intensity for a variety of cast aerogels.

As a proof of operation, several samples will be illustrated including using the scatter to quantitatively measure the density of silica aerogels, using the x-ray scatter to identify the voids in a silicone foam material in 3D and finally to collect 3D elemental image of a surface mount resistor for an integrated circuit.

Instrument:

The current prototype bench top design (X-ray Optical Systems, (XOS), East Greenbush, NY), except for the associated electronics, fits on a 2' by 2' optical bread board, and is housed and interlocked inside a cabinet. There is currently no vacuum chamber. The instrument uses an XOS X-beam Ag tube powered by a Spellman XLG power supply (25 W max) as the source, with an Amptek Si pin diode (XR-

ABPatterson.indd 1 06/21/2008 1:06:12 PM

Would You Bet Your Company's Reputation on Your EDS Results? We Did.

Place Your Bet at M&M Booth 1122



We've Expanded Our Product Range with the Most Powerful SDD for EDS

- ***New*** **Apollo Silicon Drift Detector Enables Complete Spectrum Maps to be Collected in Seconds**
- ***New*** **Hikari High Speed EBSD Detector**
- **Seamless Integration of EDS, EBSD, and WDS**

The original expectations of the development of the Silicon Drift Detector are now achievable with the EDAX Apollo SDD. Fulfilling the promise of the new technology, the Apollo SDD is capable of collecting high count rates with excellent resolution in an LN_2 free environment. The Apollo SDD, when seamlessly integrated with the LambdaSpec WDS and the Hikari EBSD Detector, provides the ultimate in high speed analysis.

Results with Confidence…Even Faster

The Apollo SDD is the latest innovation from EDAX. As the world's leader in Electron Beam Microanalysis, EDAX continues to raise the performance standard with features that provide faster results that you can trust to be complete and accurate.

For more information on EDAX's latest product developments visit our web site at ***www.EDAX.com/NEW*** *or call* ***1-201-529-4880****.*

EDAX®
advanced microanalysis solutions

AMETEK®
MATERIALS ANALYSIS DIVISION

MT Full Page Ad Master.indd 1 06/21/2008 1:12:00 PM

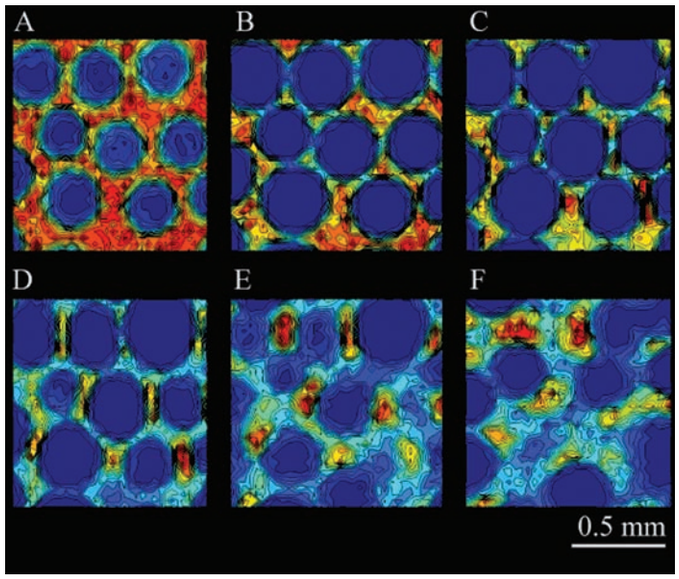


Figure 3: Array of sequential x-y contour plots displaced in z direction using region of interest indicated in Figure 2A. Pixel size (x-y) is 30 µm and z step size (from A-B, B-C, etc.) is 50 µm. Each slice took approximately 30 minutes to collect with a 1 second dwell at each location. There are 20 contour lines in each plot which are not of fixed intensity values from plot to plot.

100CR) as the detector. A monolithic polycapillary is used for each of the source and detector optics with an angle between the optics of 60 degrees, providing a spatial resolution of 30 × 30 × 65 micrometers as measured with the Ta L_α line. The center axis of each of the optics cuts the sample plane along the surface normal. The 60° angle between the optics is used for better depth penetration. Using polycapillary optics with a focal spot as small as 15 µm and mounting them 90° to each other, (45° from the surface normal) improves the spatial resolution and circularizes the confocal probe volume. Samples are mounted on three Newport 850G stages. The associated electronics are mounted on a single rack below the instrument. The instrument is controlled by a Dell computer running proprietary XOS software.

This instrument geometry enables the collection of MXRF spectra at a single point or line scans as either *x, y*, or depth profiles, *z*, as well as collect 2D regions of interest elemental maps at selected depths below the surface of the sample. These 2D slices can then be stacked into a full 3D image of the sample. Without the vacuum purge, elements with an atomic number greater than potassium can be identified and mapped. However, even low atomic number samples can be characterized and mapped based upon x-ray scatter. The confocal volume can be useful for density measurements of low atomic number matrices such as foams and aerogels. The amount of scatter produced by the sample (Figure 2) is dependent upon the mass of material within the confocal volume. Since the volume of the confocal beam is fixed, the amount of scatter is proportional to density. The 3D data is plotted using Matlab (Mathworks).

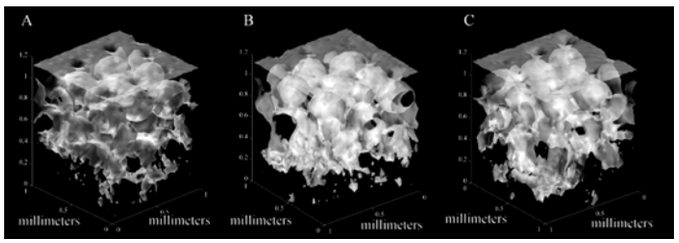


Figure 4: 3D constructs of PDMS foam scatter data from Figure 3. Each 3D image is rotated 90° counter clock-wise (A-C). Plot is 1 mm³. No modeling of x-ray attenuation is shown. Information is being collected from 1-mm depth, but signal is below user selected isovalue threshold of 20 counts.

Results:

Several cast aerogel samples with densities measuring between 10- 55 mg/cm³ were examined. These aerogels were cylindrical in shape and were mounted vertically with a flat surface pointing up. This orientation kept the beam path distance through the sample constant as the sample was moved through the beam. Measuring the x-ray scatter (Figure2a) for 4 seconds at each point (Figure 2b) and collecting a cross section profile can be used to measure the bulk density of an aerogel as well as density variations throughout the sample[3]. We have found good correlation between the amount of scatter in the center of the sample versus the density of the sample measured using a shadow graph and an analytical balance (Figure 2c). A higher density or 'skin' of aerogel has been measured on all aerogel samples examined. This 'skin' density is not seen on other samples such as polystyrene foams with similar densities and geometries. Work is ongoing with this phenomenon using confocal MXRF as well as micro-CT and is probably due to void collapse of the aerogel at the surface.

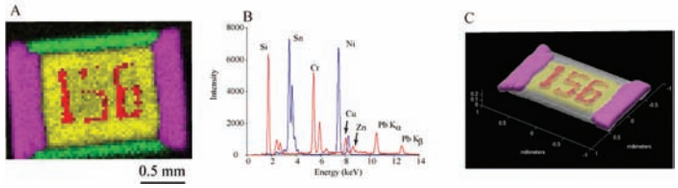


Figure 5: A) MXRF image of resistor using an EDAX Eagle II. Ti = red, Pb = yellow, Al= green, and Sn/Ni in pink. B) Spectra of the center (red) and edge (blue) of the resistor using the Eagle MXRF. Center spectrum indicates the presence of Si, Cr, Cu, Zn, and Pb. Edge spectrum shows Sn and Ni. A spectrum collected with the confocal would be exactly the same except that Al and Si peaks would not be present. C). 3D rendering of elemental images from the confocal MXRF. The same colors as A are used. Al is not identified by the confocal MXRF instrument, but is detected by its x-ray scatter shown as gray.

A piece of polydimethylsiloxane foam was also examined using confocal MXRF. Slices at various '*z*' locations were collected (Figure 3) and stacked into a single 3D image (Figure 4). As the sample is raised higher into the beam to collect information at depth, the x-ray scatter signal is attenuated by the upper layers, leading to the overall intensity dropping below the chosen cutoff isovalue and the sample is no longer resolvable. The image was plotted using Matlab with no data treatment or compensation for attenuation. There is still useful x-ray scatter signal at over 2 mm below the sample surface, and could be plotted with a signal attenuation correction versus depth. Current work is ongoing characterizing these foams using FT-IR, XRF, and micro-CT.

As a third example, a surface mount resistor for an integrated circuit is shown illustrating the ability of confocal MXRF to image a sample in 3D based solely on the elemental signal. Data was collected with a 1 second integration of each 50 × 83 *x, y* data points and 11 total slices in *z*. All spacing's were 30 µm in all three dimensions. Each slice required approximately 2 hours to collect, 22 hours for the entire data set. Eleven regions of interest were collected simultaneously, representing, the full range of channels, which were assigned to the elements Sn, Ti, Cr, Mn, Fe, Ni, Cu, Zn and Pb. The regions of interest and their corresponding energies that were mapped out are shown in Table 1, below. Understanding the distributions of lead and tin are important for mitigation of tin whisker formation which

ABPatterson.indd 2 06/21/2008 1:06:13 PM

cannot be measured in 3D using any other bench top technique nondestructively.

Table 1: Regions of Interest and their Corresponding Energies		
Element	Detector Channels	Energy Range (keV)
Scatter	0-1022	0-36.7
Sn	85-115	2.9-4.04
Ti	127-137	4.4-4.8
Cr	137-152	4.8-5.3
Mn	152-164	5.4-5.8
Fe	168-178	5.9-6.3
Ni	192-209	6.8-7.4
Cu	209-225	7.4-8.2
Zn	251-275	8.9-9.8
Pb	281-307	10-10.9

Conclusions:

Confocal micro x-ray fluorescence offers a previously unobtainable dimension to the elemental characterization of a material. Using this technique the sample does not need to be put under a vacuum, no coatings are needed, such as in electron beam techniques, and most importantly, 3D elemental information can be extracted from the sample non-destructively. Either samples can continue to be examined using other techniques or, the same sample that is examined can later be used in the field. Further developments to this technique focus primarily upon the construction of a second-generation instrument with fully automated data acquisition, a vacuum chamber for identifying and measuring low atomic number elements in samples, and automated data processing. Data processing may include full 3D mapping based upon region of interest, and full spectral mapping. Full spectral mapping/imaging has already shown great utility in many other techniques such as XRF and EDS, FT-IR, and UV/Vis fluorescence and can be used beyond simple elemental mapping. Full spectral imaging is often used to create maps of chemical phases. Confocal MXRF has demonstrated considerable characterization utility and yet it still offers undiscovered potential for further developments. The relative low cost and exciting capabilities of this technique, offers new opportunities for materials characterization. ■

Acknowledgments:

The authors wish to thank Brent Espinoza for making the silica aerogels. This work was funded by the ICF and Enhanced Surveillance Campaign programs. Los Alamos National Laboratory is operated by Los Alamos National Security LLC under contract number DE AC52-06NA25396 for the US Department of Energy.

References:

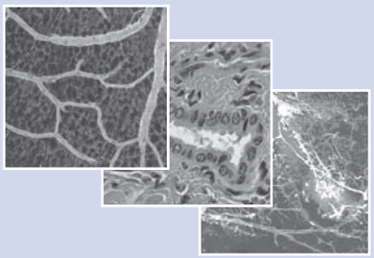
1. B. M. Patterson, G. J. Havrilla, and J. R. Schoonover, *Appl. Spectrosc.* **60**, 10, 1103 (2006).
2. G. J. Havrilla, Abstracts of Papers, 223rd ACS National Meeting, Orlando, FL, United States, April 7-11, 2002, NUCL (2002).
3. P. A. Keiter and G. A. Kyrala, *Review of Scientific Instruments* **75**, 10, Pt. 2, 4057 (2004).

PELCO
BioWave® Pro

Fast, Low Temperature
Microwave Tissue Processing

- Rapid Specimen Turnaround
- Low Temperature Environment
- Programmable Processing
- Consistent Quality Results





Application kits for paraffin processing, decalcification, confocal, light and electron microscopy are available.

TED PELLA, INC.
Microscopy Products for Science and Industry

sales@tedpella.com • Tel: 800-237-3526 • www.tedpella.com

ABPatterson.indd 3 06/21/2008 1:06:14 PM

Hardware and Techniques for Cross-Correlative TEM and Atom Probe Analysis

Brian P. Gorman[1], David Diercks[1], Norman Salmon[2], Eric Stach[2], Gonzalo Amador[3], Cheryl Hartfield[3]
[1]*Dept. of Mat. Sci. and Eng. and Center for Advanced Research and Technology, University of North Texas, Denton, TX*
[2]*Hummingbird Scientific Instruments, Salem, OR*
[3]*Omniprobe, Inc., Dallas, TX*
Brian.Gorman@unt.edu

Introduction

Atom probe tomography has primarily been used for atomic scale characterization of high electrical conductivity materials [1]. A high electrical field applied to needle-shaped specimens evaporates surface atoms, and a time of flight measurement determines each atom's identity. A 2-dimensional detector determines each atom's original position on the specimen. When repeated successively over many surface monolayers, the original specimen can be reconstructed into a 3-dimensional representation. In order to have an accurate 3-D reconstruction of the original, the field required for atomic evaporation must be known *a-priori*. For many metallic materials, this evaporation field is well characterized, and 3-D reconstructions can be achieved with reasonable accuracy.

Compared with conventional atom probes, the use of a local electrode has been shown to increase the sustainable evaporation rate and field of view [2]. The localized electric field produced by the local electrode enables arrays of specimens to be analyzed, as opposed to a single, electropolished wire needle. Specimen arrays increase throughput by minimizing exchange to UHV and cryogenic temperatures, as well as increasing material statistics through analysis of many specimens. In order to take advantage of these specimen arrays, preparation techniques utilizing *in-situ* FIB liftout techniques were developed [3]. These techniques allow routine preparation of nominally 100nm diameter specimens. The FIB also enables much improved control of the specimen diameter so the atom probe experiments can be tuned accordingly.

The maturation of local electrode and laser pulsed atom probe hardware, as well as FIB specimen preparation techniques, have enabled atom probe analysis of non-traditional materials such as semiconductors, ceramics, and some organic materials to become more commonplace [4]. For most of these materials, the evaporation field is not well characterized. For example, oxides and III-V materials tend to evaporate in clusters of atoms, rather than individual atoms [5]. The physics of cluster evaporation in atom probe experiments are not well understood, and the evaporation field required is also not well characterized. In order to increase the accuracy of the 3-D reconstructions in non-traditional materials, the evaporation field and its progression during an atom probe experiment should be calculated using the specimen geometric features, such as tip radius and shank angle.

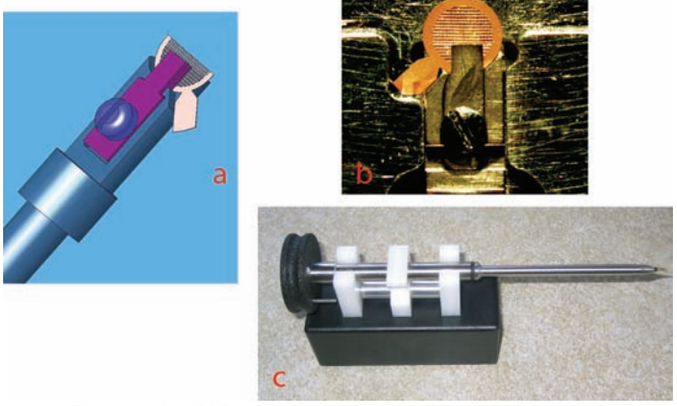


Figure 1. (a) CAD representation of the FIB / TEM / Atom Probe specimen effector and grid design. (b) Grid and effector mounted in loading jig. (c) Specimen carrier mounted on a TEM stage designed for the FEI Co. TF20ST.

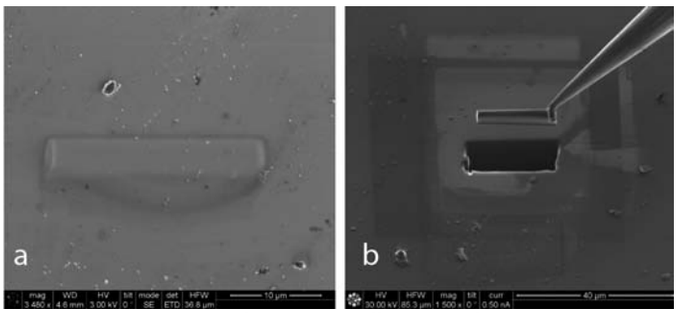


Figure 2. SEM and FIB images illustrating the in-situ specimen extraction and mounting of atom probe specimens. (a) Protective Pt deposition over area of interest using FIB-based gas injector deposition. (b) In-situ liftout of the wedge-shaped area of interest.

While a combination FIB and SEM can give some information about atom probe specimen structure, higher resolution characterization of specimens using TEM and STEM can further increase reconstruction accuracy. TEM can image not only the specimen radius and shank angle with higher precision, but also can give the internal structure of interfaces and precipitates. Diffraction and high resolution imaging can give information about the orientation of crystallographic axes with respect to the specimen, and thus allow accurate scaling of the reconstruction in the *z*-direction. Analytical

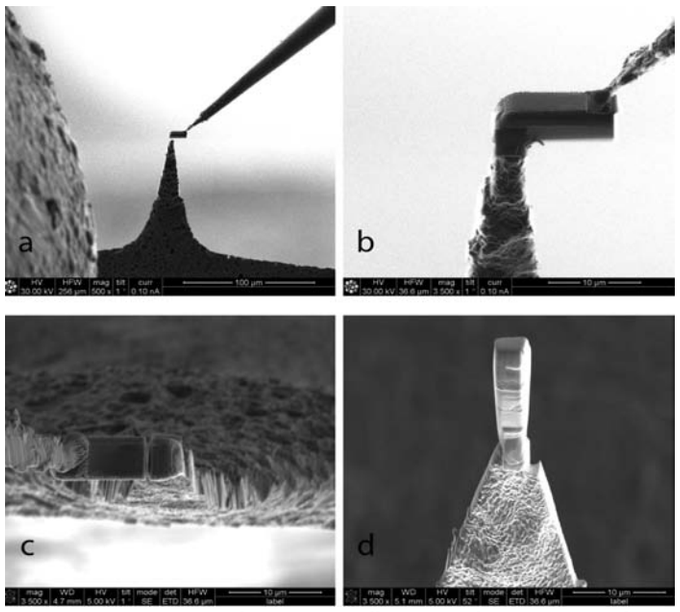


Figure 3. SEM and FIB images illustrating the specimen wedge mounting to the TEM grid posts. (a) Specimen approach to the TEM grid post, also showing the Pt GIS. (b) Specimen mounted to the TEM post with Pt. (c) Top-down image of the specimen wedge sectioned from the mounted specimen using the FIB. (d) Specimen mounted on the post before final preparation.

ABGorman.indd 1 06/21/2008 1:38:14 PM

SII

SII NanoTechnology USA Inc.

Silicon Multi-Cathode X-Ray Detector

NO LN2 • Active area ~ 50 mm² • <133 eV FWHM at 5.9 keV • ICR 1.5 Mcps • OCR up to 600 kcps



SO FAST
IT WILL TAKE YOUR "BREAK" AWAY!

introducing e-Xpress EDS

EDS - Fast Mapping • SEM - Microanalysis • Process Control

SII NanoTechnology USA Inc. • 19355 Business Center Drive, Suite 9, Northridge, CA 91324 • TEL: 818-280-0745 • FAX: 818-280-0408 • www.siintusa.com

MT Full Page Ad Master.indd 1 06/21/2008 1:49:28 PM

techniques such as EDS and EELS as well as STEM-HAADF imaging can also give preliminary information about the composition of precipitates and interfaces, which again can aid in the scaling of the evaporation field during atom probe analysis and reconstruction.

In addition to pre-atom probe TEM analysis, post-atom probe analysis gives insight into how specimens with varying compositions evaporate under the influence of a high electrical field or laser pulse. This is particularly useful in the simultaneous analysis of high and low conductivity materials (such as high-*k* dielectric / gate interfaces or oxide precipitates in metals), where the lower conductivity materials alter the local electric field and thus the sequence of evaporation. It has been previously observed that oxide inclusions evaporate much later in sequence than a metallic glass matrix [6], purportedly due to the lack of sufficient field to break the oxide bonds and cause evaporation.

Post-atom probe analysis can also give insight into why certain atom probe specimens fail during analysis, such as delamination at interfaces or dielectric breakdown. Finally, post-analysis also has the advantage of quantifying specimen irregularities induced by the laser or electric field, such as amorphization or phase separation.

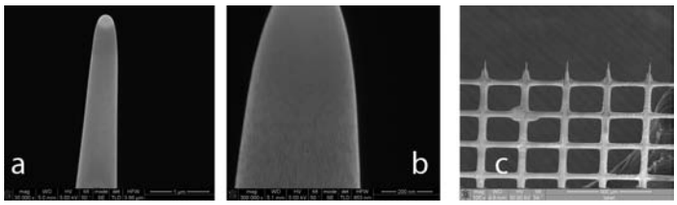


Figure 4. SEM images of the final specimen preparation steps. (a) Final shaped specimen following 5kV cleanup step also illustrating the region of interest. (b) Higher magnification image illustrating structure in the ROI. (c) Image of the grid posts after final preparation of the specimens.

Top-down specimen preparation

The usefulness of performing TEM and atom probe on the same specimen makes it beneficial to have an easy method for transferring specimen arrays from the FIB to the TEM and finally to the atom probe. To that end, as well as to minimize the handling of the fragile specimens, UNT and Hummingbird Scientific Instruments developed hardware to accept FIB liftout specimens onto 1-D arrays (Figure 1). Since the geometry of the local electrode necessitates

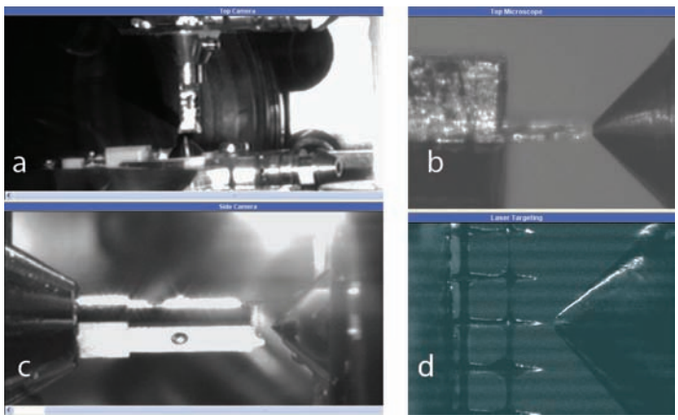


Figure 5. Optical microscope images of the TEM grid mounted specimens inside of the local electrode atom probe. (a) Top and side low-magnification images of the grid mount in proximity to the local electrode. (b) Higher magnification images of the grid mounted specimens in the analysis position next to the local electrode.

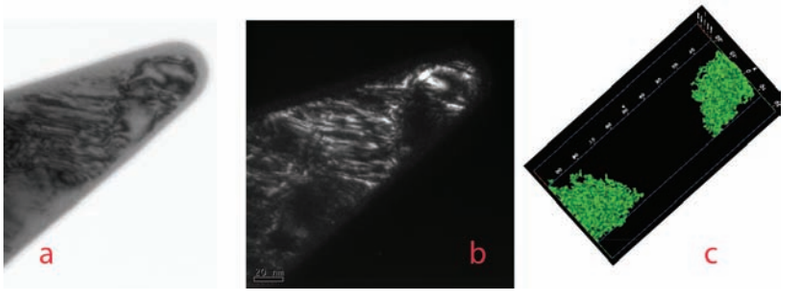


Figure 6. (a) Bright field and (b) dark field TEM images of a TiNiPt specimen. (c) Atom probe reconstruction of the same specimen in (a) and (b), illustrating the location of Ni-rich regions of the specimen.

specimens be separated by approximately 200 μm, we utilized standard 3 mm diameter, 100 mesh grids sectioned such that a vertical portion of each grid bar extended approximately 150 μm beyond each horizontal grid bar.

A jig was specially designed to guide the grids into proper position, after which the grids are secured into the end effectors by a clamp tightened with a screw (figure 1b). The jig also is designed to align and position the grid for proper sectioning. Once securely held in the grid effector, the grid does not need to be directly handled again for any of the processing or analysis. Figure 1c shows the grid effector loaded onto the TEM stage, specifically designed for an FEI Co. Tecnai F20ST. Since the grid effector has a narrow horizontal cross section of approximately 3mm, very high tilts (±80° using the center post) are possible. Using a modified grid effector and specialized grids, similar tilts have been demonstrated in small pole piece instruments. Once loaded into the TEM, the atom probe specimens are inherently positioned directly down the alpha tilt axis of the stage, allowing excellent tomography data to be acquired [7].

Once loaded and sectioned, the grids are further processed to minimize the bar cross section and therefore minimize FIB milling time. The grid effector can then be loaded into the FIB (in this case an FEI Nova 200 equipped with an Omniprobe Autoprobe 250) with the grid bars oriented vertically. FIB specimen preparation is similar to that developed for 2-D arrays. First, a region of interest is protected with e-beam and ion beam deposited Pt (Figure 2). FIB cutting is next used to cut a wedge-shaped cantilever from the region of interest. This piece is attached to an *in-situ* manipulator and transported to the posts on the grid. There, it is sectioned into an individual specimen by attaching the base of the wedge to a post and then FIB cutting to remove this area from the rest of the extracted wedge (Figure 3). This process is repeated to produce between 6 and 8 specimens for each liftout.

Sectioned specimens now attached to the grid posts are tilted parallel to the ion beam and sharpened using a series of decreasing diameter annular mills to produce the geometry required for atom probe analysis. Figure 4 shows a series of SEM images illustrating these final preparation steps. Milling can be terminated before the region of interest is reached by continual imaging with the SEM column. Reducing the FIB accelerating voltage to 5kV or lower removes a significant portion of the amorphization damage induced by the FIB [3].

Due to their diameter typically being in the electron transparency region, sharpened atom probe specimens can be directly transferred to the TEM stage (figure 1) and analyzed for relevant

ABGorman.indd 2 06/21/2008 1:38:15 PM

Tulane Univ (New Orleans) Seeks Experienced Confocal Microscopist.

MIN QUALIFICATIONS: BS
PREFERRED QUALIFICATIONS: MS

JOB DUTIES: Supervises CIF confocal microscopy lab, which includes Zeiss LSM510. Performs microscopy analysis, sample prep and data reduction.

Trains users in proper prep of samples and use of lab instruments.

Monitors instrument performance. Performs routine maintenance. Assists with repairs.

Collaborates with faculty and other scientists.

Qualified applicants should apply on-line at www.profilesams.com/tulane

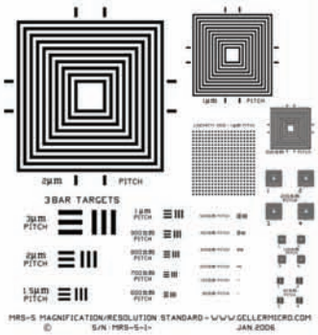
MRS-5

We are ISO-9000 certified and ISO-17025 accredited

Microscopy Calibration Standard

Now you can calibrate from 1,000X to 1,000,000X!

This is our fourth generation, traceable, magnification reference standard for all types (SEM, FESEM, Optical, STM, AFM, etc.) of microscopy. The MRS-5 has multiple X and Y pitch patterns ranging from 80nm (±1nm) to 2µm and 3 bar targets from 80nm to 3µm. There is also a STM test pattern.



Free web resource guide!

GELLER MICROANALYTICAL LABORATORY, Inc.

426e Boston St., Topsfield, Ma 01983
www.gellermicro.com

STOP HASSLING WITH MULTIPLE SERVICE CONTRACTS!

START by putting all of our instruments under one service contract with MAS (regardless of make or model). Our expert **EM SERVICE GROUP** has the knowledge and skills to keep your instrument working at its best.

TEM'S / SEM'S		PREP EQUIPMENT	SPECIAL SERVICES
HITACHI	TOPCON	VACUUM COATERS	STAGES
JOEL	ISI	PLASMA ASHERS	BEAM BLANKERS
AMRAY	CAMBRIDGE	SPUTTER COATERS	CUSTOM DEVICES
		ION MILLS	

NEW NEW NEW

Authorized service representatives for Gatan preparation equipment and Topcom TEM'S.

Contracts and On-Demand Emergency Service at Reasonable Rates from Factory Trained Specialist

MAS

800-421-8451

3945 Lakefield Court Suwanee, Georgia 30024 770-866-3200 FAX 770-866-3259
ADVANCED ANALYTICAL PRODUCTS AND SERVICES

MT_Half over 2 qtr pg ads.indd 1 06/21/2008 1:57:53 PM

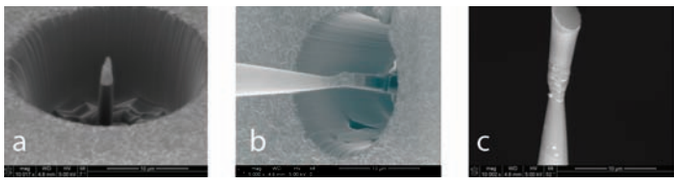


Figure 7. SEM images of (a) a FIB milled site-specific cylindrical specimen and (b) a manipulator needle attached to the top surface of the specimen using Pt deposition. (c) SEM image of the specimen following a FIB cut to remove the site-specific specimen.

structural information including their geometry, crystallography, and internal interfaces. As noted earlier, the specimens can also be easily examined using TEM tomography to high tilts. While obvious, it is nonetheless worthwhile noting that cylindrical specimens do not have the difficulties of planar specimens, in that the effective thickness remains constant with tilt angle.

Following TEM examination, the 1-D specimen effector then fits directly into a specimen holder ("puck") for atom probe analysis. The grid effector was designed such that the specimens sit at the center of the TEM stage and also have the clearance to fit near the local electrode within the atom probe. Figure 5 illustrates the 1-D grid design when used in the atom probe. The 1-D array allows for simple alignment of the specimens with the local electrode as well as with the laser pulse. One particular advantage of the 1-D array over 2-D arrays is that when properly aligned in laser pulsed mode, any laser energy that is not absorbed by the specimen simply passes through. 2-D arrays can facilitate the absorption of excess laser energy by specimens sitting within the laser's flight path beyond the sample being analyzed.

An example of cross-correlative TEM and atom probe analysis is illustrated in figure 6. This particular specimen is a TiNiPt alloy where segregation at the nanoscale can dominate the high temperature mechanical properties. Bright field and dark field images of a specimen prior to atom probe analysis are shown in figures 6a and 6b. These images were used to set the specimen diameter and shank angle for the atom probe reconstruction, as well as to note initially where phase segregation may be occurring. Figure 5c shows a nickel isosurface reconstruction of the atom probe analysis, completed using an Imago Scientific Instruments LEAP 3000x in laser pulsed mode. From this reconstruction, the atomic concentration and geometry of the Ni-rich particles and the matrix was directly determined in 3-D and compared with the TEM images of the particles.

Site-specific backside specimen preparation

In many applications, atom probe and TEM analysis is desired at highly site specific positions. Examples include phase segregated region in alloys, grain boundaries in ceramics, individual devices in semiconductor components, or even mechanical failures such as crack tips and indentations. In some cases, the FIB wedge-liftout specimen preparation technique can be utilized, but for others it may be difficult to properly align the feature of interest axially on the post and retain the feature of interest at the specimen tip after FIB milling. This is especially true for materials that have different sputtering rates, such as oxides in metallic matrices and the widely varying compositions present in semiconductor devices.

Atom probe analysis can be significantly inhibited by the presence of insulating materials within the specimen. Dielectric layers can lead to field concentrations, and ultimately specimen fracture during analysis. Our group has noted this effect significantly in semiconductor devices processed on silicon-on-insulator (SOI) wafers. In order to eliminate this issue, we have utilized backside (substrate side towards the atom probe detector) specimen preparation where the SOI layer is FIB milled away before analysis. Typically, this requires *ex-situ* specimen and nanomanipulator rotations that are time consuming and unreliable.

In order to expedite site-specific, backside atom probe specimen preparation, a simple adaptation to Omniprobe's Short Cut ™ technique [8] and grid geometry enabled this technique to be utilized. Preparation begins similar to the wedge liftout technique, where our area of interest is first protected using a combination of e-beam and ion beam deposited Pt to define and protect our area of interest. The major difference between the two techniques is in the amount of area defined. For the wedge technique, an area approximately 2 × 20 μm is required, where the site specific technique only requires a circular area approximately 500 nm in diameter.

After the area of interest has been defined by the metal deposition, a cylindrical post is cut from the sample (Figure 7a). The specimen is then rotated such that the nanomanipulator is parallel to the long axis of the cylinder. Again using FIB deposition, the nanomanipulator is attached to the cylinder (Figure 7b), and the cylinder cut loose (Figure 7c).

Once removed from the sample, the specimen is left attached to the nanomanipulator and loaded into the Short Cut jig *ex-situ* (Figure 8). An anvil subsequently cold forms the nanomanipulator needle into the grid material while concurrently sectioning the needle. The final specimen form (Figure 8b) gives line of sight access from the specimen tip to the atom probe optics. A specific advantage of forming the manipulator tip to the grid material is that TEM examination of the atom probe specimen is still achievable. If TEM is not going to be used, the nanomanipulator needle itself can be loaded into the atom probe. It should also be noted that since this

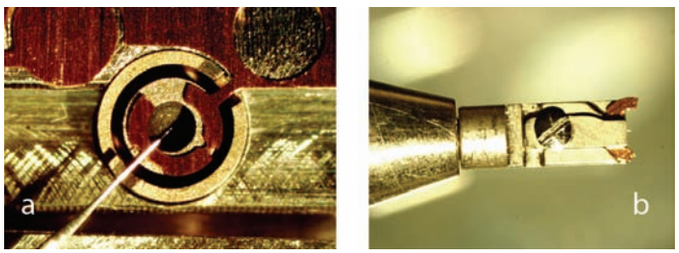


Figure 8. (a) Optical image of the nanomanipulator placed in the Short Cut™ anvil alignment jig. (b) Optical image of the nanomanipulator and site-specific specimen mounted to a TEM grid and placed in the TEM holder. The Cu grid is specially designed to allow atom probe analysis of the prepared specimen.

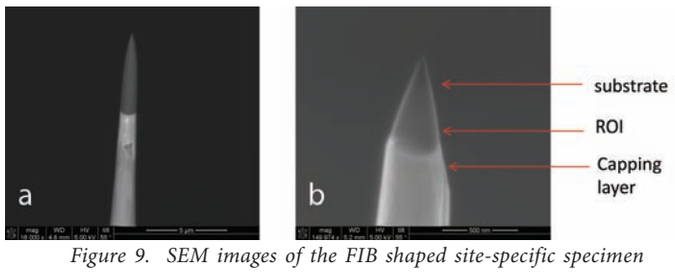


Figure 9. SEM images of the FIB shaped site-specific specimen illustrated in figures 7 and 8. (a) Image of the manipulator needle, Pt capping layer and weld, and specimen. (b) Image of the specimen after 5kV cleanup FIB mill. Note the specimen orientation difference from the first technique, with the substrate to be analyzed by atom probe before the ROI.

ABGorman.indd 3 06/21/2008 1:38:15 PM

technique produces only a single specimen, a local electrode atom probe is not required.

Site-specific specimens prepared using this technique can subsequently be loaded into the grid effector used with the 1-D array (Figure 1). The effector and grid are then placed back into the FIB for final preparation of the specimen. Figure 9 shows the final geometry of these specimens once prepared. Again, in contrast with the wedge liftout technique, the sample substrate is facing the detector with the region of interest protected during FIB milling by the substrate.

In addition to being site-specific and eliminating layers that would normally cause difficulty during atom probe analysis, this technique is also much more rapid compared with the wedge liftout technique. This technique also requires less FIB time during initial metal deposition and specimen removal, as well as during final preparation FIB milling. Disadvantages are that only a single specimen is prepared (not usually a concern for site-specific preparation), and that some of the preparation must currently be completed *ex-situ*.

Utilizing EDS and EBSD in a combination FIB and SEM makes the best utilization of this site-specific technique. EDS spectral maps can illustrate areas of varying composition that are most interesting for atom probe analysis. EBSD maps illustrate variations in crystallographic phases and grain boundary orientations, again which may be of most interest for atom probe analysis.

The geometry of the specimens when using these site-specific techniques is particularly advantageous for TEM tomography. Cylindrical specimens do not change thickness with tilt angle, and the geometry of the grid and specimen are such that the grid will not enter the specimen field of view during tilting, making 360° rotations possible.

Summary

Techniques and hardware are introduced that enable the simple, reliable cross-correlative examination of FIB prepared atom probe specimens in the TEM. Utilizing previously developed FIB techniques in 1-D arrays, cross-correlative TEM and local electrode atom probe characterization is demonstrated. Adapting the Short Cut™ technique to atom probe specimens allows for rapid preparation of site-specific specimens from the substrate side of the sample rapidly and with high precision. ■

Acknowledgements

The use of instrumentation at UNT's Center for Advanced Research and Technology is gratefully acknowledged. Laboratory assistance at UNT from Kris Mahdak is also gratefully acknowledged.

References

1. Miller, M.K. (2000). *Atom Probe Tomography: Analysis at the Atomic Level*. New York: Kluwer Academic.
2. Kelly, T. F., et. al. (2004) First Data from a Commercial Local Electrode Atom Probe. *Microsc. Microanal.* **10**, 373-383.
3. Thompson, K., et. al. (2007) *In-situ* Site-specific Specimen Preparation for Atom Probe Tomography. *Ultramicroscopy* **107**, 131-139.
4. Kelly, T. F., et. al. (2007) Atom Probe Tomography of Electronic Materials. *Ann. Rev. Mat. Res.* **37**, 681-727.
5. Gorman, B. P. , Norman, A. G., Yan, Y. (2007). Atom Probe Analysis of III-V and Si-based Photovoltaic Structures. *Microsc. Microanal.* **13**, 493-502.
6. Gorman, B. P., *et. al.* (2008) Cross-Correlative TEM and Atom Probe Analysis of Partial Crystallization in NiNbSn Metallic Glasses. *Mat. Sci. and Tech.* in print.
7. Gorman, B. P., Diercks, D. R, Jaeger, D. (2008) Cross-correlative TEM and Atom Probe Tomography. *Microsc. Microanal. Suppl. 2*, in print.
8. Moore, T. M. (2006) Apparatus for Preparing a TEM Sample Holder. *U. S. Patent 7126132*.



ABGorman.indd 4 06/21/2008 1:38:18 PM

Imaging Skin Epidermal Stem Cells: A Review

Hilda Amalia Pasolli
The Rockefeller University New York, NY
pasolla@rockefeller.edu

Nature has provided us with a wonderful outer surface, the skin. We humans are fascinated with our epidermis and hair. We spend an exorbitant amount of time and money on skin and hair maintenance. We try hard to keep it soft, smooth, radiant, tan or pale, clean or made-up. We try to remove hair from some areas as hard as we try to keep it on others. Only when our skin is afflicted by disease, burns, wounds, or scratches is it apparent that this amazing outer shell protects us from dehydration and infections. To perform this crucial protective function and to be able to respond to injuries, skin needs to undergo self-renewal to repair damaged tissue and to replace old cells. For this formidable task, skin depends on stem cells. Stem cells have the ability to self-perpetuate and to give rise to differentiating cells that constitute one or more tissue types.

Epidermis and hair follicles

Epidermis is composed of layers, the outermost of which is the skin surface. The innermost layer, the basal one, is composed of proliferative cells, which attach to the underlying basement membrane. The basal layer stratifies to give rise to the differentiated cell layers of the spinous layer, granular layer and the stratum corneum (Figure 1). This wonderful architecture is maintained through a diversity of intercellular junctions such as adherens junctions, desmosomes, and tight junctions while hemidesmosomes and focal adhesions provide attachment to the basement membrane. Epidermis homeostasis is maintained by balancing cellular proliferation in the basal layer with the outward flux of terminally differentiating cells moving outward to form the spinous, granular and stratum corneum layers, which will eventually be sloughed from the skin surface.

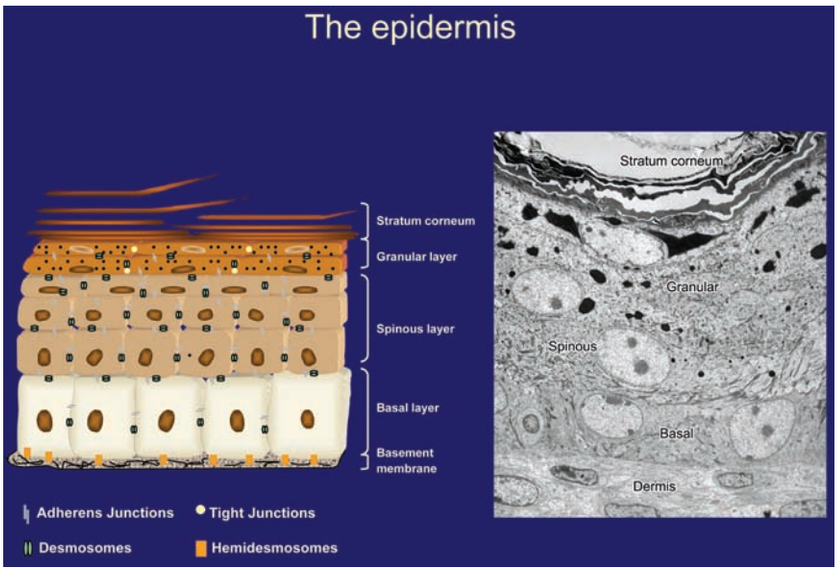


Figure 1. Mammalian skin consists of the epidermis and dermis, separated by a basement membrane. The epidermis is a stratified squamous epithelia that is composed of several cell layers. Resting on the basement membrane is the basal layer (BL), consisting of proliferating, transit-amplifying cells (see text). The basal layer stratifies to give rise to differentiated cell layers of the spinous layer (SL), granular layer (GL) and the stratum corneum (SC).Epidermal cells is kept together by different types of intercellular junctions (adherens junctions, desmosomes, tight junctions) and attach to the basement membrane by hemidesmosomes. At the right, micrograph of mouse epidermis as viewed with the transmission electron microscope.

One of the most remarkable features of mammalian epidermis is its ability to generate appendages, such as hair follicles, sebaceous glands, and sweat glands. I will focus on the description of hair follicles. Hair follicles are amazingly complex structures (Figure 2A): they are composed of an outer root sheath (ORS) that is contiguous with the epidermis, an inner root sheath (IRS), and the hair shaft itself. The IRS and hair shaft are each composed of three different layers. The hair bulb, at the base, contains actively proliferating undifferentiated cells, the matrix, which gives rise to the IRS and hair shaft cell layers. The matrix encloses a pocket of specialized mesenchymal cells called the dermal papilla (DP).

The lower segment of each hair follicle cycles through periods of active growth (anagen), regression (catagen), and rest (telogen) (Figure 2B). During anagen matrix cells divide rapidly. As they move upward they differentiate, giving rise to the IRS and hair shaft layers. During catagen the lower follicle undergoes apoptotic cell death. The DP moves upward until it rests beneath the bulge, where it remains during telogen. The follicle can then prepare for the next cycle of growth. The bulge resides in the ORS, in a small niche below the sebaceous gland, at or near the insertion of the arrector pili muscle.

How to identify stem cells: label retention

One of the most distinctive attributes of stem cells of the hair follicle is that they divide infrequently. This is most probably in order to preserve their proliferative potential and to avoid errors in DNA sequence that could occur during replication. In their search for skin stem cells, Cotsarelis and colleagues (Cotsarelis et al, 1990) made a major breakthrough when they noticed that mouse skin stem cells that retained a DNA label ([^{3}H] thymidine) were located in the hair follicle bulge. Cells that rarely divide (such as stem cells) will be able to keep their DNA label and hence can be identified as label-retaining cells (LRCs). On the contrary, cells that are actively proliferating will soon 'dilute out' the DNA label in subsequent cell divisions. The bulge is an attractive location for skin epithelial stem cells for several reasons: it resides at the base of the permanent part of the follicle where stem cells are in a convenient position to regenerate the hair at the end of each hair cycle, and they are in a close and contiguous position to reconstitute wounded epidermis. The deep position of the bulge also guards the stem cells from mechanical stress and from sunlight-induced mutations, which is crucial for cells that must maintain an intact genome for many years.

Label-retaining cells work as stem cells

Following the identification of LRCs, the next challenge was how to verify that these cells can indeed function as stem cells. Purifying and characterizing LRCs as stem cells required a method to isolate these cells and permit their manipulation for prospective therapeutic use. The Fuchs and Cotsarelis labs utilized fluorescence activated cell-sorting (FACS) to sort bulge cells from mouse hair follicles based on specific labels.

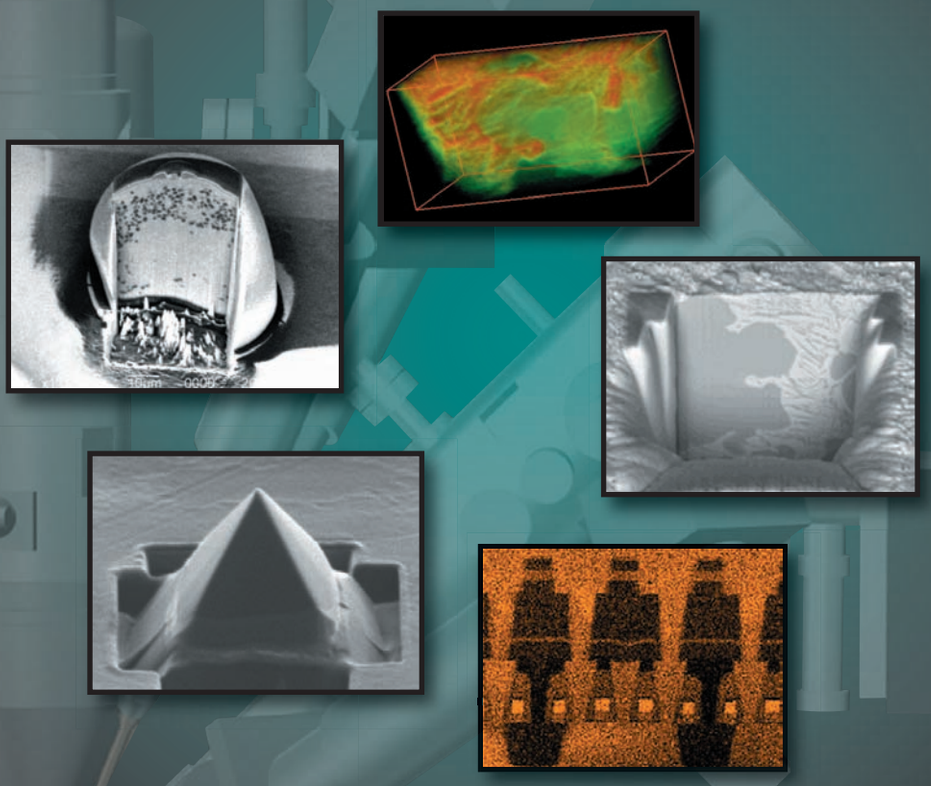
The Fuchs lab induced for a limited time the expression of a keratin 14 (K14) promoter-driven transgene, encoding a long-lived histone tagged with green fluorescent protein (GFP) (Tumbar et al, 2004).

ABPasolli.indd 1 06/21/2008 2:19:05 PM

Power Tool for Grownups

MultiBeam - look - build - analyze - in real time

NanoFabrication





JIB-4500

Another
Extreme imaging
solution

JEOL

Stability • Productivity • Performance
www.jeolusa.com • salesinfo@jeol.com
978-535-5900

Who says you can't afford to have it all? High-resolution imaging, bitmap milling, TEM sample prep, and high-speed slicing and sampling in real time with this all-in-one SEM/FIB. The new JEOL MultiBeam combines the world's most popular low vacuum LaB_6 electron column with high resolution ion beam optics. Utilize the full power of the MultiBeam power tool for your next nanofabrication project. For more information visit www.jeolusa.com/multibeam.

MT Full Page Ad Master.indd 1 06/21/2008 2:38:13 PM

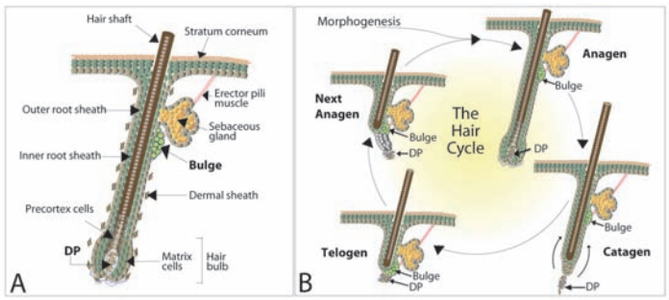


Figure 2: Schematic of an anagen (A) and cycling (B) hair follicle. Hair follicles undergo periodic cycling from anagen (hair producing) through catagen (regression), and into telogen (resting). (A) In the anagen hair follicle the dermal papilla (DP) is enclosed within the hair bulb, and the bulge is nestled below the sebaceous gland. (B) During the hair cycle, the proximity of the DP and the bulge varies, with the closest contact occurring at telogen as the follicle prepares for a new anagen. Reprinted by permission from Cold Spring Harbor Laboratory Press: Laura Alonso and Elaine Fuchs, **G***enes Dev. 2003; 17: 1189-1200*

The isoform keratin 14 is specifically expressed in the basal cells of epidermis and ORS cells, which includes bulge cells. Histones are proteins that bind to the DNA. Therefore we could make all cycling keratin 14 expressing cells GFP-positive. By administering a drug to the mice, we could turn off the expression of the transgene and wait for months to 'wash out' the GFP label from actively dividing cells. We found, as predicted, that the GFP-label-retaining cells were located in the hair bulge. Then, standard FACS could be used to isolate and characterize the cells expressing high levels of GFP.

In addition to this, research by the Morris and Cotsarelis group showed that the intermediate filament protein keratin 15 (K15) was primarily expressed in the bulge region and relatively rare in other skin epithelial cells (Morris et al, 2004). They proceeded and marked LRCs. They engineered mice in which the K15 promotor drives the expression of GFP, thus also allowing FACS-based sorting of cells into those expressing high levels of GFP. More recently, the purification of bulge stem cells have been accomplished in our lab by FACS based on the expression of bulge surface markers such as α6 integrin and CD34 coupled with K14-GFP expression (Blanpain et al, 2004).

The new methods to purify bulge cells allowed researchers to perform clonal analyses and engraftment and demonstrate the two defining features of stem cells, namely self-renewal and pluripotency. When cultured bulge cells and dermal cells were grafted onto the back of *Nude* mice (*Nude* mice are a mice strain which due to a genetic defect lack hair), they were able to regenerate epidermis , hair follicles and sebaceous glands showing that our bulge-derived skin cells were indeed multipotent stem cells (Blanpain et al, 2004). The Cotsarelis group showed that the K15 bulge cells could produce all the epithelial components of the anagen follicle (Morris et al, 2004).

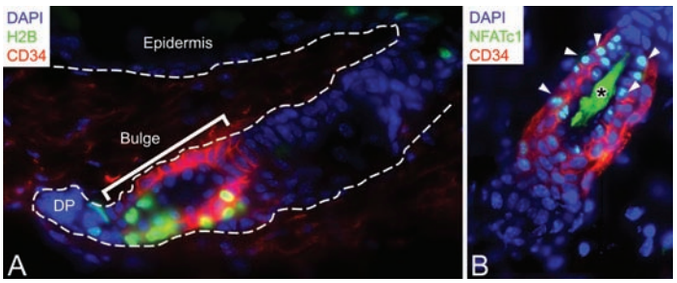


Figure 3. Bulge stem cell markers. *Hair follicles in resting phase (telogen). Skin stem cells reside in their niche, the region of the hair follicle known as the bulge. Slow-cycling cells retain the label for histone 2B-green fluorescent protein (A) The stem cells express a surface marker, CD34. Fig. B: NFATc1 is expressed in bulge stem cells (arrowheads) DAPI stains all nuclei. Asterisk indicates hair shaft autofluorescence. DP, dermal papilla.*

These methods have allowed to not only identify and image bulge LRCs, but also to characterize their gene expression by performing microarray analyses. Approximately 150 genes are preferentially expressed in the bulge relative to the proliferating basal cells of the epidermis. Although each of these procedures purifies slightly different cell populations, the array data are in quite good agreement, enabling researchers to exploit this information to learn more about follicle stem cells. Analysis of genes expressed by bulge stem cells allowed researchers to identify further markers of this population such as the transcription factors Lhx2, NFATc1, and Sox9 (Horsley et al, 2008, Rhee et al, 2006) and to elucidate how these transcription factors act to maintain the bulge stem cell niche.

Skin epidermal stem cells: future challenges

Bulge cells are so far the best characterized stem cells in skin. We know that they can regenerate the hair follicle, the sebaceous gland and repair wounded epidermis. There are still other mysteries. Questions such as how is the homeostasis of unwounded epidermis maintained? How is the differentiation of other important skin appendages such as sebaceous and sweats glands specified and maintained? Do they also have their own stem cell population? There is more and more evidence that interfollicular epidermis has its own population of stem cells. Progress in our lab has shown that the sebaceous gland has its own progenitor cells (Horsley et al, 2006; for a review see Horsley and Fuchs, 2008).

The characterization of skin stem cells triggers additional exciting questions: could they be used to repair skin and regenerate hair in humans? Could they be used as a means to deliver corrective gene therapy for skin disorders and maybe even non skin disorders? Would these stem cells have the plasticity to differentiate into non skin cell types? The answer to these exciting questions will most probably be revealed in the coming years. ■

Acknowledgments

My thanks to Bob Marks for correcting the manuscript and to my colleagues: Valerie Horsley for critical reading and for valuable suggestions, Valentina Greco and Geraldine Guasch for providing immunofluorescence pictures.

References

Blanpain C, Lowry WE, Geoghegan A, Polak L, Fuchs E., Self-renewal, multipotency, and the existence of two cell populations within an epithelial stem cell niche. *Cell*. 2004 Sep 3;118(5):635-48.

Cotsarelis G, Sun TT, Lavker RM., Label-retaining cells reside in the bulge area of pilosebaceous unit: implications for follicular stem cells, hair cycle, and skin carcinogenesis. *Cell*. 1990 Jun 29;61(7):1329-37.

Fuchs E, Horsley V., More than one way to skin . . ., *Genes Dev*. 2008 Apr 15;22(8):976-85.

Horsley V, Aliprantis AO, Polak L, Glimcher LH, Fuchs E., NFATc1 balances quiescence and proliferation of skin stem cells. *Cell*. 2008 Jan 25;132(2):299-310.

Horsley V, O'Carroll D, Tooze R, Ohinata Y, Saitou M, Obukhanych T, Nussenzweig M, Tarakhovsky A, Fuchs E. Blimp1 defines a progenitor population that governs cellular input to the sebaceous gland. *Cell*. 2006 Aug 11;126(3):597-609.

Morris RJ, Liu Y, Marles L, Yang Z, Trempus C, Li S, Lin JS, Sawicki JA, Cotsarelis G., Capturing and profiling adult hair follicle stem cells. *Nat Biotechnol*. 2004 Apr;22(4):411-7. Epub 2004 Mar 14.

Rhee H, Polak L, Fuchs E., Lhx2 maintains stem cell character in hair follicles. *Science*. 2006 Jun 30;312(5782):1946-9.

Tumbar T, Guasch G, Greco V, Blanpain C, Lowry WE, Rendl M, Fuchs E., Defining the epithelial stem cell niche in skin. *Science*. 2004 Jan 16;303(5656):359-63.

ABPasolli.indd 2 06/21/2008 2:19:05 PM

Side-By-Side Comparison? Difficult When Our Coaters Stand Alone.



High Resolution Sputter Coater 208HR for FE-SEM

Superior Features:

- High Resolution Fine Coating
- Wide Choice of Coating Materials
- High Resolution Thickness Control
- Multiple Sample Stage Movements
- Wide Range of Operating Pressures
- Compact, Modern, Benchtop Design



Find out about our complete line of sample coaters.

TED PELLA, INC.
Microscopy Products for Science and Industry

4595 Mountain Lakes Blvd., Redding, CA 96003-1448
Phone: 530-243-2200 or 800-237-3526 (USA) FAX: 530-243-3761
Email: sales@tedpella.com Web Site: www.tedpella.com

MT Full Page Ad Master.indd 1 06/21/2008 2:43:42 PM

Signature Analysis Applied to EDS Microanalysis

J.W. Colby & D. C. Ward
xk, Incorporated, Clackamas, OR[1]
denniscward@earthlink.net

Most spectroscopies (FTIR, XRD, RAMAN, MS, etc.), were developed in order to identify materials. This is accomplished by capturing the spectral "signature" of an unknown and matching it to those of a comprehensive database of reference materials. Development of these spectroscopies has included efforts to embellish the associated database. EDS evolved as a resource to provide qual/quant, and development has been to improve the accuracy of quantation. Until recently, EDS was not considered a spectroscopy to provide identification of materials.

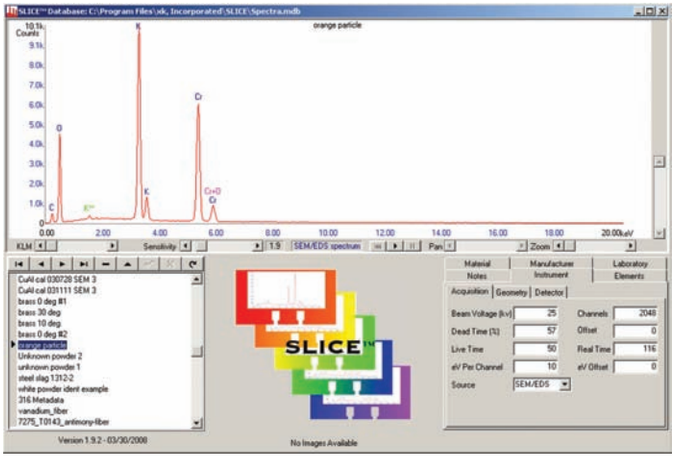


Figure 1 – Main spectral display window

In order to fully utilize SEM/EDS the Federal Bureau of Investigation evaluated the current capability to meet mission requirements for trace material characterization. It became readily apparent that a compositional approach was not sufficient, as; comparison of composition is not sufficiently discriminating, the composition of many materials is not known, and the determination of composition could not always be determined accurately for the variety of materials anticipated.

Even for the "suitable" sample, the difficulty in selecting the model and parameters for quantitation can be demonstrated in a computer program developed and patented by C. E. Fiori and C. R. Swyt at NIST in 1994, which allowed one to calculate a spectrum theoretically from a hypothetical sample. In use, the operator could pick any one of several models and parameters from many sources, to achieve the calculated spectrum, and as might be anticipated, the resulting spectra varied considerably. In fact, by choosing the parameters and model properly (or improperly), one could obtain nearly any result anticipated.

It appeared that a "traditional" spectroscopy approach to EDS could be a powerful addition to quantitation. Therefore, in 1998, the FBI awarded xk, Inc. a contract to develop a relational database architecture and software to query the database. This led to the development of SLICE™ (Spectral Library for Identification and Classification Explorer). The program and database have evolved into a fully functional database program, which not only includes the

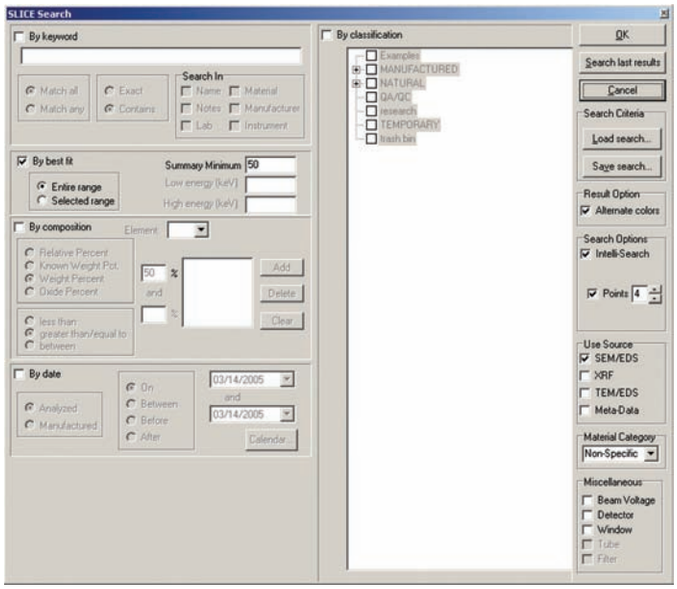


Figure 2 – Search Window for "Orange Particle"

spectra and chemistries, but also other metadata to facilitate and further refine the classification of spectra from unknown materials. Data mining, enhanced spectral display and comparisons, and a materials classification tree are also part of SLICE. In practice, the spectra in standard EMSA format as developed by Nestor Zaluzec, *et.al.* in 1991 and implemented by most EDS companies, are imported into SLICE. Chemistries may be imported if contained in the EMSA file, or may be determined within SLICE. Both peak ID and quant results may be executed within SLICE. Chemistries may be displayed as weight %, atomic %, relative %, or in the case of minerals, clay, *etc.*, as oxide %. Any additional known metadata are added to the stored spectrum, including text notes, sources, physical and instrumental parameters, *etc*. In addition, the spectrum may be archived with SEM and optical images, x-ray maps, PDF documents, spreadsheets, *etc,* all readily retrievable. Laboratories or individuals may build their own database and materials classification tree (text document) to suit their particular requirements. The current database[2] contains nearly 6000 spectra, from many material categories (alloys, SRM materials, minerals, commercial products, *etc.*). The main window of SLICE is shown in Figure 1, and

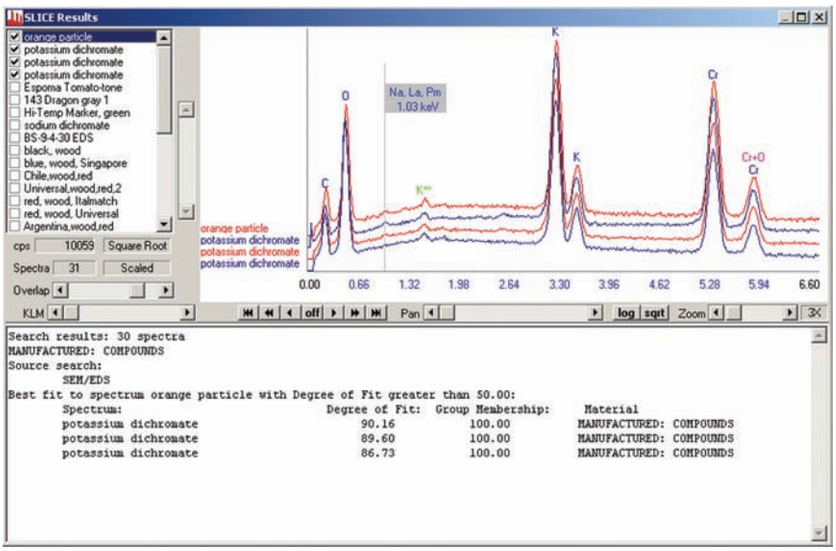
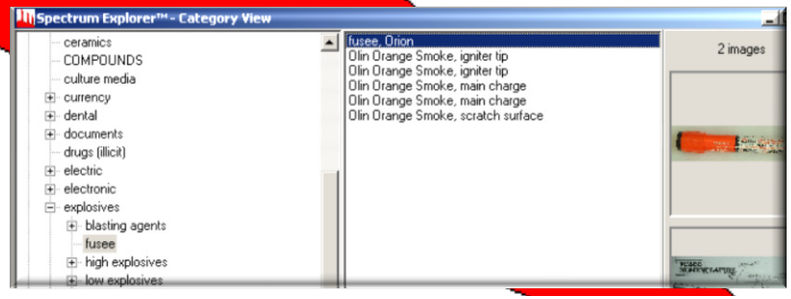


Figure 3 – Search results for the "orange particle". The spectra are displayed in the square root mode, and normalized about the cursor.

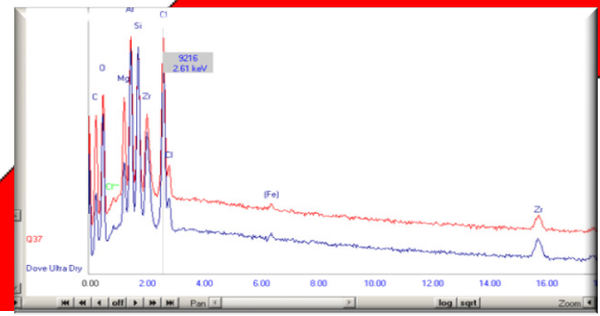
ABWard.indd 1 06/21/2008 3:01:41 PM

MT Full Page Ad Master.indd 1

Did you know there is much more to EDS than qual and quant?

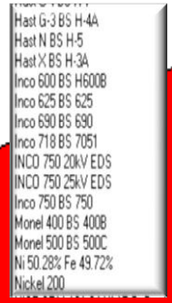


Explorer based data management

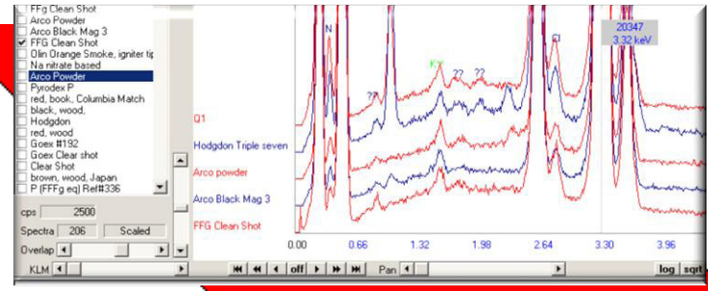


Best fit analysis for "identification"

SLICE*



1000's of reference spectra



Enhanced spectral display



And much more . . .

*Spectrum Library Identification and Classification Explorer

xk, Incorporated
www.xk.com
503.799.6015

06/21/2008 2:53:09 PM

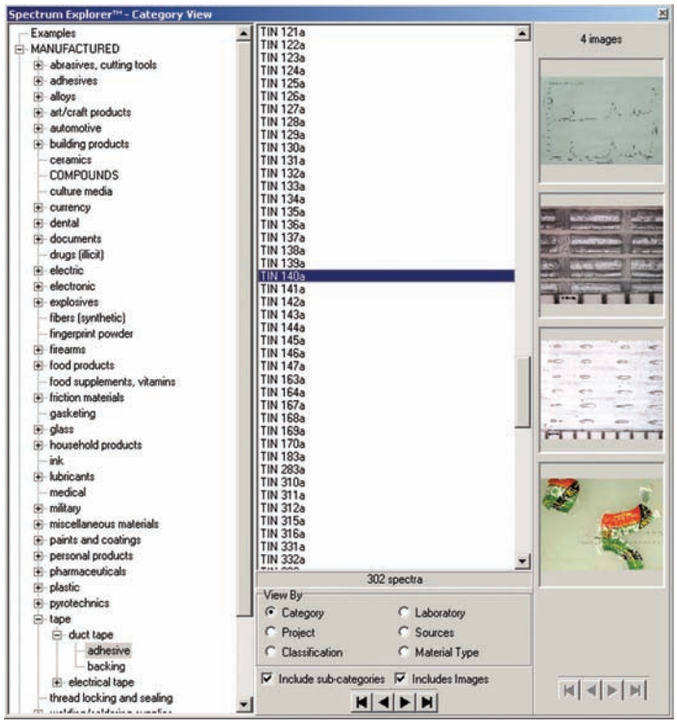


Figure 4, Spectrum Explorer, showing the classification tree on the far left, the associated images on the right, and the list of spectra in between.

consists of the spectrum from an "orange particle", and the metadata stored under the various tabs.

The notes section may contain URLs in addition to text information, and clicking the URLs will link to the appropriate web site if an external internet connection is available. Clicking the image or other documents displayed will automatically open them to full size images or documents. In this case, no images were stored with the spectrum.

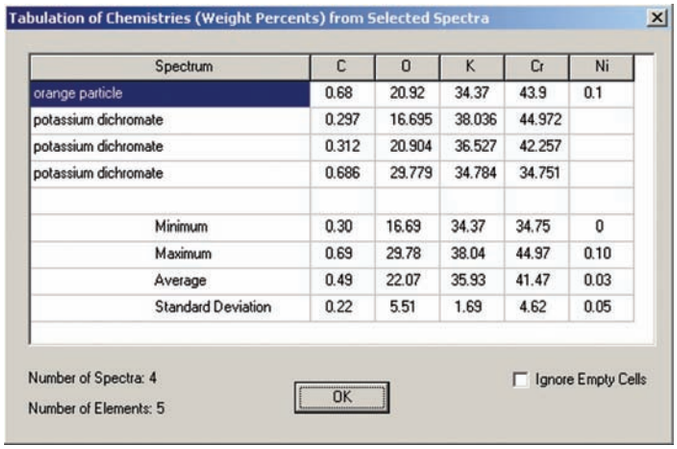
Users may create their own proprietary databases in addition to the one supplied with SLICE[2]. In cases of failure analysis or defect revue, SLICE and the associated database become an historical resource of similar prior defect occurrences, comparable to forensic evidence relating to serial criminal activities. Since the failure analysis report (*e.g.* MS Word or PowerPoint document) may be associated with the spectrum as an "image", subsequent to the database query, a simple click opens the document for comparison to the current problem.

Queries can be executed based on key words (names, material, laboratory, *etc*., and text within the notes section), best fit, composition, date, properties, classification, instrument parameters, source, and source properties, separately or in combination with each other. As an example, from the Search Page (Figure 2), the database is searched to find likely candidates to identify/classify the "orange particle" shown in Figure 1. The best-fit algorithms have been developed and optimized to be relatively insensitive to instrumental and operating parameters, to avoid some of the problems listed above.

Spectra may be compared as the result of Search queries (Figure 3), or by direct choice from within the Spectrum Explorer shown in Figure 4. Compared spectra can be displayed in the usual linear and log modes, and in square root mode. Overlapped spectra may be tightly or loosely overlapped, and normalized at any point in the spectra, statically or dynamically to facilitate comparison. The number of spectra overlapped can be chosen dynamically, and the metadata can be examined from any of the overlapped spectra. Data associated with the spectrum can also be tabulated.

The tabulated data can be properties specific to the material, or properties that are more general. Chemistries can also be tabulated (weight %, atomic %, *etc*.) and both chemistries and properties can be sorted in ascending or descending order. Statistics may also be displayed. The tabulated data can be copied and pasted into a document (*e.g.* MS Word or Excel) for further processing and/or report generation. The tabulated chemistries for the "orange particle" and potassium dichromate spectra are shown in Figure 5. The variations in chemistry are significant, and are due in part to the sample themselves not being flat, polished and homogeneous, as well as other uncertainties in the analysis. Nevertheless, the SLICE results strongly point to the particles being potassium dichromate. No other database entries are remotely close.

The majority of spectra in the current database are SEM/EDS spectra but TEM/EDS and XRF/EDS spectra are also included, and spectra of one type can be searched against spectra of another type (*e.g.* unknown XRF spectrum against both SEM and TEM spectra) although in general better results can be obtained against spectra of the same type.



Spectrum	C	O	K	Cr	Ni
orange particle	0.68	20.92	34.37	43.9	0.1
potassium dichromate	0.297	16.695	38.036	44.972	
potassium dichromate	0.312	20.904	36.527	42.257	
potassium dichromate	0.686	29.779	34.784	34.751	
Minimum	0.30	16.69	34.37	34.75	0
Maximum	0.69	29.78	38.04	44.97	0.10
Average	0.49	22.07	35.93	41.47	0.03
Standard Deviation	0.22	5.51	1.69	4.62	0.05

Figure 5 – Tabulated chemistries as weight percents from the "orange particle" and other potassium dichromate spectra

By providing utilities for archiving and querying data, SLICE provides EDS with significantly enhanced capability, putting it on a par with other, more classical spectroscopy. Although EDS has not historically been considered a spectroscopy that provides "identification," the inclusion of this capability is significant for disciplines such as forensics, failure analysis, and process control, where material sourcing is required. ■

References:

1. www.xk.com
2. The original spectral database for this project was heavily populated by the FBI. The database, as subsequently modified is provided with SLICE.

Editor's Note

This article was submitted along with the included advertisement in mid-May 2008 with instructions to place both items in the July 2008 MT issue. By mistake, I placed the article in the May issue, which upset xk's marketing plan. For this I extend my apologies. I deemed repeating the article, along with the advertisement in the July issue where it belongs as the only fair solution to this situation. Ron Anderson, MT Editor

ABWard.indd 2 06/21/2008 3:01:41 PM

DiATOME
diamond knives

Development, Manufacturing, and Customer Service since 1970

What have we achieved in this period?

ultra 45° the first diamond knife with an absolutely score-free, hydrophilic cutting edge.

semi the first diamond knife for alternating sectioning ultrathin/semithin.

cryo the diamond knife for sectioning at low temperature.

histo the first diamond knife for semithin sections for light microscopy.

ultra 35° the diamond knife for optimized sectioning results in almost all applications.

STATIC LINE II the ionizer for eliminating electrostatic charging in ultramicrotomy.

cryo-P a cryo knife with a patented platform for section pick up.

cryo immuno the optimized cryo diamond knife for the Tokuyasu technique.

ultra sonic the oscillating diamond knife for room temperature sectioning.

cryotrim 45 and 25 optimizing trimming with diamond blades.

ultra AFM & cryo AFM the first diamond knives for AFM at room and low temperatures.

cryo 25° for sectioning frozen hydrated specimens.

What services can we offer you?

- Technical assistance in all fields of ultramicrotomy.
- Free sectioning tests for all types of samples.
- Make use of our many years of experience in perfecting our knives.
- Custom knives, tools, and boats.
- Special purchase programs.
- Workshops and training.



For more information, please call or write us today, or visit us online at:

www.emsdiasum.com

DiATOME
for all your sectioning requirements

P.O. Box 410 • 1560 Industry Rd.
Hatfield, Pa 19440
(215) 412-8390 • Toll Free: 1-(800) 523-5874
Fax: (215) 412-8450 or 8452
email: sgkcck@aol.com • stacie@ems-secure.com
www.emsdiasum.com

MT Full Page Ad Master.indd 1 06/21/2008 2:47:28 PM

Cryo-Fracture or Freeze-Fracture, a Method to Expose Internal Tissue Surfaces and Cell Surfaces for Viewing in the Scanning Electron Microscope

Jeannette Taylor
Emory University, Atlanta, Georgia
jvtaylo@emory.edu

Cryo-fracture, in conjunction with critical point drying is a method used to prepare biological samples in order to expose, for viewing via scanning electron microscopy, those naturally occurring surfaces which might otherwise remain obscure. For example, the Bowman's capsule and tubules of a kidney, tiny blood vessels on any organ, inter-cellular spaces in liver or alveoli in the lungs. Also, some surfaces, not normally exposed at all such as the membrane surface of a nuclear envelope, mitochondria or chloroplasts or the cytoplasm of a cell, can be brought to light with this method. Herein is a review of the development of cryo-fracture and how it is currently used at our facility.

Cryo-fracture of biological material was introduced by G. H. Haggis in 1970 (1). Haggis presented two methods of freeze fracture. In one method, the tissue samples, about 0.5 mm in one dimension, were fixed for 24 hours in 2% glutaraldehyde in a buffered sucrose* solution, pH 7.4, and rinsed in distilled water for 4 hours to wash off any buffer salts that might crystallize on the tissue surface. The fixed tissue was plunge frozen in Freon 22 at -150°C, fractured at -170°C by a chilled blade and freeze dried at -80°C for 15 hours. A 20 to 30 nm coat of gold was evaporated onto the mounted samples for examination in the scanning electron microscope. An alternative method proposed was to plunge freeze unfixed (washed or unwashed) tissue and fracture it as above then freeze dry, mount and coat for viewing. As the sample prepared using both these methods were frozen while wet with water, there was ice crystal damage.

Combining critical point drying with freeze fracture was introduced by W. J. Humphreys, B. O. Spurlock, and J. S. Johnson in 1973 (2) as an alternative to freeze drying the freeze fractured tissue. The authors pointed out that critical point drying takes less time than the 15 hours for sublimation in freeze-drying. One major change in the freeze fracture method of Haggis was that the tissues were fixed and then dehydrated to 100% ethanol prior to freezing and fracturing in liquid nitrogen (-196°C). This technique was elaborated and refined in 1974 (3) by the same authors who described utilizing the Parafilm packets used to contain the dehydrated samples in the 100% ethanol during the freezing and fracturing steps. Substituting ethanol for the water in the specimens prior to freezing appeared to have eliminated ice crystal damage. The ethanol, held in place by the Parafilm packet, also filled all the voids and supported the tissue through the trauma of fracture. The authors described using a 2 cm strip of Parafilm wrapped around a 2 mm wooden dowel to form the cylindrical packets. The sealed Parafilm packets, filled with 100% ethanol and the ethanol-dehydrated tissue were submerged in liquid nitrogen until frozen. The frozen cylinder was next placed on a metal block chilled by liquid nitrogen and with a chilled razor blade, gently fractured while submerged in liquid nitrogen. The fractured pieces were immediately placed into a container of fresh 100% ethanol and allowed to thaw. Critical point drying followed.

The fracture surfaces, described as distinctly smoother and shinier, were mounted face up. A layer of 20 to 30 nm of gold was evaporated onto the samples prior to viewing in the scanning electron microscope. The authors cryo-fractured onion root tips, leaves, and the perused kidney and liver of a mouse.

The authors, Humphreys, Spurlock, and Johnson, ran a parallel study of tissues prepared through critical point drying after which they were placed into propylene oxide, embedded, and thin sectioned for transmission electron microscopy (TEM). Though these samples appeared to be well preserved, at the request of a reviewer, the authors followed with another parallel study in 1975, this time embedding and sectioning samples that had been not only prepared by freeze fracture and critical point drying but also coated and viewed in the scanning electron microscope. The gold-coated fractured surfaces were cut in cross-section exposing the plane of the fracture, the organelles at that edge and the metal coating (4). This work demonstrated that there was no cytoplasmic loss or shift at the freeze-fracture surface. The authors did note, however, that the evaporated coat of 37 nm of gold had an effect of obscuring any detail their scanning electron microscope might have been capable of resolving and suggested a thinner metal coating.

In 1977, G. H. Haggis, with B. Phipps-Todd, (5) presented a modification of the freeze fracture method, wherein the samples are fixed, dehydrated to 100% ethanol, frozen in liquid nitrogen and critical point dried. Their modification was to first infiltrate small (<0.5 mm) pieces of tissue samples with dimethylsulphoxide (DMSO), freeze in Freon 22 chilled by liquid nitrogen, fracture the tissue and then let it thaw in fixative containing 25% DMSO, followed by dehydration and critical point drying in that order. Their aim as they described it was to "wash out" the soluble proteins at the fracture face, thus revealing the 3D structure of the internal membranes, cytoskeleton, and cytoplasmic and structures of the plant and animal tissues which they used. They did have to contend with ice crystal damage but the DMSO helped to reduce it. The samples started in an appropriate buffer to which was added DMSO in 5% steps until 25% DMSO was reached. Haggis and Phipps-Todd described the 25% DMSO as a compromise between a higher concentration to reduce ice crystal damage and a lower concentration to reduce possible tissue damage by the DMSO itself.

As was noted previously, the fracture face of a fixed, dehydrated, freeze-fractured sample revealed little detail. This new freeze-fractured, thawed, fixed protocol offered whole nuclei, fibers, globules, lobes, fractured nuclei, chloroplasts and vacuoles. Haggis and Phipps-Todd prepared samples using both fracture methods but critical point dried their tissue, using CO_2 as the transition medium, rather than freeze- drying as Haggis had previously done. This fracture protocol seems to open up the cell to easy viewing but a lot can be lost. Using both methods in tandem would provide a fuller picture of cell organization. Alternatively, perhaps a very light fixation could be employed to just firm up the organelles.

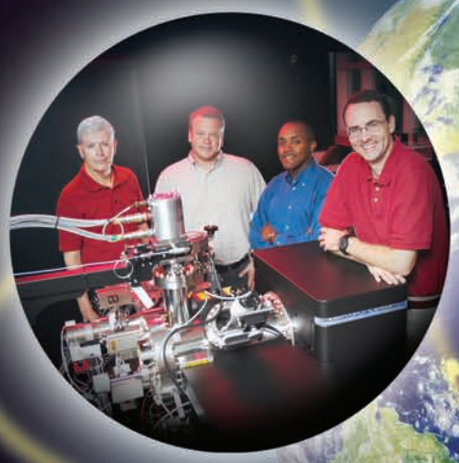
A further refinement on the pretty much standard freeze-fracture method of first fixing the tissue, dehydrating to 100%

ABTaylor cryo.indd 1 06/22/2008 8:56:55 AM

IMAGO SCIENTIFIC INSTRUMENTS

FEI COMPANY™
TOOLS FOR NANOTECH

Atom-Scale Information: Global-Scale Solutions





FEI® Titan™ S/TEM systems bring atom-scale imaging to labs around the world, and a growing number use Imago™ LEAP™ atom probe microscopes for atom-scale compositional analysis. It's a powerful combination for scientists and R&D labs working on global challenges in energy, water, food, disease, terrorism, crime, education, and the environment.

Now FEI offers the entire range of these state-of-the-art atom probe and S/TEM platforms, as well as industry-leading DualBeam™ systems for sample preparation. With FEI, you have a global partner to enable you with the most advanced atom-scale technologies for global-scale results.

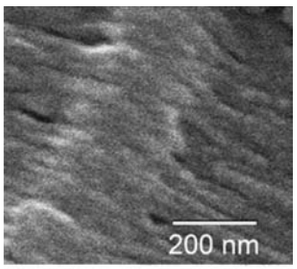
See more at fei.com

© 2008. The FEI logo, Titan and DualBeam are trademarks or registered trademarks of FEI Company. The Imago logo and LEAP are trademarks of Imago Scientific Instruments.

ethanol and then freeze-fracturing the tissue followed by critical point drying was made in 1981 by R. Apkarian and J. C. Curtis (6). Their study of ovarian follicles of immature rats employed cryofracture (same as freeze-fracture) to prepare samples for viewing in the scanning electron microscope. The authors made three refinements in the protocol. The fixative was highly oxygenated. The fixed samples were washed in distilled water for a long time to eliminate salt deposits on the sample surface. Sample dehydration was performed using a linear gradient apparatus to provide a very gentle dehydration. And last, the specimens were fractured using a modified Smith-Farquhar tissue chopper. In this modification to the freeze-fracture method, the 100% ethanol infiltrated samples were sealed in little Parafilm packets pre-filled with 100% ethanol, plunge frozen in a chilled Freon 22 slush, and transferred to liquid nitrogen, in which the submerged samples were fractured. The Smith-Farquhar chopper was equipped to hold liquid nitrogen in a trough and the height of the razor was adjusted so that when it was released to fall on the sample, it would only just cleave the top, not cut through the sample. The shock of the impact propelled the fracture and the fractures were well controlled. The fracture pieces were then placed into fresh 100% ethanol to thaw after which they were critical point dried, mounted, and coated.

A. E. Hotchkiss, V. J. Martin, and R. P. Apkarian employed this same method in 1984 in their study of the planulae of a hydrozoan (7). The samples were fixed, rinsed with buffer, rinsed briefly with distilled water, dehydrated to 100% ethanol, sealed in little Parafilm packets filled with 100% ethanol, plunge frozen in chilled Freon 22 at -160°C and fractured in liquid nitrogen at -196°C using the modified Smith-Farquhar tissue chopper, after which the samples were placed into fresh 100% ethanol and critical point dried, mounted and coated.

The cryo-fracture protocol as currently practiced at our facility is based on a long history, which began with simply fracturing frozen fixed and unfixed wet tissue. The next development produced what is essentially the protocol as practiced here today, that is, ethanol dehydration prior to cryo-fracture followed by drying using the critical point method. However, many refinements have been made over the years to tissue handling and to the process of critical point drying. Freons are no longer used as they are now recognized as an environmental hazard.



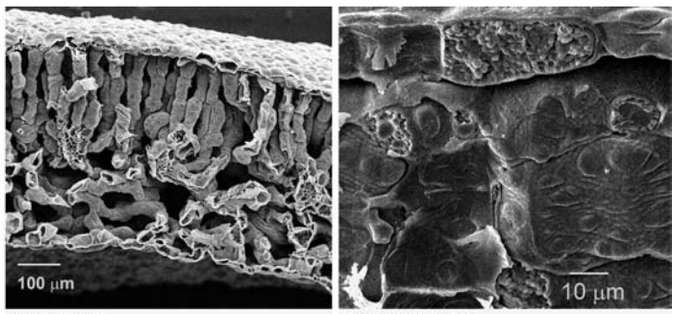
Skeletal muscle

The cryo-fracture protocol followed at our facility is to fix the small pieces of tissue, rinse in buffer and distilled water and dehydrate through 100% ethanol, seal the tissue inside little Parafilm packets filled with 100% ethanol, freeze the samples in liquid nitrogen and gently fracture the samples using a liquid nitrogen-chilled razor blade while submerged in liquid nitrogen. The complete infiltration with 100% ethanol would seem to be adequate protection against ice crystal formation in the tissue. One point to make about using the Parafilm packets is that at no time are any samples exposed to air. The samples are placed into the packets and sealed while everything is submerged in 100% ethanol. The freshly cryo-fractured tissue is removed to a container of fresh 100% ethanol to thaw and the Parafilm discarded. Critical point drying, mounting and coating proceed from there.

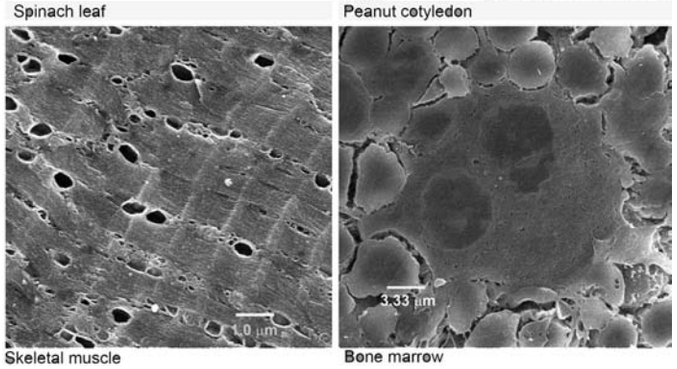
The 12 nm of sputtered gold applied to samples for conventional scanning electron microscopy (SEM) in our facility is just a third of the thickness of that used by Humphreys, Spurlock, and Johnson in their work and the 1 to 2 nm of sputtered chromium applied to samples requiring high resolution SEM imaging might seem almost invisible in a comparative TEM cross section.

The images are SEM micrographs of a Cryo-fractured spinach leaf, peanut cotyledon, mouse bone marrow and mouse skeletal muscle. Please note the nicely preserved organelles and membranes such as fat storage droplets in the peanut. Some membranes look like sheathes broken away revealing the cell contents. But particularly note the nearly flat plane of the fracture. In the marrow one can see nuclei in cross section and in the muscle one can see the banding; higher magnification shows detail.

These samples were sputter coated with 12 nm gold then viewed using a Topcon DS130 SEM at 10 kV. ■



Spinach leaf
Peanut cotyledon



Skeletal muscle
Bone marrow

References:

G. H. Haggis, "Cryofracture of Biological Material", *Scanning Electron Microscopy*, April, 1970, pp. 97-104 *Though sucrose is an osmotic agent rather than a buffering agent, in his report, Dr. Haggis' indeed describes his fixative as "2% glutaraldehyde in sucrose buffer at pH 7.4".

Walter J. Humphreys, Ben O. Spurlock, & Janet. S. Johnson, "Critical Point Drying of Freeze-Fractured Tissue for Scanning Electron Microscopy", *Proceeding of Thirty-First Annual EMSA Meeting*, 1973, pp. 452-453

W. J. Humphreys, B. O. Spurlock, & J. S. Johnson, "Critical Point Drying of Ethanol Infiltrated Cryofractured Biological Specimens for Scanning Electron Microscopy", *Scanning Electron Microscopy, Part I*, April 1974, pp. 275-282

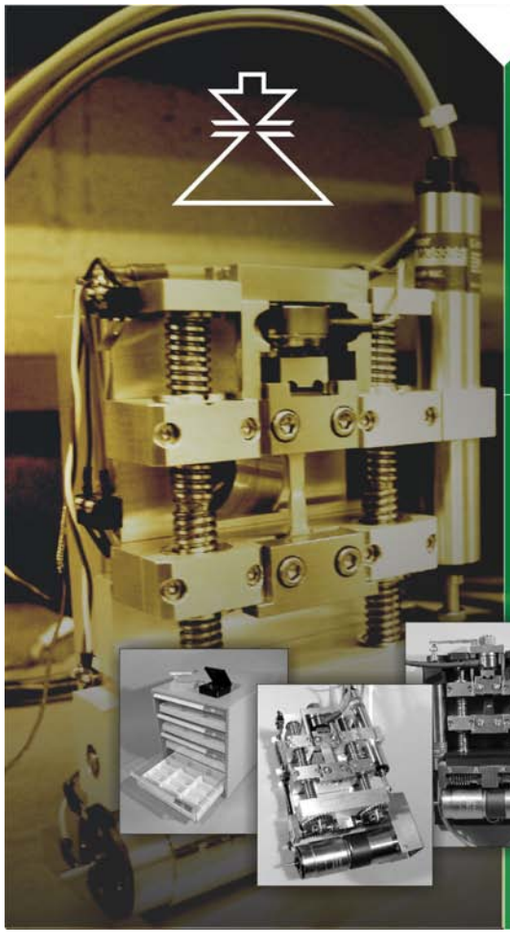
Walter J. Humphreys, Ben. O. Spurlock, & Janet S. Johnson, "Transmission Electron Microscopy of Tissue Prepared for Scanning Electron Microscopy by Ethanol-Cryofracture", *Stain Technology*, 1975, pp. 119-125

G. H. Haggis & Beverly Phipps-Todd, "Freeze Fracture for Scanning Electron Microscopy", *Journal of Microscopy*, Vol. III, Part 2, November 1977, pp. 193-201

R. Apkarian & J. C. Curtis, "SEM Cryofracture Study of Ovarian Follicles of Immature Rats", *Scanning Electron Microscopy, Vol. VI*, 1981, pp. 165-172

Anne E. Hotchkiss, Vicki J. Martin, & Robert P. Apkarian ,"A Scanning Electron Microscopic Surface and Cryofracture Study of Development in the Planulae of the Hydrozoan, *Pennaria tiarella*", *Scanning Electron Microscopy, Vol. II*, 1984, pp. 717-727.

ABTaylor cryo.indd 2 06/22/2008 8:56:55 AM



CUSTOMIZING
TO YOUR SPECIFIC NEEDS

Micromanipulators, preparation materials, darkroom and general lab supplies, books, grids and apertures. Many items are manufactured in our machine shop, so customizing to your specific need is not a problem.

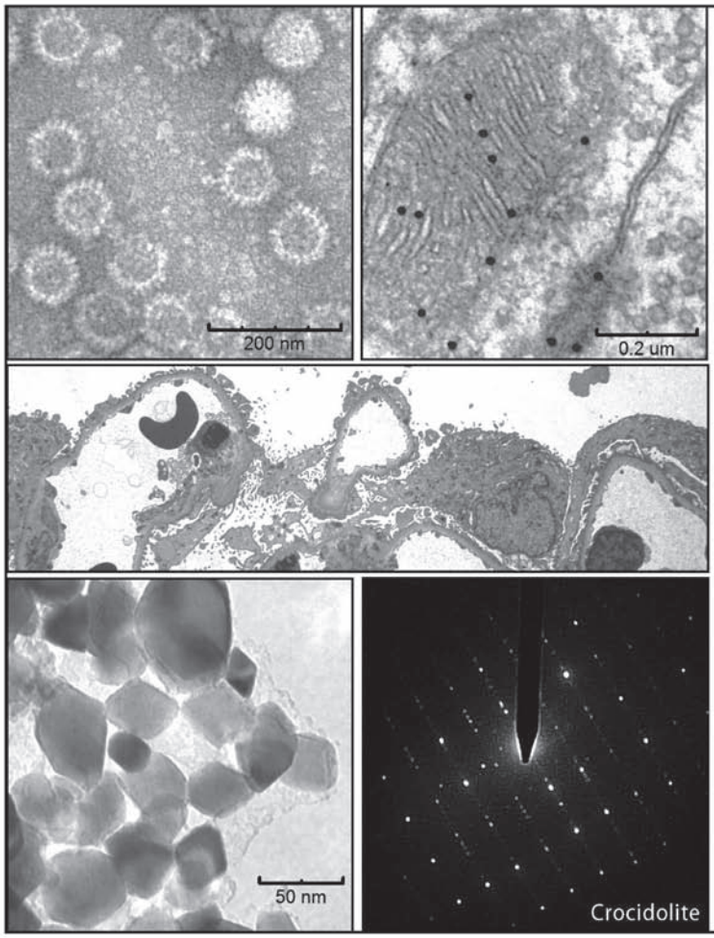
Some of the accessories and laboratory supplies we can supply are tweezers, tools, TEM CCD imaging systems, tensile testers, turbo evaporators, sputter coaters, substages, specimen holders, standards, carbon coaters,

CONTACT US

750 Pierce Road, Suite 2.
Clifton Park, New York 12065-1303
Phone: 518-877-0820, 800-833-4024
Fax: 518-877-3885

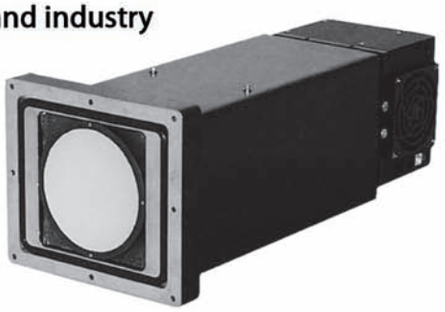
ERNEST F. FULLAM, INC.
Microscopy & Laboratory Supplies

sales@fullam.com \ www.fullam.com



Affordable TEM camera systems for research, healthcare, education, and industry since 2001

SIA



1 to 16 Megapixels, slow scan and TV

Magnification factor of 1 on bottom mounted cameras

Diffraction beam stop on side mounted cameras

Reliable, easy to use and upgrade

Standard and custom configurations for any TEM

Compatible with existing TEM accessories



Scientific Instruments and Applications
2773 Heath Lane; Duluth, GA; 30096
(770) 232 7785; www.sia-cam.com

MT_Half over 2 qtr pg ads.indd 1 06/22/2008 9:19:56 AM

SEM Remote Control with a 3D Option

F. Mighela[*], C. Perra[***], R. Pintus[**], S. Podda[*], M. Vanzi[***]

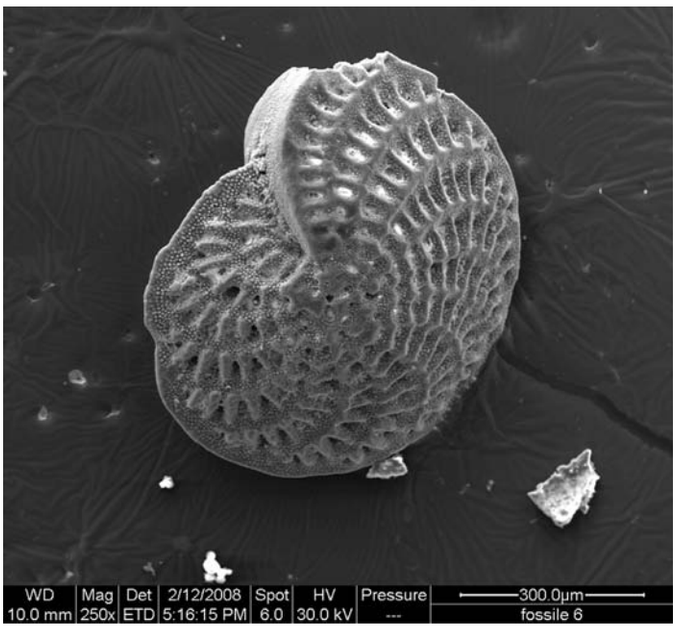
[*]*Telemicroscopy Laboratory, Sardegna Ricerche, Edificio 3, Località Piscinamanna, Pula (CA), Italy* [**]*3D Model Laboratory, Sardegna Ricerche, Edificio 1, Località Piscinamanna, Pula (CA), Italy*

[***]*DIEE, University of Cagliari, Piazza D'Armi, Cagliari, Italy*

francesca.mighela@diee.unica.it

Remote control of a scientific instrument is a topic gaining more and more attention between instrument users and operators. The project presented in this article reports results obtained from two distinct research efforts. The main outcome from the first research was the realization of an application to remote-control a Scanning Electron Microscope (SEM), while the main outcome from the second research was the implementation of a procedure to reconstruct 3D surfaces.

The remote control application is a server/client application [1], and [2]. The server/client structure is comprised of two different applications. The server application, resident on a computer locally, is connected to the instrument and it works as middleware between the instrument and the client. The client application is implemented on the remote user's computer, and is able to control the instrument through a TCP/IP connection. The main aspect of this server/client application is that it has been designed not only for working on local networks but, in particular, for providing good performance when used over the Internet. The remote commands implemented on the client application concern the connection to the server application, the connection to the microscope, the management of microscope controls, communication with the local operator, video streaming of specimens' images, and the management of the 3D surface reconstruction engine. Excluding the video streaming, the communication between client application and the microscope is practically in real-time.



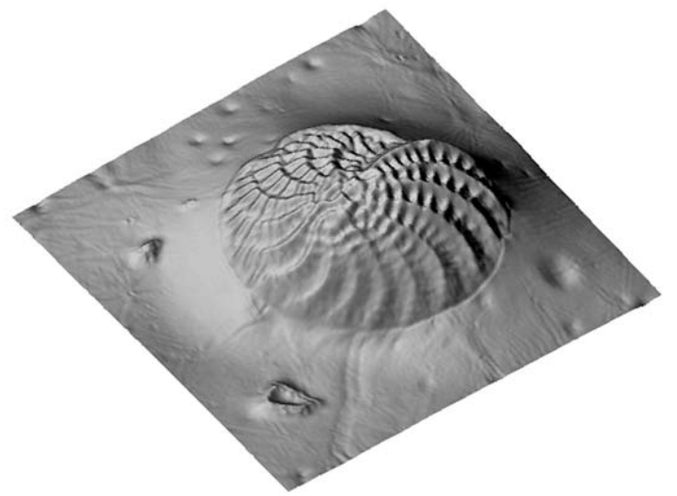


FIG. 1a, top: The image of a shell fossil with the Scanning Electron Microscope operating in high vacuum. 1b, bottom: The fossil foraminiferan surface 3D reconstruction obtained by the method briefly explained in this paper.

The procedure for 3D surface reconstruction was originally designed as a local application [3] and was modified during work for providing remote control functionalities. The 3D tool extracts the third dimension from back-scattered electrons [3]. This method for reconstructing the depth map in the SEM is founded on a 4-Source Photometric Stereo (PS) technique, which is based on the so-called reflectance map that uses several images of a surface, taken from the same viewpoint but under different lighting directions, to estimate the relative surface depth at each image point.

The image acquisition process may require specific instrumentation (4-sector, independent channel axial BS detector), or a strictly standard SEM configuration with specimen rotation/translation. In this last case, an alignment procedure had been developed [4] to simulate different lighting conditions in a standard SEM. It is necessary to rotate the specimen under the fixed detector and to acquire four images sequentially of the same specimen view after imposing three 90° rotation steps on the specimen. A sequence of four pictures of the same area will be obtained, each of them apparently illuminated from a different lighting direction. All these microscope operations are executed via remote control without any delay utilizing the 3D reconstruction tool available in our remote control application. Fig. 1a and Fig. 1b show an example of 3D reconstruction using this technique.

The results demonstrate that it is possible to remotely control an SEM on a public network, both for conventional and non-conventional operations, even if the video streaming is affected by network limitations. Starting from this point, a new research project was undertaken. The topics of this project are several: on one hand, it is important to obtain real-time video streaming on a public network. On the other hand, it will be useful to realize a distributed architecture where it is possible to share instruments through tools for conventional and non-conventional operations on a public network.

Real-time video streaming on a public network will be best handled via new internet communication protocols; new telecommunication network features, like wide band and low latency; and exploiting standard video coding techniques tuned and adapted to the nature of the video signals being encoded. The current implementation is based on H.264/ACV [7] standard encoder optimized for fast encoding of the RGB digital signal coming from the SEM.

The development of a distributed architecture requires a complete revision of the way the remote control was implemented in previous projects. In fact, despite the good results obtained with

ABMighela.indd 1 06/22/2008 10:13:58 AM

61:Layout 1 6/26/08 1:54 PM Page 1

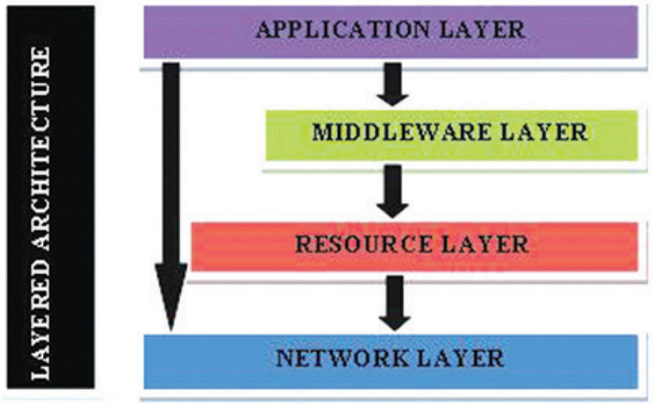


FIG. 2: Example of layered structure.

the server/client application, some aspects restrict the utilization of remote control. The main problems are that the server/client application requires that remote clients install the client application on their own workstations, and that it is necessary to implement a server/client solution for each instrument when sharing more than one instrument. In order to overcome these limitations we identify distributed computing protocols, more commonly known as Grid technology, as the available technology to reach our goals. The first phase has been a research effort concerning the state of the art of this technology, in order to identify the best solution. The features of Grid technologies are explained in [5] and [6]. The main property is that Grid architectures are layered structures. Fig. 2 shows an example of a possible layered structure. The advantages of applying Grid technology on different instruments are listed below:

- Security access;
- Security connection;
- Real-time interaction;
- Interoperability;
- Real-time streaming video;
- Concurrent access by multiple users to the same resource;
- Public network availability.

In this Grid example, every layer has a dedicated role, and implements the solution to these questions. In particular:

- Network layer connects all resources and contains the interfaces implementing local control and managing the security aspects;
- Resource layer groups resources such as computers, storage systems, instruments, sensors, electronic data catalogue, data base;
- Middleware layer is the layer where there are all the tools that allow the interaction between the grid resources available;
- Application layer is the only one accessible by the user. Here are the User Interfaces of the available applications.

Among the several advantages provided by Grid architectures, there is a point particularly relevant to remote control of microscopes: instrumentation security. It is obtained by observing that layers containing the application interfaced directly with the instruments are completely hidden to unauthorized remote users. Only the layers with Graphical User Interfaces (GUI) of the applications pertaining to remote control of the instruments by authorized researchers, with conventional and non-conventional operations, are available to those specific remote users. Moreover, Grid architecture is accessible through an electronic certificate, that improves the security of Grid shared resources. Another favourable point is that the layered structure allows an easier configuration of the remote control operation, because it is possible to develop a unique GUI to remote control different specific instruments. When the remote client accesses the Application Layer, and selects the resource to use, just the commands related to it will be enabled. In this way, it is easier to include other options, like the 3D surface reconstruction engine, which are not specific for the instruments, but is an option developed *ad hoc* for improving the instrument's performances and experimenting with new technologies and applications. ■

References

[1] F. Mighela, C. Perra, M. Vanzi "Long Distance SEM Remote Control", *The 16th International Microscopy Congress Proceedings*, September 2006.

[2] F. Mighela, C. Perra: "Remote Control for Microscopy Applications", *Instrumentation and Measurement technology Conference Proceedings*, April 2006.

[3] R. Pintus, S. Podda, F. Mighela and M. Vanzi, "Quantitative 3D Reconstruction From BS Imaging" *Microelectronics Reliability* 44, 2004 1547-1552.

[4] R. Pintus, S. Podda and M. Vanzi "An Automatic Alignment Procedure for a 4-Source Photometric Stereo Technique applied to Scanning Electron Microscopy" in press on *IEEE Transactions on Instrumentation and Measurement*.

[5] I. Foster, C. Kesselman, S. Tuecke "The Anatomy of the Grid: Enabling Scalable Virtual Organizations", *International Journal of Supercomputer Applications* 15 (3), 2001, pp. 200-222.

[6] http://gridcafe.web.cern.ch/gridcafe/

[7] T. Wiegand, G.J. Sullivan, G. Bjontegaard, and A. Luthra, "Overview of the H.264/ACV Video Coding Standard", *IEEE Transaction of Circuits and Systems for Video Technology Proceedings* (2003)

TGSTechnologies
TEM SAMPLE HOLDER SERVICE & MODIFICATION SPECIALIST

A New Alternative to your TEM Specimen Holder service and repair needs.

TGS Technologies provides High Quality TEM Specimen holder service with 25 years experience.

We offer competitive rates for our quality services.

Contact Us Today

TGS Technologies
Phone: 724.453.3865
Fax: 724.453.2968
E-mail: tom@tgstechnologies.net
Web: www.tgstechnologies.net

Coloring Pictures for Electron Microscopists or Elements of Digital Image Manipulation for Students

V.M.Dusevich, J.H.Purk, J.D.Eick
University of Missouri School of Dentistry, Kansas City, MO
DusevichV@umkc.edu

Coloring pictures is an educational exercise, which is fun, and helps develop important skills. Coloring SEM micrographs is especially suitable for electron microscopists. Color micrographs are not just great looking on a lab wall; they inspire both microscopists and students to exercise digital picture manipulation. Many microscopists enjoyed looking at the beautiful color micrographs by D. Scharf, but were frustrated to learn they needed a very particular scanning electron microscope equipped with multiple secondary electron detectors in order to color their own pictures. Fortunately, there are other ways to color SEM micrographs. Most SEMs are equipped with at least two detectors, for secondary and backscattered electrons. Most microscopists use Adobe Photoshop™ or similar programs capable of combining several digital pictures into one. Therefore, most microscopists have the means to successfully color pictures. Three somewhat different black and white pictures of the same object could be used as Red, Green, and Blue layers in Photoshop to produce a color picture. "Somewhat different" pictures could be produced by utilizing different detectors, different detector configurations, or different accelerating voltages in the SEM while taking pictures of the same object in the same position at the same magnification. In some cases these pictures would not coincide precisely; this can be corrected by sliding RGB layers slightly relative to each other (in Photoshop), or it can be avoided by utilizing lower magnifications.

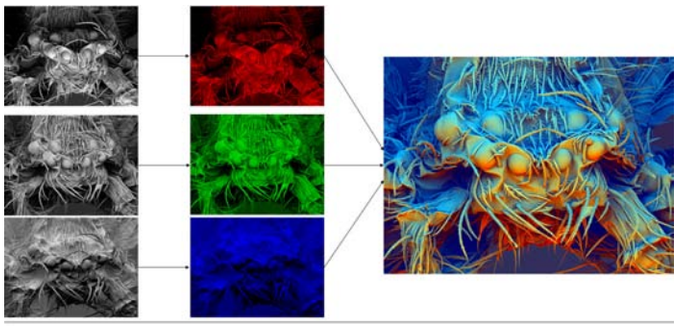


Figure 1. Spider

Figure 1 represents the process of colorizing a portrait of a spider. Just one detector was used, a solid state BSE detector, consisting of two sectors (4 quadrant systems could offer even greater flexibility). Three black and white pictures of the first column of Figure 1 are (from top to bottom): picture taken with sector A of the BSE detector; picture taken with sector B; and picture taken in the so-called "topography" mode, *i.e.* utilizing the A-B signal.

Utilizing Adobe Photoshop™, the pictures were converted into Red, Green and Blue layers correspondingly (second column of Figure 1). Each layer was then subjected to various manipulations with Photoshop tools, such as brightness/contrast changes and tweaking with a tool called *Levels*. Next the picture was "flattened" so that the layers were combined in a single color picture



Figure 2. Micrographs of a bug taken at 15 kV (a, left), 5 kV (b, center) and 1 kV (c, right)

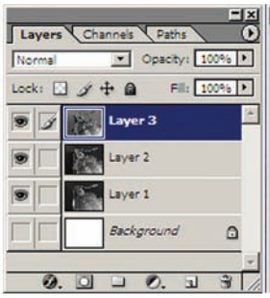


Figure 3. Layers window

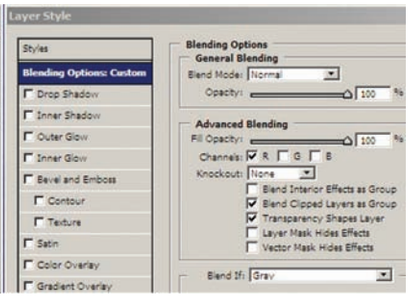


Figure 4. Layers Style window

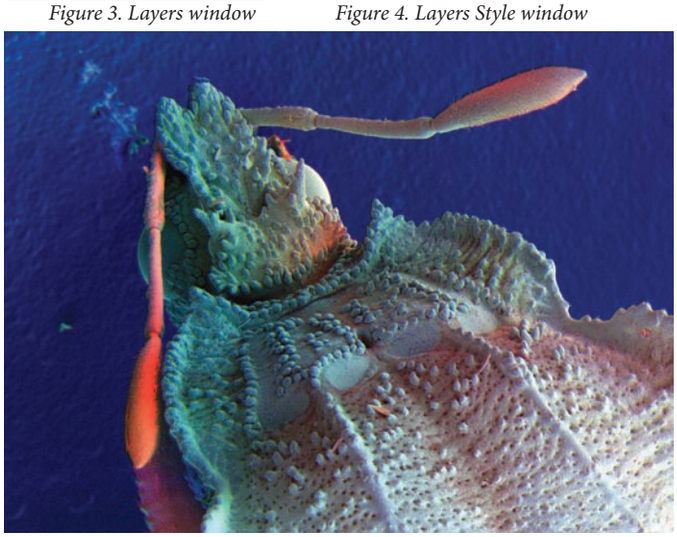


Figure 5. Bug in psuedo color

to decrease the size of the file and make it easier to read in other programs. This picture was again subjected to tweaking with the *Hue/saturation*, *Color balance*, *Levels*, and *Curves* tools to suit the tastes of the electron microscopist.

The next example is a step by step instruction for coloring the picture of a bug with the help of Adobe Photoshop™. Three initial black and white pictures were taken with a secondary electron detector at different accelerating voltages: 15, 5 and 1 kV (Fig. 2). Some charging could be observed on the left antennae of the bug at 15 kV, but it will give a nice accent in the final color picture.

- Open the three initial pictures in Photoshop, select the window with the picture taken at 15 kV, in Photoshop menu click on *Select*, in submenu click *All*, and then copy the picture to clipboard (*Edit – Copy*).
- Open a new window by selecting *File – New*. The new window will be the same size as the picture on the clipboard.
- Paste the first picture in the new window with *Edit – Paste* to create Layer 1.
- Highlight the second picture (5 kV), repeat *Select – All* and *Edit – Paste*, creating Layer 2.
- Repeat for the third picture (1 kV).
- In the *Layers* window (Figure 3) click on the Eye icon next to the line *Background* to make the background invisible.

ABDusevich.indd 1 06/22/2008 10:27:55 AM

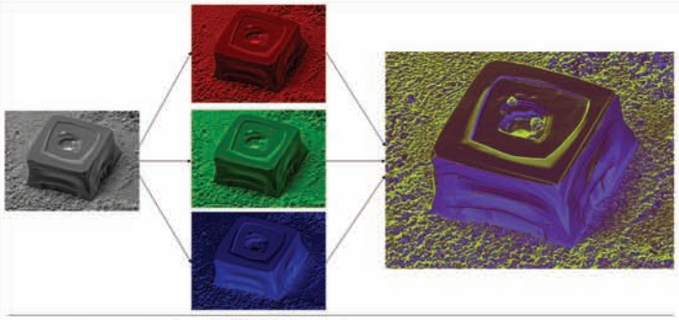


Figure 6. Sodium chloride crystal

- In the Photoshop menu select *Image – Mode – RGB Color* and in a pop-up window choose *Don't Merge*; although the image remains visually black and white, it could be colored now.
- Right click on the line *Layer 1* and in the submenu choose *Blending Options…*
- In the pop-up window (Figure 4) in the *Channels* row, uncheck G and B options, making Layer 1 the red channel of the final picture.
- In the same manner make layers 2 and 3 Green and Blue channels.
- Now the picture is colored, but in full resolution (*View – Actual Pixels*) the blue layer (Layer 3, picture taken at 1 kV) is misaligned with the other layers. *Layer 3* should be selected in the *Layers* window and then moved with *Move Tool* (the upper right corner of Photoshop Toolbox) so that it coincides with the Red and Green layers.
- The image can be "flattened" (*Layer – Flatten Image).*

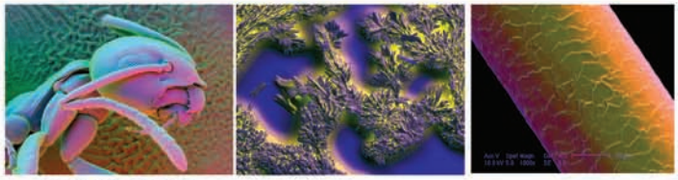


Figure 7, left. Ant
Figure 8. Crystals of sodium bicarbonate
Figure 9, right. Hair

- Some adjustment with the *Levels* tool (*Image – Adjustments – Levels)* produces the final image (Fig. 5).

Even if the microscopist has no means of producing "somewhat different" pictures of the same object, a color micrograph can still be produced from a single black and white picture, as shown in Figure 6. The same black and white micrograph of a salt crystal was used for all RGB channels (layers), except that in the blue channel an inverted (negative) picture was used. After multiple manipulations with layers and the intermediate picture, the final colored micrograph was produced.

Figure 7, a colored micrograph of an ant, was made from micrographs taken with a secondary electron detector and the sector A and sector B of a BSE detector. The picture from Figure 8, soda crystals, was made with a BSE detector: composition (A+B), topography (A-B), and A modes. For Figure 9 one of the authors donated his hair. The image was composed of micrographs taken with a secondary electron detector, sector A of a BSE detector, and A-B signal of BSE detector. ■

Supported in part by USPHS Grant K23-DE016324.

When people discover how well the Evactron® De-Comtaminator cleans SEMs they ask:

Could You Make it Clean My Kitchen?







Electron Microscope operators are so impressed with Evactron D-C's gentle and effective cleaning power, they ask us if we can make a bigger Kitchen Evactron with the same powerful oxygen radicals that sweep out grease and oil from SEMs. Fantastic idea. We're considering it!

OVER 700 EVACTRONS D-CS SOLD WORLD-WIDE TO CLEAN SEMS, FIBS, & HIMS

XEI Scientific

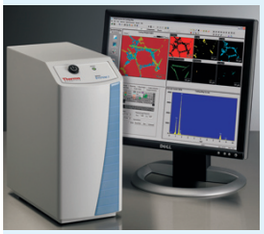
http://evactron.com/
1 (800) 500-0133
General technical inquiries:
information@evactron.com
Sales and quotations:
Sales@evactron.com

M&M Booth 720

ABDusevich.indd 2 06/22/2008 10:27:56 AM

Thermo Fisher Scientific Inc. announces that HUNT Biobank has selected its **Thermo Scientific Nautilus LIMS™** to gather, store, manage, track and retrieve the biological data of approximately 100,000 people from Nord-Trøndelag County, Norway, as part of one of the largest population-based health studies ever performed. Initiated to support epidemiological, clinical and preventative medical research, HUNT Biobank studies provide insight into disease status and progression, particularly in relation to quality of life measures such as environment, education and occupation. Spanning almost 25 years, HUNT Biobank now represents an integrated family and personal database. For more information about Thermo Scientific Nautilus LIMS, please e-mail marketing.informatics@thermofisher.com or visit www.thermo.com/informatics.

Thermo Fisher Scientific Inc. has unveiled the **Thermo Scientific NORAN System 7**, the most advanced EDS X-ray microanalysis system available. Equipped with a high throughput pulse processor, spectral imaging capability and a sophisticated software suite, NORAN System 7 is the fastest complete EDS X-ray microanalysis system available on the market. The new system produces accurate and dependable results in just a few seconds, accelerating the microanalysis capabilities of modern electron microscopy laboratories. The Thermo Scientific NORAN System 7 incorporates a powerful new analyzer designed to achieve fast and precise acquisition of data. The system automatically analyzes both the x-ray spectrum and images during data acquisition to obtain the correct identification of the material under analysis. This exclusive "analysis during the acquisition" technique produces results more than ten times faster than other systems. This comprehensive system also features the latest in large area UltraDry silicon drift detectors for the detection of X-rays down to Beryllium. The high-resolution UltraDry detector ensures optimum collection efficiency and throughput. The Thermo Scientific NORAN System 7 software uses advanced peak shape fitting algorithms to accurately identify the elements in the sample while also enabling high-speed analysis and the production of high quality spectra. For more information about the new Thermo Scientific NORAN System 7 EDS X-ray microanalysis system, please visit booth #834 at Microscopy and Microanalysis 2008, Albuquerque, New Mexico, August 3-7. Alternatively, please call +1 800-532-4752, email analyze@thermofisher.com or visit www.thermo.com/microanalysis.



FEI Company announced that it has selected Shimadzu Corporation, developer of analytical measuring and technology systems, as a sales agent in Japan. Shimadzu, located in Kyoto, Japan, will sell FEI systems, including Quanta™ and Inspect™ scanning electron microscopes (SEMs) and the Quanta 200 3D small-stage DualBeam™ focused ion beam/scanning electron microscopes (FIB/SEM), to its established base of customers in Japan. More information can be found at: www.fei.com.

NanoImaging Services, Inc. announces **NanoImaging Data Browser**, a new data delivery service that provides its customers quick, efficient and complete access to the massive data sets generated by image-based structural investigations. The ability to directly visualize supra-molecular structures has tremendous value in all phases of the drug development pipeline, and any improvement in analytical speed has the potential to accelerate the entire development process. For more information, visit www.nanoimagingservices.com.

Leica Microsystems introduces the **Leica FCM1000**, an imaging solution developed for real-time *in vivo* and *in situ* imaging of fluorescence in mice and rats. This fibered, micro-endoscope allows researchers to image deep brain events, peripheral nerves, and angiogenesis in a minimally invasive fashion with cellular resolution. The Leica FCM1000's microprobes are designed to access virtually anywhere inside the living animal. By simply contacting the tissue of interest, the user can generate high-speed recordings of cellular or vascular events. The flexibility and minute diameters of the Leica Fibered and Miniaturized (FM) Microprobes enable endoscopic access to the living animal, with minimal animal preparation.

The former Bal-Tec AG, based in Liechtenstein and now part of the Leica Microsystems family, is an important manufacturer of both mechanical and cryo sample preparation equipment for Scanning Electron Microscopy and Transmission Electron Microscopy. Products such as the EM VCT100 Vacuum Cryo Transfer system for SEM, which provides sample transfer from preparation equipment to analysis systems for EM, and the EM HPM100 High Pressure Freezing unit, are now available from Leica Microsystems. For more information contact Molly Baker, Leica Microsystems Inc. 847/405-0123, or visit www.leica-microsystems.com

NanoAndMore USA, Inc. the North and South American distribution arm of NanoWorld Holding, AG, today announced that it has **signed a distribution agreement for the US market with BioForce Nanosciences Holdings, Inc.**, a producer of integrated biological and mechanical systems for life science researchers at the micro and nano scales. NanoAndMore USA joins the sister company of NanoAndMore GmbH, already a distributor of BioForce Nanosciences' products., in distributing these leading edge products. www.nanoandmore.com

NANOSENSORS™ today announced the introduction of new Gold and Platinum coated variations of its well-known speciality probe type for Atomic Force Microscopy - the **AdvancedTEC™ SPM probe**. The Platinum Iridium and the gold coated AdvancedTEC™ AFM probes will be available in different force constants and resonant frequencies for contact mode, non-contact/tapping mode and force modulation mode measurements. These new variations extend the range of applications for the AdvancedTEC to Electrostatic Force Mode (EFM), Scanning ElectroChemical Microscopy (SECM), Scanning Capacitance Mode (SCM), Scanning Kelvin Probe Microscopy (SKPM) as well as to usage in combined imaging techniques such as: Atomic Force Microscopy (AFM) – Scanning Electron Microscopy (SEM) imaging, Infra Red – Scanning Nearfield Optical Microscopy (IR-SNOM) or Electrical Micro-Nanprober systems. For further information please visit the NANOSENSORS website at: www.nanosensors.com

Together with the Foundation for **Innovative New Diagnostics (FIND), Carl Zeiss has developed a special microscope to improve the diagnosis of tuberculosis**. Compared to the traditional technique of diagnosing tuberculosis by Ziehl-Neelsen staining, diagnosis with the Primo Star iLED fluorescence microscope is four times faster with a ten percent improvement in sensitivity. The market launch of this new fluorescence microscope has been scheduled for October. The outstanding feature of the new microscope is its energy-saving LED illumination which is specially designed for use in the countries concerned. FIND and Carl Zeiss will sell the Primo Star iLED at a reduced price to 24 developing countries defined by the WTO World Trade Organization. For more information on the breadth of solutions offered by Carl Zeiss MicroImaging, please visit www.zeiss.com/micro.



Carl Zeiss SMT has launched the **ParticleSCAN VP**, a newly developed work-flow solution for automated full-scale high-resolution particle analysis. The newly developed system in particular allows for the analysis of non-conductive samples based on proprietary Variable Pressure technology. The system is a further development of the high vacuum ParticleSCAN particle detection and analysis system introduced in 2007 and based on Carl Zeiss´ field proven mobile Scanning Electron Microscope (SEM) platform. The highly automated system has been designed for frequently repeated analysis of material samples in industrial production and research environments. It is used in process control for the detection and monitoring of ultra-fine particles. Combined with an optional X-Ray analysis tool (EDS) the system can automatically record

AAIndustry_News 08n4.indd 1 06/22/2008 10:44:43 AM

the morphology of samples, i.e. measure, classify and record their size, shape and chemical composition. Thereby the system enables customers for highly efficient and automated process control, yield improvement and manufacturing capability. Provided with the dedicated SmartPI ™ software, ParticleSCAN VP can be adapted to a broad spectrum of particulate analysis – from pharmaceutical powders to inclusions in metal alloys. The new Variable Pressure mode now also enables the rapid examination and analysis of non-conducting samples. You can find the complete text under http://www.zeiss.de/C1256A770030BCE0/WebViewAllE/BF193D25EA-BA49E4C125746B004F7A4A

The McCrone Group Inc. announced a significant expansion of "**The McCrone ATLAS of Microscopic Particles,**" a comprehensive online particle reference resource, and its associated website. "The McCrone ATLAS of Microscopic Particles," is a comprehensive online particle reference resource available to Forensic Scientists, First Responders, Researchers, and Teachers on a subscription basis. McCrone's ATLAS is designed as a reference tool to assist scientists in the identification of unknown particulate samples. This exclusive ATLAS is the first comprehensive web-based particle reference source for scientists, microscopists, and criminalists engaged in materials analysis and identification and for science educators to use in classroom learning. The ATLAS now includes 846 historical characterizations from THE PARTICLE ATLAS Edition Two - Volumes Two and Five. There are now over 1,000 particle characterizations on the site. During the next several years additional characterizations and updates will be posted on a regular basis. The new expanded ATLAS site provides excellent detail for particle identification and it now permits several subscription options and payment methods. Available at: www.mccroneatlas.com, the ATLAS combines the knowledge of the world's foremost particle analysts into one of the most wide-ranging reference tools ever developed for forensic scientists and others in the scientific community. For further information about The McCrone Group, please visit www.mccrone.com.

Gatan, Inc. successfully **obtained ISO9001:2000 certification**. This milestone corroborates Gatan's long-lived commitment to improve the quality of our products and services to our customers. Since our inception, Gatan has and continues to set and implement measureable and definitive quality objectives throughout the company to advance our quality management system. Our ultimate goal is to become the benchmark of quality and service for imaging and analysis products in the electron microscopy industry. Website: www.gatan.com

Wells R&D Introduces the **OS200B Lens Test Bench, Classic Lens Test Bench** Plus Live Video And MTF Analysis Software. If you are evaluating performance of commercial lenses for use in larger systems, validating performance of custom lens prototypes, tracking the performance of incoming batches of lenses, or diagnosing imaging problems, then the OS200B from Wells Research and Development is the lens test bench system you need.

Technical Manufacturing Corporation's (TMC) new TableTop PZT™ is an active hard-mount vibration cancellation system that is ideal for small precision instruments, particularly those instruments in buildings where floor vibration is severe. Incorporating TMC's patented STACIS® technology, the cost-effective TableTop PZT features a lightweight, compact design; extended stroke piezoelectric actuators; sub-Hz vibration cancellation, both vertical and horizontal; and it has no soft air suspension. The TableTop PZT has a payload capacity up to 300 lbs. Contact Steve Ryan Technical Manufacturing Corp., 978-532-6330, sryan@techmfg.com

Ted Pella, Inc, introduces a new glow discharge system for cleaning and surface modification of TEM grids and support films. With increasingly demanding imaging applications, using clean or surface modified TEM grids and support films has become more important than ever. The new **PELCO easiGlow**™ has been designed as an affordable, quick and easy to operate glow discharge system for any TEM lab. The PELCO easiGlow™ is a compact, standalone system that fits easily in a TEM lab. The practical chamber size with its newly designed UC glow discharge head and adjustable stage with glass slide holder allows for easy loading and fast turnaround times. The system is fully microprocessor controlled and includes an intelligent touch screen device for operation and display of parameters. The PELCO easiGlow™ supports both hydrophilic and hydrophobic treatment for either a negative of positive charge and includes two separately controlled gas inlets. The required vacuum level is set by an electronically controlled precision proportional valve, eliminating manual setting with a needle valve. A soft venting procedure ensures that the TEM grids are not disturbed when the system is vented. For the most common glow discharge application, making TEM supports films hydrophilic using air, the PELCO easiGlow™ includes a automated and quick cycle with fully selectable parameters. This function is widely used for TEM preparation using aqueous solutions and for Cryo-TEM applications. The microprocessor controlled systems also offers full manual control for all parameters and an advanced protocol programming feature for custom glow discharge treatment applications. The PELCO easiGlow™ combines both true ease of operation for simple cleaning procedures and sophisticated control for advanced custom glow discharge applications. For those labs which needs both hydrophilic and hydrophobic surface treatment a dual glow discharge system is available to avoid cross contamination of the glow discharge chambers. www.tedpella.com



Ted Pella, Inc, introduces the **next generation of Silicon Dioxide Support Films** for analytical electron microscopy. Utilizing advanced MEMS technologies with novel stress reducing techniques, smooth freestanding silicon dioxide membranes with unsurpassed flatness are now available. The film thickness of these flat membranes is 40nm, offering enhanced imaging capabilities for analytical TEM applications.

As a response to the increased demand for affordable high-quality AFM calibration standards, **BudgetSensors®**, a Bulgarian manufacturer of silicon and silicon nitride probes, as well as AFM accessories for Atomic Force Microscopes (AFM), announces the commercial introduction of **two different AFM height calibration standards – the HS-100MG and the HS-20MG**. Both height calibration standards feature silicon dioxide structure arrays on a 5x5mm silicon chip. The fabrication process guarantees excellent uniformity of the structures across the chip. This in turn ensures easy and reliable Z-axis calibration of any AFM system. Arrays of structures with different shape and pitch are integrated on each chip. Aside from Z-axis calibration, this design also allows X- and Y-axis calibration for bigger scanners (40-100µm range). The HS-100MG features structures with 100nm and the HS-20MG features structures with 20nm step height. For more detailed product specifications, please visit BudgetSensors®' website www.budgetsensors.com/calibration_standards.html.

Biomedical Photometrics Inc., announces the launch of its latest generation of panoramic confocal fluorescence and brightfield **slide scanners, the TISSUEscope™ 4000** for the pathology, medical research, genomics and general microscopy markets. The latest instrument comes equipped with 4 solid state fibre-coupled lasers as standard, (405, 488, 532 and 639 nm). This enables it to acquire images from slides stained with fluorescence markers such as DAPI/Hoechst in the violet, all the way into the far red. The new TISSUEscope™ 4000 instrument comes with the latest version of the MACROview software including a streamlined user interface, which provides the instrument operator with a significantly more efficient workflow, substantially reducing image scanning set up time. With the addition of a 5" x 7" motorized stage the TISSUEscope™ 4000 offers researchers the flexibility to acquire a wide range of specimen sizes, all in stunning high resolution (0.5µm/pixel) detail. Biomedical Photometrics Inc. (519) 886 9013 ext 38 www.confocal.com

AAIndustry_News 08n4.indd 2 06/22/2008 10:44:43 AM

NETNOTES

Edited by Thomas E. Phillips, Ph.D.
University of Missouri
phillipst@missouri.edu

Selected postings from the MSA Microscopy Listserver (listserver@msa.microscopy.com) from 04/15/08 to 06/15/08. Postings may have been edited to conserve space or for clarity.

SPECIMEN PREPARATION – acetonitrile as a dehydration agent

I remember well that acetonitrile (AN) has been advised as a substitute for propylene oxide (PO) between ethanol dehydration and Epon embedding. I have always used ethanol and then PO until now but I am eager to use AN instead. Now I wonder if I could not use AN for dehydration too, so it could be used all along! For dehydration factors like penetration time, lipid extraction and hardening of the tissue are important to take into account but having no experience with AN, I have no idea. Do some of you use AN for dehydration and Epon embedding? Are there differences between ethanol and AN dehydration (time, hardness,...) to take into account? Also, I have to split the whole procedure into 2 days, usually I stopped in ethanol 70%. Where should I stop until next day with AN? Stephane Nizets nizets2@yahoo.com Apr 17

I have only ever-substituted acetonitrile in place of the PO, I've never tried to use it to dehydrate, only for the infiltration steps. It works great for that purpose. Jo Dee Fish jfish@gladstone.ucsf.edu Tue Apr 29

I tried dehydration and Epon embedding with only acetonitrile as agent. I used it instead of ethanol dehydration then PO (propylene oxide) then Epon in my classical protocol. Well...it didn't work. The sections contain holes or cracks that really look like bad polymerization. Especially artifacts (holes or cracks) are visible along the nuclear envelope and with lipidic organelles like the mucus-filled vacuoles of goblet cells (I tried with pieces of gut). Nothing is visible in LM on semi-thin sections, only under the TEM. Apart from the artifacts, the morphology is excellent and the contrast too. I can only guess that acetonitrile dehydration requires longer or more frequent steps than ethanol. My dehydration protocol for small pieces of organ in ethanol is 2x10' per step (50%-70%-95%-100%) and I did the same with acetonitrile. I could of course wash 3x or extend the incubation time but I wish not to experiment further with acetonitrile. Stephane Nizets nizets2@yahoo.com Apr 29

SPECIMEN PREPARATION - wicking or blotting grids

The following replies were made in response to a query about the best material with which to blot grids.

Whenever I had something like that being necessary, for instance for removing surplus methylcellulose over ultrathin cryosections, I used wet filter paper, or wet tissue. That will remove the solution to be blotted off very slowly. Jan Leunissen leunissen@aurion.nl May 19

If speed is an issue, you could try using 'paper points'. These are thin enough (there are different sizes so that you can pick the correct wicking speed) that you can have lots of control over the process. David Elliot elliott@arizona.edu May 19

The only materials I have experience with of that wet slowly and are brittle are nitrocellulose (and similar) membranes, used for protein/RNA/DNA blots or in micropore filters. The wet filter paper idea seems the simplest and cheapest, though! rosemary.white@csiro.au May 19

Living multiple lives as both microscopist and molecular virologist I think I've probably used most options for doing negative staining, and have done all sorts of transblotting. The first thought would have been points or filter paper cut so that you had no loose fibers for wicking as with Dave Elliot's point. However, Rosemary's observation is probably best. Your description of the brittleness and flow rate for what the post-doc used fits something like Zetaprobe right down the line. Go over and borrow a little from your local contact in the molecular biology group and try it. It should do the job. Paul R. Hazelton paul_hazelton@umanitoba.ca May 19

I don't know what your original material might be but I have tried many different filter papers for the purpose of slow and even wicking of grids and have found that a #40 Whatman has a nice rate. Bob Underwood underwoo@u.washington.edu May 20

As already suggested, wet filter paper (Whatman Qualitative grade "1") is ideal. If you hold the piece of wet filter paper at an angle so that it contacts the edge of the underside of the grid that also helps to pull the suspension down rather than straight to the edge. Ted Dunne drteddunne@yahoo.com May 28

SPECIMEN PREPARATION - sample mounting

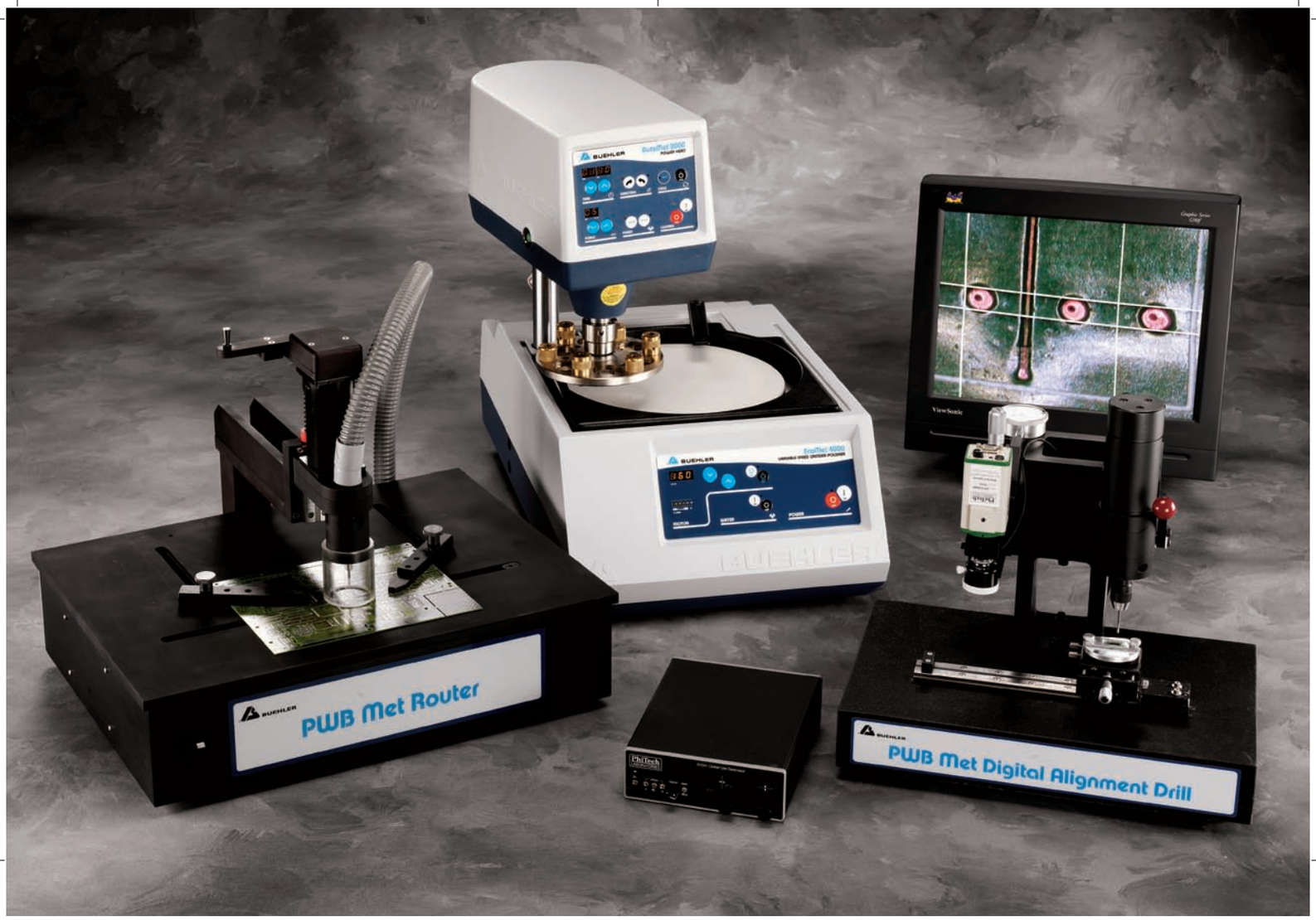
What is a good method of attaching a silicon chip to an aluminum SEM stub, so that: a) the electrical contact is good, allowing high-resolution imaging (50 kx or higher); and b) the mechanical stability is good, so that the specimen can survive shipping? I am aware of the following materials: colloidal carbon in isopropyl alcohol conductive carbon adhesive tabs and I am curious about the experience of other microscopists. Don Chernoff donc@asmicro.com May 9

Normal way is to use carbon double sticky tabs. If the die is SOI, then coat the outer edges with colloidal Ag. This will prevent it from charging. For shipping, single stub storage tubes work well. Another mounting method is to use colloidal Ag to mount the die. Care is needed to avoid wicking over the edges of the die. Gary Gaugler gary@gaugler.com May 9

We have had problems in the past with high-resolution imaging (>100,000x) of samples secured with double-sided carbon adhesive discs, although I use them all the time for routine, low-magnification work. At high magnifications, the sample crept under the beam. I use cyanoacrylate ("super glue") to hold the sample securely, then a bit of colloidal carbon in one corner to ground them. Unfortunately, you cannot then recover them. I have also used a hot-glue gun to secure samples, again grounding with colloidal graphite. Soaking in acetone later will remove the colloidal carbon and loosen the glue, so the sample can be removed. Mary Fletcher maryflet@interchange.ubc.ca May 9

I will second Mary's problems with double-sided carbon tabs. I have the same trouble with double-sided carbon tape. I use colloidal carbon paint to mount my samples for high magnification work, making sure the paint is fully dry before I put the sample in the SEM. I've also used Mary's SuperGlue suggestion. Use minimal glue and ground with carbon paint. CrystalBond thermal adhesive works well and has the added ability to be removed with acetone. Becky Holdford r-holdford@ti.com May 9

AANetNotes 08n4.indd 1 06/22/2008 1:19:02 PM



Follow Our Direct Route to Success

Buehler is pleased to introduce a new set of tools for the printed wiring board (PWB) industry that will ensure successful plated through-hole preparation for both rigid and flexible boards. We understand the electronic industry's need to meet higher reliability standards, RoHs regulations and advancements in small hole technology.

Success begins with the PWB Met™ Router, which minimizes stress introduced while removing samples from standard or multilayer boards. Rout a test coupon from most locations on the printed wiring board to find the answer you need.

Reduce preparation costs by mounting multiple coupons at once and create a common reference plane for targeted features with the PWB Met™ Digital Alignment Drill. The digital camera, color monitor, and reticule system provide precise, incremental alignment required for microvias.

Upgrade to a complete system with our Nelson-Zimmer® 3000. It combines accuracy of the PWB Met™ Small Hole Accessory with robustness of the EcoMet® 4000 grinder-polisher and AutoMet® 2000 Power Head. As many as 18 coupons can be mounted and prepared simultaneously with desired results. Precision diamond stops enable you to consistently reach a centerline of through-holes as small as 0.004" (100µm) in diameter.

Whether inspecting rigid or flexible through-holes we have the solutions you need.

BUEHLER®

Worldwide Headquarters
Buehler Ltd • 41 Waukegan Road • Lake Bluff, Illinois 60044 • USA
Tel: (847) 295-6500 • Fax: (847) 295-7979
Email: info@buehler.com • Web Site: http://www.buehler.com

PROVIDING SOLUTIONS FOR OVER 70 YEARS

MT Full Page Ad Master.indd 1 06/22/2008 1:41:49 PM

I too have experienced stability issues with carbon tape. In my line of work, the Z axis is also critical and carbon tape contracts for many hours after the SEM is evacuated. I have had very good results with putting the silicon chip directly on an aluminum sample holder and using single sided SEM compatible copper tape with nickel colloid adhesive to tape it down. I use my tweezers to burnish the tape onto the chip top, edges, and aluminum holder. The conductive adhesive on the edges of the chip gives a good electrical connection. One nice feature of this technique is that you do not have any solvents that have to dry before imaging. The negative side of this technique is that some part of the chips top will have tape covering it and adhesive residue is left if you peel off the tape. Acetone will remove the residue. I have successfully shipped samples all over the world that have been prepared this way. Richard Stallcup rstallcup@zyvex.com May 11

Single sided copper tape works fine. I have also successfully used double sided copper tape on the aluminum stub instead of the double sided carbon tape. Smitha Dronavilli vvi@cypress.com May 12

SPECIMEN PREPARATION – drying carbon paint for SEM

I use a hot glue gun to stick my samples to the stubs, since I have found in the past that carbon paint is not always a reliable glue. Just paint over the glue with a bit of carbon paint, after the glue is set. Mary Fletcher maryflet@interchange.ubc.ca May 28

Depending on the sample type I use either of three methods: A cheap hair dryer, an old vacuum chamber, or a heat lamp. Coming soon method #4: New lab poster! "For urgent work, give me one week. For impossible demands, give me one day". Evelyn York eyork@ucsd.edu May 28

The use of carbon paint to mount specimen-carrying stubs in a scanning electron microscope is a potential source for a serious vacuum problem, as described on page 76 of my book, "Vacuum Methods in Electron Microscopy". Often the user smears the entire under surface of the specimen stub with a thick coating of carbon paint, places it on the microscope stage, waits a few minutes until the visible ring of paint around the bottom edge of the stub appears to be dry (assumes all of it is dry) and proceeds to pump the instrument out. What usually happens then is that this user comes around complaining that the SEM's vacuum system is not functioning properly because it is taking an abnormally long time to pump down. What happens in a situation like this is that whereas the visible ring of carbon paint around the bottom edge of the stub appears to be dry, the large quantity of paint underneath the stub remains un-dry, and the solvent that it contains is slowly diffusing out through the "dry ring" causing the rate of evacuation to slow down markedly. A better approach is to set the stub on the stage dry, and then to place a few small isolated dabs of carbon paint around the bottom edge of it. Three or four such small dabs will dry quickly, and if allowed to become truly dry, will usually hold most stubs in firmly place. There will then be no trapped paint to bleed solvent into the vacuum system, and operation should proceed smoothly in a normal manner. -- Wilbur C. Bigelow bigelow@umich.edu Thu May 29

SPECIMEN PREPARATION – dispersing particle for SEM

I am interested in liquid suspension/dispersing techniques that will allow me to disperse small particles (10 to 0.1 microns in size) onto an SEM substrate so the individual particles are well separated (i.e. no clumping/flocculating etc.). While I suspect this is a well-known problem in SEM sample prep, maybe with some known techniques, I have been trying things without any outside help so far. I have had some success using ethanol with a few drops of a high quality commercial surfactant, but after the ethanol evaporates the oily surfactant is left as a coating on the particles, which makes SEM impractical. The material I am working with are small inorganic (mineral) particles. However, the material aside, I'm wondering in particular if the life science side of the EM house has some suggestions that might help. Roy Christoffersen roy.christoffersen-1@nasa.gov May 21

The closest I come to a problem like yours is putting 10 nm Au particles on cryoTEM grids. They have a tendency to aggregate, and I want them well-dispersed, so I try to evaporate the water they're suspended in rapidly. I have found that putting the grids in a 50-70 degree oven does the job. You can also try to tailor the properties of your SEM substrate. If the particles bind to the substrate, then they should have less tendency to clump. Another thought is to use an atomizer to deposit small drops of your suspension onto the substrate. If the substrate can be kept warm, the drops will evaporate quickly, so the particles should be in fixed positions, more or less, and this should give you a good distribution. Bill Tivol tivol@caltech.edu May 21

Chuck Garber described a technique for separating particles in an email to the listserver some time ago which I've attached below. I don't know if it will help in your situation, but it is probably worth looking at. Cheers, Henk Colijn -- [From: Garber, Charles A. * EMC.Ver #3.1] -- Oldrich Benada wrote: I need some advice. I was asked to do some analysis of silica particles (size distribution) for chemist in our institute. Particle size should be in the range of 3 to 6 um. I do not have any experiences with such sample. Could someone give me a tip how to prepare sample for TEM (or SEM)? Charles Garber reply: The problem is that those pesky silica particles don't know that they are supposed to separate and stay away from each other when dispersed in a liquid followed by a droplet of this liquid suspension being placed on a solid surface. They tend to agglomerate very quickly leading to a difficult- to-analyze situation, especially using automated means of analysis. You are correct in that the size range expected could be on the order of 3-6 nm. This is the ideal application for the camphor/naphthalene method which I described several years ago. Credit for the technique, or at least the one who taught it to me was an innovative microscopist then working at the DuPont Experimental Station in Wilmington, DE by the name of Robert P. Schatz, in about 1968, now deceased. Take a 60% camphor/40% naphthalene mixture and heat it to twenty or so degrees above room temperature on a hot plate in a small beaker or flask, the two organics are miscible in each other and this is the eutectic composition. Once a clear liquid, add a small amount of the silica (not more than 0.1%), which disperses quite readily. Then, using a pipette, take out some liquid and put a drop onto a carbon coated glass slide, at which time the drop is instantly frozen solid (it is at room temperature). Put the slide into your vacuum evaporator to pump out all night, and the "magic" is that the solid eutectic sublimes at room temperature at a rate that by morning, it is completely gone, leaving the silica particles uniformly dispersed on the carbon film! The rest is obvious. You can pick this up on

AANetNotes 08n4.indd 2 06/22/2008 1:19:02 PM

Beating the Competition is Easy, When You've Got Products They Don't Offer!

Si-Li EDS Detectors,
IXRF offers guaranteed, premium ≤ 130eV, resolution Si-Li detectors. *(*industry standard detector resolution 133-138eV)* that carry a three year warranty.

New 30mm^2 at 133eV, three year warranty available for cost effective fast X-ray Mapping.



X-Beam, Micro XRF,
40-60 micron spot. 10,000 times more analytically sensitive than EDS. Out performs WDX for less than half the cost.

fX SEM XRF,
400-1000 micron spot. 10,000 times more analytically sensitive than EDS.
Perfect for environmental applications as well as non-conductive samples.

50mm^2 Silicon Drift Detector, the largest Active Area in the industry (50mm^2). 133eV resolution, with optimum peak stability, and high input count rates. Who says "Bigger isn't better"?

IXRF does not stratify their software suite into low, medium, and high-end levels; there's only one high-end package that includes a myriad of **Spectra Analysis, Image Analysis, X-ray Mapping,** and unsurpassed **SEM/EDS Automation.**

Free Software Upgrades for Life…no compromises.

IXRF SYSTEMS

IXRF Systems, Inc. 15715 Brookford Dr, Houston, Texas, 77059 (Tel): 281/286-6485 (Fax): 281/286-2660
www.ixrfsystems.com

MT Full Page Ad Master.indd 1 06/22/2008 1:46:51 PM

a grid, as is, or in order to bring out more contrast, Pt/C shadow, probably using an angle not more than 30 degrees. You can float the "replica" off of the slide directly onto a grid and viola! you have particles completely dispersed, virtually no doublets or triplets, and a field quite amenable for automated image analysis (as a bonus). One important further suggestion: Sometimes these silica particles tend to fuse together as little "chains". If you suspect this is happening, be sure to take the micrographs as stereo pairs because you can in fact capture this three dimensional spatial information. Disclaimer: We do not sell either the camphor or naphthalene so have no vested interest in whether people use this method or not. It is just a really neat method for the preparation of fine particle samples in this size range. We are obviously set up to use this method as a service for others, however. Charles Garber - reposted by Henk Colijn colijn.1@osu.edu May 21

FYI - The published version of the camphor-naphthalene article is: Thaulow, N. and E. W White: General method for dispersing and disaggregating particulate samples for quantitative SEM and optical microscopic studies, Powder Tech, 5, 6, 377-379, 1972. Andrew Anthony Havics ph2@sprynet.com May 21

I would make sure that your substrate is very flat: a glass cover slip or vitreous carbon. Suspend your particles in pure alcohol and sonicate for a minute, don't use the surfactant for the reasons you mention. Put one drop of your suspension onto the substrate and it should spread out quite well. The alcohol should evaporate quite quickly, but particles at that size range should not agglomerate too badly. You should be able to find good areas on your sample to examine. Mary Fletcher maryflet@interchange.ubc.ca May 21

Another way to disperse particles dry is by simply pouring slowly into the top of a long tube or pipe held vertically over your substrate. The pipe should be something like 3-4 feet long and 2-3 inches in diameter. Just hold it vertically over an adhesive substrate. The fall through the still air in the tube breaks up the particles and reduces agglomeration. John Mardinly a.mardinly@numonyx.com May 21

There are numerous strategies that might be worth a try for your samples. It will require significant trial and error to determine what works best for your samples and analytical needs. All will have advantages and disadvantages and prep artifacts so you will need to experiment and decide what produces the best dispersion (particle loading, particle separation, and substrate) for your samples. In general, if you are starting with a dry powder there are a few paths you might try (in no particular order). 1. Dry "puffing" of the sample in a box with your sample substrate. A home-made "puffer" box is pretty cheap and easy to make. You basically use compressed air to puff the dry sample into the air around a sample substrate and allow it to settle. Works well for narrow size distributions of larger particles (~500nm or greater). 2. Resuspension and filtration. Suspend your sample in water (or other solvent) with a surfactant, ultrasonic briefly, and filter onto polycarbonate membrane filter. Remove a section of the filter, place it on a substrate and carbon coat. This is a good general purpose method, but dispersion of particles can be difficult with some minerals (clays in particular). Your sample will also end up on a carbon-rich substrate, but methods are available to produce carbon films supporting particulate on TEM grids (See any of the TEM asbestos analysis methods) 3. Spray mounting. This is basically making a heavy suspension of your sample in a solvent and airbrushing it onto a suitable substrate. One of the microscopy supply vendors makes a spray mounting device. Makes good dispersions of fine particulate, but introduces the possibility of size fractionation during prep. 4. Drop mounting. Sounds like you have already tried this, but if you try different solvents and try heating your substrate slightly to allow for rapid evaporation it might work. 5. Film casting. Suspend sample in collodion solution (~2% or less) and cast a thin film on H20 surface. Pick the film off the water with a polished substrate and heat to sublimate the collodion. This takes a lot of trial and error to get the technique down and to figure out the best particle loading. Your particles also need to be able to withstand higher temperatures and need to be insoluble in H2O. Those are the few that come to mind. There is opportunity for significant amounts of creativity so have fun playing with this. Just beware that some will introduce significant prep artifacts depending on the particle size. Lehigh used to offer a course called "Particle Characterization and Preparation, Microscopy and Analysis" during their summer Microscopy School. It was taught by John Small and Cynthia Zeissler et al. from NIST. All of these general methods can be refined to suit what you have and what you want to do, but all will likely introduce artifacts on the particle size distribution. Bryan Bandli bbandli@d.umn.edu May 21

SPECIMEN PREPARATION - sputter coating

A question regarding applying conductive coatings. We're in the process of procuring 2 new FESEMs and I need to update our sample prep equipment. We have an Edwards Auto 306 and a vintage (workhorse) Polaron E5000. I am aware that we need to update to a new sputter coater with e.g. Pt/Pd targets; however it has been suggested to me that we use the Edwards Evaporator for all our coatings needs. I don't think that this will suffice - but apart from the evaporator being slower, can anyone help me build a list of reasons why we need a new sputter coater? Emer emer.ryan@dit.ie Apr 18

I have been operating an EMS575X Turbo Sputter coater for nearly two years. Besides the fact that it is fast as you already knew, the samples rotate so all sides get an even coat and the machine is built to be compatible with a "Film Thickness Monitor" (FTM) which we chose as an option. This has proven to be a great help and money saving component in that the sputter coater now stops sputtering automatically when the desired coating thickness is obtained - no guessing or timing! Less electricity is used per run and a pre-determined amount of target is used for each run (thickness easily changed for different types of samples) eliminating wasted expensive metal. The negative was the additional cost of the FTM. Patricia Stranen Connelly connellyps@nhlbi.nih.gov Apr 18

I am going to put a disclaimer up front. We manufacture and sell the IBS/e ion sputter coating system. Now, having said that, consider a sphere sitting on the tilting and rotating holder of your sputter system. Now consider the amount of time each surface element of the sphere is pointed at the sputter target. When your stage is tilted at 90°, if it doesn't stay there longer to account for the amount of time to cover each surface element with the same amount of material as when the stage is at 0°, then the coating over the surface will not be uniform. In other words, the stage should spend less time going through 0° than when it is turning around at 90°. Further, because you want to coat the sample uniformly, it

AANetNotes 08n4.indd 3 06/22/2008 1:19:03 PM

11 MEGAPIXELS

High Definition Digital TEM Cameras

AMT's HOT NEW LINE

TEM INTEGRATION

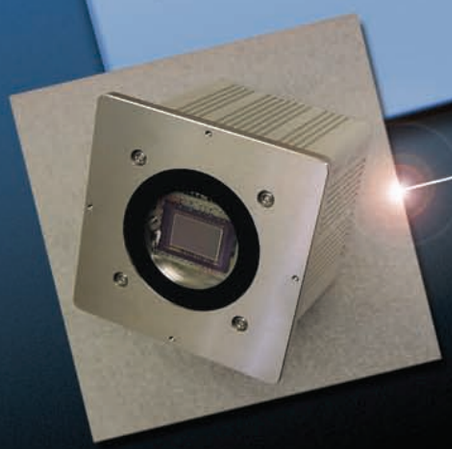
FASTEST DISPLAY

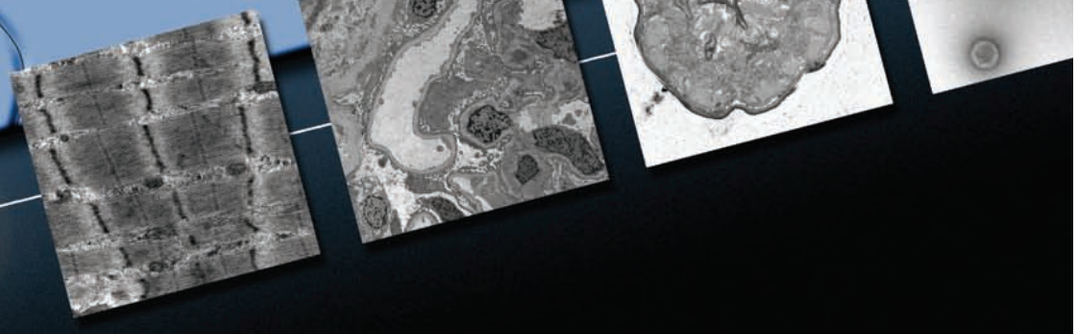
LARGEST FIELD OF VIEW

BUILT-IN RELIABILITY

PROVEN SUPPORT

SIDE MOUNT & BOTTOM MOUNT





AMT

Advanced Microscopy Techniques Corporation

3 Electronics Avenue • Danvers, MA 01923

978-774-5550 • www.amtimaging.com

MT Full Page Ad Master.indd 1 06/22/2008 1:51:29 PM

is not beneficial to coat the sample fast. You want to grow the film slowly so that you have better control over both the film thickness growth and the uniformity of the film by allowing your stage to go over all possible angular ranges over the duration of growth. In our system, I will actually purposely grow some films slower to enhance the uniformity of highly topographic samples. Magnetron sputter systems are fast, but they have a couple of disadvantages. Magnetron systems can "spit" material sometimes. These are larger particles that can be incorporated into the film. Also, the distribution of the sputtered material changes over time as a function of the wear pattern in the target. This can affect the accuracy of a quartz crystal thin film monitor system. Don't forget that you also have to run the unit a little before coating to get rid of any surface oxide on the target. Different target materials oxidize differently, so the amount of time that you have to pre-sputter the target is dependent on the material. In practice, what this means is that you have to have a shutter for your sample so that it is not coating the sample while you are conditioning the target. On the other hand, an ion beam system has a fairly stable deposition pattern over time. The deposition rate has a cosine distribution that doesn't matter too much about how the target is eroded over time. It is slower, which I think is a good thing for high resolution SEM coatings. And it does not "spit". One other thing that separates the systems: You can't deposit magnetic materials easily with magnetron sputtering. Why is this important? Several investigators are using Ni and Fe thin films to use as catalyst layers for the growth of carbon nanotubes. Another thing is that you can readily change targets with an ion beam. In our system, we can have up to four targets that can be switched while under vacuum. The Gatan system has two targets. What this means is that you can use these systems to put down multi-layer thin film coatings that can be used for calibration samples and standard samples for TEM. I've actually performed the calculations for using a bi-layer thin film with known thicknesses to act as a thin film binary standard for AEM. I just haven't done the experiments yet. Scott D. Walck walck@southbaytech.com Apr 18

We had an older dual beam VCR Group microsputter coater mounted on an Edwards 306A. Both units integrated fine. However, it was a bear to change the Edwards back and forth between microsputtering and other thermal evaporations. 1. The Edwards is a fine unit but it is oil pumped. That was not a big problem with our Cr coatings but others wanted a turbopump on it. 2. We had to cover all the feed throughs with a steel bell jar that was more like a collar. The collar was very heavy and had a large diameter. The microsputter coater fit on top of this collar. It took two of us to change back and forth from the microsputter coater mode to regular Edwards' modes. 3. You need lots of bench space for the bell jar, the heavy collar, and the sputter unit. A desktop sputter unit is MUCH smaller, lighter, and takes less bench top space. 4. Cycle times are longer with a large free standing large bell jar evaporator. They have their place and uses. However, then there is the LN_2 trap issue and waiting for cooling and pump down with LN_2. Then you might need a rotator system. Do you really want to go there? I took a 30+ year old vacuum evaporator from another group that was headed to the dumpster and rebuilt it. It was not fun. Some nut opened all the valves and pumped the thing overnight with the diffusion pump heater on and the vent valve open. Don't hire a plumber as a vacuum technician. The diffusion pump chimney had carbon foam in it the next day. That's just one of the 15+ things that were wrong with the evaporator before I got it. It took three months of my spare time to finish the rebuild. Once I got it working, then I had to convert my new used evaporator from a dual thermal boat unit. I installed a Ladd carbon rod and tungsten basket unit in the evaporator. So I got the new smaller evaporator unit working and we seldom had to change the Edwards over again. What's the moral of the story? That's how much I/we hated converting the Edwards. If you are a weight lifter, you will love converting back and forth. I eventually passed on converting. The dedicated carbon rod evaporator setup I built put a stop to the repeated conversions between carbon to chrome to carbon to Pt, to carbon, etc. Paul Beauregard beaurega@westol.com Apr 18

There is a new bench-top high vacuum platform for research & development from Oxford Vacuum Science. It uses thermal evaporation, providing a real, low-cost alternative to electron beam technology: www.oxford-vacuum.com. Dietrich von Diemar didi@specs.com Apr 18

SPECIMEN PREPARATION – coating for SEM

Does someone in the community have some experience/opinion about the osmium coating for FE-SEM as a replacement for conventional gold coating? Any particular comment about Os vs Au or Au/Pd or Pd/Pt for biological specimens (collagen, cells, etc) Alejandra acamacho@rd.us.loreal.com Alejandra Jun 2

Consider Pd and Ir. If EDS is not an issue, these will work well. The caveat is to coat at high vacuum. This is typically about 15-20mT. With rotation, you can get a very nice coating. At high magnification, Au/Pd and Au are seen. Pt works well too at high vacuum. Gary Gaugler gary@gaugler.com Jun 2

SPECIMEN PREPARATION – evaporating thick Al layers

We have several researchers who need to coat some wafers with 1-2 micrometers of aluminum. We tried using our conventional technique (10 cm of 10 mil Al wire evaporated from a tri-wire tungsten filament) but can only obtain extremely thin layers. What should we be doing to obtain the thick layers? John J. Bozzola bozzola@siu.edu May 16

I had success producing thick Al layers by evaporating Al foil in a basket of W, which can be obtained from a number of EM supply houses. The basket has two arms and is conical with the wire wound to form the part that a ball of crumpled foil will fit into. I think that one could use as much foil as necessary, since Al has a relatively low boiling point. (The same is not true for Ti, which can melt and short enough W wire that the temperature never achieves the >3000 K necessary to evaporate it.) I cannot say how flat or uniform the layer is except that Al evaporated onto plate glass makes a good mirror. You could also evaporate as usual, then repeat until a 1-2 um layer is built up, but this may not be practical unless you can get ~100 nm or more per individual layer. Bill Tivol tivol@caltech.edu May 16

Thermal evaporation of aluminum from W baskets is problematic. The molten Al reacts with the W to form a eutectic (Al-W dendrite sample anyone!) and the W wire often breaks before you get a very thick film. Also, when making thick (>100nm) metal films, internal stress in the film becomes a problem. I've had films peel

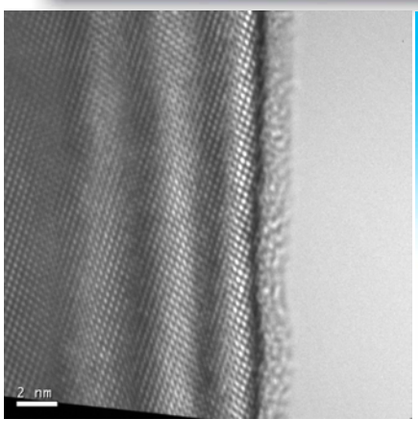
AANetNotes 08n4.indd 4 06/22/2008 1:19:03 PM

New Plasma Trimming™ Tools

Patent Pending

Thins and Removes Amorphous Ion Damage

TEM Sample Preparation





PTR-2000 Plasma Trimming™ Rod



PCPT Plasma Trimmer™

- Easy to use.
- Compatible with all FIB instruments.
- Compatible with different gases and gas mixtures.
- 0 to -1000 Volts (PCPT)
- Programmable 0 to -500 Volts (PTR-2000).
- Uses modified Fortress™ holders.
- Compatible with SampleSaver™ storage containers.
- Does not affect plasma cleaning capabilities.

South Bay Technology, Inc. has developed two Plasma Trimming™ tools for cleaning the amorphous damage from FIB-prepared, ion milled, or Tripod polished TEM samples with low energy ions. Five modified Fortress™ holders and the SBT SS-100 SampleSaver™ with FIB rack are included to minimize re-oxidation of the samples until they are ready to be imaged.

New UVO Cleaner® Station*

Stores and Cleans TEM Sample Holders in Air!

*UVO-Cleaner® is a registered trademark of Jelight Company Inc.



The UVO Cleaner® Station is designed to store multiple TEM specimen holders while periodically cleaning them using specially designed, spiral UV lamps using the UVO cleaning method. Each specimen holder is securely held in an adapter that is specific to its manufacturer's design. This adapter is mounted on the rear panel of a sliding drawer. When the drawer is closed, the rods are centered within the spiral lamps while keeping the rods in a dust-free container. When on, the spiral lamps surround the rod within a few millimeters and completely bathe the rod in UV light - generating active oxygen species for cleaning.

Available Models:

UVO-CS2-2: 2-position, 2 active lamps

UVO-CS4-2: 4-position, 2 active lamps

UVO-CS4-3: 4-position, 3 active lamps

UVO-CS4-4 4-position, 4 active lamps

SBT SOUTH BAY TECHNOLOGY INC.

1120 Via Callejon, San Clemente CA 92673 USA
Voice: 949 . 492 . 2600 • FAX: 949 . 492 . 1499 • Sales: 800 . 728 . 2233
e-mail: sbt@southbaytech.com • Visit us at http://www.southbaytech.com

©2007 South Bay Technology, Inc.

from the substrate due to the stress. I'm not sure if this is more of a problem with thermally evaporated films compared to sputtered films or not. Perhaps someone more familiar with the deposition processes can further clarify the issue. Since thick films are grown, there must be ways to do it. Would it be better to grow a thick film by electro-deposition similar to the way they grow TEM grids? Hendrik O. Colijn colijn.1@osu.edu May 16

IMMUNOCYTOCHEMISTRY – brain tissue for EM

Can you all lend some expert advice as how to optimize a protocol for post-embed labeling on brains? I have a user who has been doing post-embed labeling on brain tissue which has been embedded in Araldite with the traditional fixation and embedding protocols (Karnovsky's, OsO4, ethanol, propylene oxide and Araldite). She has to etch her sections and other damaging things which limit ultrastructural beauty and labeling prettiness. I'm suggesting LR White but I want to know what the experts are doing. Paula Sicurello vapatpxs@yahoo.com Jun 11

The specimen as you describe it is probably not the best situation to start with, although there have been reports of successful immune-labeling on tissue that was OsO_4 fixed and epoxy embedded. So if that is what you get, you might have to give it a go. LR White embedding means you have to go through another run of specimen preparation. While you are at that...is there no way you could consider a pre-embedding approach? Jan Leunissen leunissen@aurion.nl Jun 11

Using Epon may not be far off the mark when it comes to brain immunocytochemistry. There is a group in Norway who have been successfully using it for a while (O.P Ottersen). More recently they switched to Durcupan (Gundersen et al J Cerebral Blood Flow & Metabolism (2001) 21, 41–51; http://www.nature.com/jcbfm/journal/v21/n1/abs/9591036a.html;jsessionid=178E36E3B37B167B1C682EA6ED331497). Although other resins may be more favorable, they will bring other problems. For example, LR White is a very good solvent that may take away brain lipids. You may also encounter polymerization problems too if you are not using this resin routinely. There will also be a different contrast that your collaborator may not appreciate (low contrast myelin) Of course, the final answer to your question is to try one or two different options and see which works best for your antigen and antibody combination. Have you considered cryosections of cryoprotected material? This would be an excellent approach for antigens that are not washed away during aldehyde fixation. The only disadvantage could be that the myelin will not have the black appearance usual for tissue treated with osmium. Interestingly, someone just told me that adding uranyl acetate to the pick-up solution will create the black (artificial) color if you really want it. Paul Webster pwebster@hei.org Jun 11

There are many approaches for immunogold labeling in brain tissue. Post-embedding labeling on conventionally fixed and Epoxy resin embedded material is one of them, however this method is only suitable for a small category of antigens, among which is a group of amino acids used by the brain as neurotransmitters. The antisera against these small amino acids usually are raised by immunizing rabbits with the respective amino acids that are conjugated to a carrier protein (e.g. BSA) using glutaraldehyde. Therefore, the preservation of the epitopes of these amino acids in brain tissue is not incompatible with glutaraldehyde fixation, and this is one of the reasons conventional embedding is fine for the labeling of these amino acids. The labeling described in the paper Paul listed in his reply is an example of this type of labeling. However, the majority of immunogold labeling in brain tissue is for antigens that are far more "vulnerable". Although using milder aldehyde fixative, omitting OsO_4, and switching to LR White resin may minimize the "damage" to the antigens, I do not recommend this approach for brain tissue. In brain tissue, the identification of neuronal structure relies heavily on the integrity of membrane ultrastructure. In addition, many labelings are for membrane bound proteins such as receptor proteins, channel proteins, or transporter proteins. In its protocol, LR White embedding is usually accompanied by the omission of OsO_4 fixation which means lipid is not stabilized so more likely to be extracted or "melted" during dehydration and thermo polymerization. For this reason, LR White embedded brain tissue will not give the adequate membrane ultrastructure required. If your user has a particular reason to insist on post-embedding labeling, I would recommend high-pressure freezing, cryo-substitution, and embedding in Lowicryl. There have been many publications using this approach for brain tissue showing good membrane integrity. In general, the far more common approach, or I should say the approach people usually start with for immuno labeling in brain tissue is pre-embedding labeling. One aspect of immunolabeling in brain tissue is to survey the distribution of the protein in a large and structurally heterogeneous area before dissecting out the right area for EM analysis. For this reason, pre-embedding labeling offers a major advantage because the labeling can be seen with LM in large Vibratome sections that cross any region of the brain. Pre- embedding immuno labeling has other benefits as well which we can discuss later. As Paul mentioned your user might want to try one of two different approaches, however, he/she should not try randomly. Again, find out first what is being labeled and what questions need to be answered with this labeling. Back to Araldite embedded material, if the etching is done right, he/she should be able to get beautiful ultrastructure. Hong Yi hyi@emory.edu Jun 12

It all depends on the antigen you are looking for. That said, it is unlikely that traditional EM processing will allow you to find what you are looking for. Before proceeding, I suggest a literature search to see how others have localized this antigen at the EM level. This could save someone a lot of time and trouble. Geoff McAuliffe mcauliff@umdnj.edu Jun 12

DIGITAL IMAGING – resolution

I have a dilemma: I have acquired images for a client on our TEM, which is equipped with a Gatan Erlangshen ES500W camera. Using Digital Micrograph, I acquired images in the DM3 format. I then batch convert to Tiff or BMP, and gave the client both the original DM3 files as well as the converted ones. I instructed them on opening the DM3 in Image J, which was not a problem. The problem is that once in Image J, they need to be converted into tiff, or other common file type for use in other programs, i.e., for preparing a manuscript. My client has a problem with a "resolution loss" once the file type is changed. The image is about half the size (~1.3MB), but their main concern is that the dpi is only 72 (when opened in Corel), and that they won't be accepted if they have that low of a dpi. I haven't been able to find any information on how important the dpi number is, and I'm a bit skeptical as the image looks to be the same quality as the

AANetNotes 08n4.indd 5 06/22/2008 1:19:03 PM

NETNOTES

original. My client thinks I should change the settings on the camera so the original image is larger than 3MB, but I don't even know how/ if this can be done! Sarah Aubut saubut@nrcan.gc.ca May 28

Your image size is not determined by the dpi - that is the display size and is a function of the software and/or output device (i.e., monitor or printer). Displaying the image at 72 dpi or 300 dpi makes the image look bigger or smaller on screen but the resolution isn't changed. The resolution is determined by the 1200 x 800 pixels (or whatever the image size is in pixels). Thomas E. Phillips phillipst@missouri.edu May 28

Digital imaging has so many things controlled by various things from the acquisition to the final output. Like Tom said, the image resolution is set by the pixel resolution at acquisition time. But ugly things can subsequently happen. A new document in Corel is typically 72 dpi by default unless changed; the assumption is that you are developing images for computer viewing and computer monitors are approx 72 dpi. Now if you drop an image onto a page at that default resolution you have to grab the "handles" and drag it to the desired size on the page. Here is the problem: when you click "Apply" (in Corel9....) it re-samples the image to the 72 dpi page resolution and the original resolution is gone. If you had started with a page at 300 dpi (near photographic) then an 1800 pixel wide image is 6" wide on the 300 dpi page and if printed on a good 300 dpi printer (true 300 dpi like a dye sublimation printer, or equivalent). I think that if an image has no scale data in the tag fields (TIFF) Corel will treat it as a 72 dpi image by default so the hypothetical 1800 pixel-wide image is (1800/72) inches in hypothetical size. There is wealth of information about digital imaging on the Molecular Expressions website: http://micro.magnet.fsu.edu/primer/digitalimaging/index.html Dale Callaham dac@research.umass.edu May 28

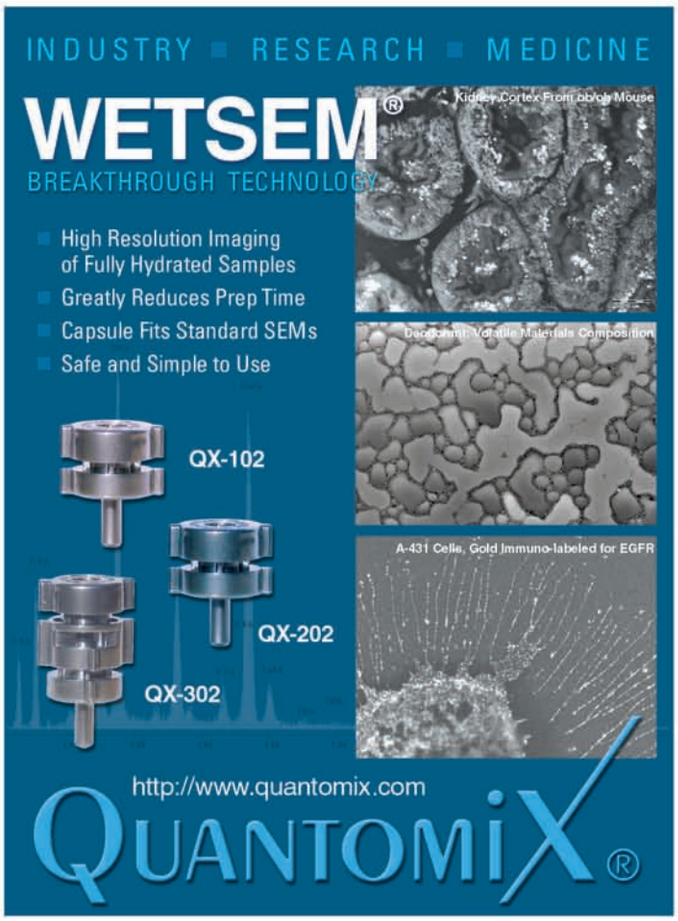
Another thing that might be related to the reduced file size is the bit depth. Image acquired from the CCD camera is likely being 16 or 32 bit. But it has to be converted to 8 bit TIFF file in order to be displayed properly in normal software such as Windows Image Viewer or MS-Word. This process will cause some information loss and reduce the file size. Fan Li lixxx326@umn.edu May 28

EM - algae in chiller

We have a conventional SEM, a FEG-SEM (the most recent acquisition) and a TEM, all with water circulation provided by the same chiller. Lately we have noticed some algae forming inside the hose of the FEG-SEM, which is a bit more transparent than the rest. We have changed the water in the chiller, but with no results. My questions are: 1) Is it possible to use some product to remove these algae without damaging any part of the microscopes? If not, what can we do? 2) Do you use distilled water in such chillers? Isabel Dias Nogueira isabel.nogueira@ist.utl.pt Apr 16

Preventing the growth of algae in cooling water systems is discussed in detail in my book "Vacuum Methods in Electron Microscopy". Two chemicals commonly used to prevent algal growth in such systems are Chloramine T and dichlorophene. Both of these chemicals can be obtained from various specialty chemical companies. You can also probably obtain algaecides from companies (and merchants) that sell water beds, and swimming pool equipment. I do not recommend the use of ethylene glycol for several reasons that are discussed in my book. Also, remember that algae require light in order to grow, and so you can substantially inhibit





AANetNotes 08n4.indd 6 06/22/2008 1:19:04 PM

their growth by fully excluding light from the system (i.e. cover the reservoir with a light-tight cover, and use fully opaque tubing). Changing from ordinary tap water to distilled water will probably not give you much of an advantage, except for possibly minimizing the formation of a bit of scale in the heated parts of a diffusion pump. However, the amount of scale formation should be quite limited since it is a closed system containing a limited amount of water. Wilbur C. Bigelow bigelow@umich.edu Apr 16

When we got a new water re-circulator a few years ago, they told me that, if it got some algae in it, empty all the water out, fill it with tap water, run it around for a while, then empty the tap water out and replace with distilled water. The tap water in most cities now has enough chlorine in it to kill the algae and flush it out, but they want the re-circulator run routinely with distilled. The other thing I have heard is that just one or two drops of bleach in the tank will kill any organisms without harming any components. Mary Fletcher maryflet@interchange.ubc.ca Apr 16

I would keep all Cl out of the system. If any remains, it will corrode the cheap brass most systems use. This brass is high in Zn and is much more susceptible to corrosion than Imperial brass (but it cost $1 more). For my Haskris chiller, I run 10% ethylene glycol with distilled water. I try to find the purest distilled water I can. I've taken selected drops from different distilled water jugs and put on a clean microscope slide. Let dry and see what remains. Most will have residue. The one that has the least or none is the one to use. Zeiss chose clear hoses for my SEM but I see no problem since using ethylene glycol. Be sure to change chiller filter(s) about twice a year. Gary Gaugler gary@gaugler.com Wed Apr 16

To protect our chillers from algal growth and freezing (chiller lives outside) we run them with the heat transfer fluid Hexid A4 from applied thermal control. http://www.app-therm.com/product_hexid.asp. It's pricey but we have no problems with algal growth. I have no commercial interest, just a satisfied customer. A. Christine Richardson a.c.richardson@durham.ac.uk Apr 17

To restrict the growth of algae in the fluid reservoir, I recommend the reservoir cover be kept in place and that all recirculation lines be opaque. This will eliminate the entrance of light, which is required for the growth of most algae. The use of Chloramine-T, 1 gram per 3.5 liters is recommended. Other algaecides can be harmful to the unit's internal components. We use a Thermo recirculating chiller for our Hitachi TEM. Thermo recommends distilled/deionized water with 0.05 to 0.1 megohm-cm reading. Highly distilled/deionized water, above the 3 megohm-cm region, may become aggressive and is not recommended for use with units with wetted parts other than stainless steel. Distilled/deionized water in the 15 megohm-cm region is definitely aggressive and should not be used. Do not use a deionization (DI) filter with inhibited EG. A DI filter will remove inhibitors from the solution rendering the fluid ineffective against corrosion prevention. Also inhibitors increase fluid conductivity. Proper reservoir cleaning is necessary. Make a monthly visual inspection of the reservoir after initial installation. After several months, the frequency of cleaning will be established. Use a soft cloth for cleaning; do not use steel wool or other abrasive materials. They can scratch the steel surface and initiate rusting. IPS Gill ipgill@gmail.com Apr 17

As suggested by one of you, I ran some tests to make sure we had algae in our system. To my surprise, the composition of the deposit I removed from the hose was mainly Fe, Zn and Cu... I suppose they come from the water pipes, and that our filters have not been changed as often as they should have been. Apart from changing the filters, cleaning the water deposit of the chiller, is there anything else I can do to remove this deposit from inside the microscopes? Isabel Nogueira isabel.nogueira@ist.utl.pt Apr 22

I am not sure I am the only one that sent you a suggestion. I sent you the procedure and suggestion to determine if you were dealing with either green algae or green copper carbonate residues. Either case is possible. So that is absolutely the first task. I am glad that someone found out what I did. Green does not mean that algae are the only cause of green deposits. See the Microscopy.com archives on Jan 21, 2008 for algae and carbonate reactions involving CO_2. As shown in the attachment article sent to Microscopy Today and you, the chemical reaction of CO_2 will attack copper sources including brass. I suspect that your zinc is from alloys like brass and not galvanized pipes. Impellers on pumps can also be bronze and slowly eroded away over the years. So tin can also be found. The iron could be from a lot of sources but stainless steel fittings or tubing makes a lot of sense. Chlorides will pit corrode stainless steel. You can never eliminate all sources of copper, its alloys, and iron in instruments or chiller loops. Water filters can catch precipitates in suspension such as calcium and magnesium carbonates (city water contamination) and/or copper carbonate (erosion of copper and its alloys). A water filter will not stop the scaling by itself but is required at the inlet of every instrument, in my opinion. The scaling problem is Ksp based and that involves dissolved ion concentrations. Removing the residual or plugging deposits that you can't see is tricky. Servicemen use Lime Away or CLR to remove the scale. Both these products contain a mild acid. They are citric acid and phosphoric acid based. Some phosphates can be insoluble. Dilute hydrochloric acid works to remove carbonates but it has some risk. You run a water circulation loop into an open bucket using a small circulating pump. Start out with a low concentration of HCl. All sorts of CO_2 bubbles and black rubber particles can be seen in a white bucket exiting the return line. In the bottom of the bucket, put a couple of old dark copper US pennies or other equivalent copper coins. They must be oxidized. Once the initial bubbles are formed and any blockage is opened up a bit, you can then slowly add HCl while still circulating. Do not dump HCl additions onto the copper coins. Remove them temporarily while adding HCl. When you see the copper penny coins turn bright and the copper oxide is removed by the return line solution, then that is the highest HCl concentration you should use. You have started to attack the copper tubing oxides in your microscope and the pennies are your indicator for that attack. Immediately switch to pure DI water from another bucket and flush the system. Do not recirculate any water at this point. This flushing can take a while and requires frequent water dumping and refilling of the buckets. Monitor the output of the circulation from the microscope with silver nitrate to test for a white silver chloride precipitate. Once you think you have not detected any more chlorides from any residual HCl, flush a few more volumes of pure DI water and switch to freshly flushed chiller lines. Circulate fresh DI water for a few days. Test for chlo-

AANetNotes 08n4.indd 7 06/22/2008 1:19:04 PM

Mini-SEM™ www.Mini-SEM.com

Mini-SEM Compact Footprint (22 x 22 x 22 inches)

15 keV or 30 keV Analytical Miniature Electron Microscope

120,000 X - Magnification (Digital Zoom)

Liquid Nitrogen Free - Light Element X-ray Detector

Easy Spectral Identification

Advanced Image Analysis & Image Processing

Ultra Fast Elemental Mapping - Spectra for every pixel

Auto Report Writing

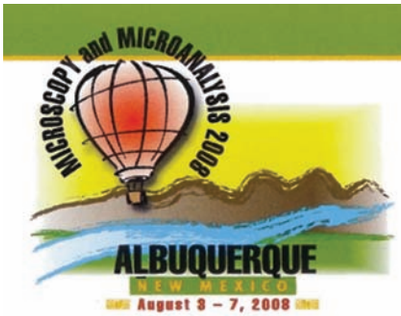
Installation & Training in Minutes!



Scanning Electron Microscope
+
X-ray NanoAnalysis

EVEX

Call Today 609-252-9192



There's Still Time To Register for the M&M 2008 Meeting in Albuquerque!

It's Fast! It's Easy! It's Secure!

Go online to **www.microscopy.org** and click on M&M 2008 Meeting, then on "Registration/Forms". You can register online, or download a PDF to fax or mail in.

Check out the comprehensive scientific program on the meeting website, as well as the impressive list of exhibitors.

Register now!

REGISTRATION DESK HOURS IN ALBUQUERQUE:

Thursday, July 31	10:00 am – 5:00 pm (exhibitors only)
Friday, August 1	10:00 am – 7:00 pm
Saturday, August 2	6:30 am – 5:00 pm
Sunday, August 3	6:30 am – 8:00 pm
Monday, August 4	7:00 am – 6:00 pm
Tuesday, August 5	7:30 am – 5:00 pm
Wednesday, August 6	7:30 am – 5:00 pm
Thursday, August 7	7:30 am – 3:00 pm

Director, Imaging Technology Group
Beckman Institute for Advanced Science and Technology
University of Illinois at Urbana-Champaign

The Beckman Institute has a position opening for one (1) Director, Imaging Technology Group (ITG). The ITG's primary mission is to provide state-of-the-art imaging and visualization resources for researchers at the Institute and the University of Illinois. This mission is accomplished through two facilities: a Microscopy Suite, and a Visualization, Media, and Imaging Laboratory. A secondary mission of the ITG is to develop advanced technologies with an emphasis on projects in remote and virtual instrumentation. The ITG Director sets the vision for this group of approximately 25 staff members, writes grants and directs special projects to support that vision, and conducts daily management of the staff. Applications must be received by July 31, 2008, for full consideration. To view the full job posting, please visit our website at http://www.beckman.uiuc.edu/about/employment.html.

The University of Illinois is an affirmative action, equal opportunity employer.

rides. If you see chlorides, flush the system again. When you find no chlorides, add your algaecide, hopefully a low PPM level of a quaternary ammonium salt surfactant and not any chlorine based "bleach". Try to seal the open reservoir airtight. It is the source of both CO_2 reactions, whether algae or copper carbonate based. As CO_2 is dissolved in the copper erosion case, the solubility product (Ksp) of copper carbonate will be exceeded before calcium carbonate. Once you exceed a Ksp, you will start to form scale. The ion concentrations will build up from CO_2 mixing in the open reservoir, even in a HVAC heat exchanger based system. Monitor any transparent lines for a green color build up in the future. If you see the green build up, then you did not exchange the old water with new DI water often enough (3-6 months). You must replace the DI water periodically to prevent exceeding the Ksp of any carbonates that are sure to form. It helps to have valves installed so that one can selectively flush the various branch lines to a diffusion pump or lenses. Deposits do not form uniformly. The output from DPs will scale more than the inlets. It would seem that hot water would keep the ions in solution. That is not what I/we found. So the green monitor tubing line should be after a DP, if possible. Check all the flow rates after cleaning out any lines. Check them against the flow specifications of the manufacturer. You said that you were surprised at the composition of the green deposits. I was not. I spent two months killing algae that didn't exist by following my supervisor's algae idea. The more Chloramine-T we added, the darker green the water turned. I took our water and added HCl and then ammonium hydroxide. The water turned green in acid and blue in NH_4OH base. After a few blue and green color cycles back and forth, I looked at him and said, "I don't think we have a blue-green alga problem in our chiller. This is how dissolved copper ions perform chemically." Like you, I got the message and eventually did some relevant inorganic testing. I would recommend having a serviceman flush the scale out with acid. If you have a good idea of how the lines run in the scope, then you can try descaling yourself. Paul Beauregard beauregard@westol.com Apr 23

EM - maximum length of vacuum lines

The oil mechanical vacuum pumps (a few each of belt drive and direct drive) for our 4 EM's are currently located in a service spline directly behind the instruments. Currently, the pump to scope distance is about 4-5 feet using rubber hose. Our safety folks are asking that we relocate the pumps. This will involve 1) moving them into the scope lab itself or into another room at the end of the hallway. I'm worried about noise and vibration if we relocate into the lab. If we put all the pumps into a single room it will involve long vacuum line runs. Safety insists we will use hard tubing. The vacuum line runs could be up to 20 or more feet between the pumps and EM's. Also, the tubing run will involved 2 right angle bends. How far can I locate the pumps from scopes? Does it matter if the bends are mitered? Should I use larger diameter tubing than the current rubber hose? Owen Mills opmills@mtu.edu May 7

Very simply the pumping speed is such that it follows the inverse square law. The further away the pump, the slower the pump down. Bends in a pumping line slow the procedure even further. When we design an instrument we expect the rotary pumps to be within 5 feet of the instrument and the facilities provided with the machine are designed to reduce vibration. The only area that you may not like is the noise from the pump, however to use an acoustic cover is a far better solution that to have the pumps at the distance that you indicate. Steve Chapman protrain@emcourses.com May 7

I would like to know the justification for moving the pumps. Is it that the exhaust is not properly ventilated? Could it be that lab equipment is not allowed in utility spaces? Fire code? http://www.lesker.com/newweb/technical_info/conductance_calc.cfm Jim Quinn jquinn@www.matscieng.sunysb.edu May 8

I have to agree with Gary. You need to know why they want them moved. Is it a fire hazard, a fume issue, etc. You might point out to them that it is far more dangerous to have the pumps in the same room than to have them isolated. This involves inhaling the fumes, etc. If they persist, you must insist that they put in writing that they will pay to fix any problems (e.g., poor vacuum to the instrument) that result from this move. They must realize the consequences of this forced move. John J. Bozzola bozzola@siu.edu May 8

Conductance of tubing is inversely proportional to tubing length, not inverse square. However, it is proportional to 4th power of diameter of tubing. So, slight increase in diameter will compensate for the increased length. Doubling diameter would enable one to increase length 16 times for same conductance. Kristian Ukkonen kristian.ukkonen@iki.fi May 8

I have been involved with several instances of moving rough pumps, and being a former student of Will Bigelow, dutifully calculated the conductance using the class notes that are now in his text book on vacuum technology. OK, the conductance and pumping speeds match, but what will surprise you is that the rough pump line suddenly has a volume that has increased by quite a lot, and when you hit that button that says "Pump", the "WHOOOMPF" you will hear the first time that roughing valve opens will really be a shock. Consider carefully whether your system can withstand the internal turbulence that this will cause. EDX vendors believe that pumping turbulence throws particulate material around with sufficient force to put pinholes in EDX detector's thin windows. There is also potential for physically moving thin apertures, lifting pole pieces, and who knows what else. The best thing to do here (aside from keeping pumping lines short) is install a throttle valve where the roughing line connects to the microscope. One way to do this is insert a butterfly valve in the large diameter roughing line in which you have drilled a small hole, maybe on the order of 0.25-0.5 inch. Close the butterfly valve before pumping, and then open it after the initial surge has subsided. John Mardinly a.mardinly@numonyx.com May 9

The "WHOOOMPF" sound and much longer pumping time which you are describing will indeed take place if entire roughing line is vented and if roughing pump is stopped during the vent. One way to deal with it will be to install a throttle valve, as you described, but in this case one still has to deal with increased pumping time due to the need to pump air from the volume of roughing line during each circle. Another way of running instrument with long roughing lines is to install into the roughing line electric (or pneumatic) shutoff valve as close as practical to the place where roughing line connect to SEM, and to control this valve from the relay which intended to stop roughing pump during vent and start it during pumping, in such a way that the valve is closed during vent and opened during pumping. Roughing pump should be connected

AANetNotes 08n4.indd 8 06/22/2008 1:19:04 PM

The Formula for Vacuum Success

DUNIWAY STOCKROOM has ***two*** ways for you to access our **complete catalog *or* selected sections** at www.duniway.com/catalogs

1. View them online & save or print them.

2. Use the online form & we'll mail you the latest printed version of the complete catalog, or

♦♦♦ NEW Sections ♦♦♦

- ♦ Q-Hardware/Supplies Section
- ♦ S-Vacuum Pump Section
- ♦ P-Vacuum Gauge Section

Duniway Stockroom Corp.
1305 Space Park Way
Mountain View, CA 94043



800-446-8811
www.duniway.com



Custom Microscopy Supplies From M. E. Taylor Engineering, Inc.

- ♦ **SEM Light Pipe Scintillators**, styles for Leo &Cambridge SEMS and custom products
- ♦ **Scintillators:** ITO Gold, Phosphor, YAG and YAP from $89
- ♦ **Recoating of Light Pipes** from $150
- ♦ **Conductive Adhesive Products**
  Silver paint, pens and epoxy
  Carbon paint, tape and tabs
- ♦ **ProScope and Dino Microscopes** and accessories

Phone (301) 774-6246

See our products on the Web @ www.semsupplies.com

McCRONE RESEARCH INSTITUTE
CHICAGO

McCrone Research Institute

2820 S. Michigan Ave, Chicago, IL
Phone: (312) 842-7100 or Fax: (312) 842-1078
www.mcri.org

Offering Basic & Advanced Microscopy Courses

- Polarized Light Microscopy
- Infrared Microspectroscopy
- Forensic Hair & Fiber
- Asbestos Identification
- Microscopy of Explosives
- Illicit Drugs & Excipients

Plus: Customized Courses at your location!

For a complete listing of courses and course descriptions please visit our website at www.mcri.org or call (312) 842-7100

MT_Half over 2 qtr pg ads.indd 1 06/22/2008 2:57:53 PM

directly to power and run all the time, even when instrument is vented, thus keeping roughing lines constantly evacuated, so this volume does not need to be pumped each circle. The operation, as far as SEM is concerned, will be the same as if roughing pump, with pumping speed limited by the conductance of the long roughing line, was installed where the shutoff valve now is. This will save pumping time with, but have downside of increased hours on the roughing pump (bill pump rebuilding costs to Safety Department. Valery Ray vray@partbeamsystech.com May 9

The question of the acceptable length of a rough pumping line has been pretty well covered by others who have already commented on this matter. However, if you want to see an actual calculation then you can find one on pages 44-45 of my book, "Vacuum Methods in Electron Microscopy" If you do install a pumping line of considerably greater volume than the existing one, and if the pump-out valve is located at the end of this line nearest to the instrument, then you should give serious consideration to the phenomenon mentioned by Dr. Mardinly. That is, assume that the vacuum chamber is at atmospheric pressure, the pump-out valve is closed, and the pumping line is evacuated. Then if the pump-out valve is suddenly opened the sudden rush of air from the chamber into the rather large volume of the vacuum line could indeed cause a serious turbulence in the instrument chamber. Wilbur C. Bigelow bigelow@umich.edu May 12

EM - magnetic interference from UPS

Do uninterruptible power supplies (UPS) cause magnetic interference to EM? If so, what solutions for UPS are in use in EM labs. The question came to us as to whether a UPS in rooms adjacent to EMs might interfere with them. Aryeh Weiss aryeh@cc.huji.ac.il May 15

We did some measurements on UPS last fall, before the installation of a new TEM, as we took the opportunity to add UPSs on the SEM and the existing TEM. The question was where localize them, on one hand to answer the same question as you and, on the other hand, to avoid long cables between them and the scopes. The specifications of the manufacturer give only some indications in the MHz/GHz range, to assure that there are no interferences with phones, WiFi etc. For EM, it's more the 0-10 kHz band which is important. We did the measure with a 100 kHz spectrum analyzer and a coil, in a room far from all power lines, at distances from 3 and 6m. The results 6 m away show that compared to the local background (UPS out), if it is powered on without load, frequency between 400 and 1500 Hz increase a bit (from 0.2 to 0.4 mG). With a resistive load of 6 kW, frequency between 1500 and 3000 Hz increase from the same order. The UPS itself has a frequency at 8 kHz of less than 0.05 mG, with its harmonics at 16, 32, etc kHz. The conclusion was that if we put each UPS 3-5 m away from its scope (in the technical room, next to the scope) we will be quite sure. The noise from the power line supplying the scope and its power supply itself will produce much more interferences. And it's the case. For the SEM, there is a level of less than 0.2 mG near the column with the UPS without load, and it goes up to 0.4 mG when I switch the SEM on! Jacques Faerber jacques.faerber@ipcms.u-strasbg.fr May 15

It depends on the particular make and model of the UPS. For the Phase One (Now Danaher) UPS for our 2010F, JEOL recommends over 30 feet distance from the UPS to the column, and that is for a 200KV microscope! John Mardinly a.mardinly@numonyx.com May 15

EM - filament life

We have problem with filament life on our Tecnai12, with diffusion pump and IGP. The scope is 5 years old. We are using W filaments supplied by FEI. We are getting between 20 to 30 hrs, rarely up to 50 hrs of life from a filament. Usually we operate at low emission settings, less than 10 μA. The filament current is stable and does not fluctuate more than 10% of the selected value. Scope performance has not changed. We have had several attempts by FEI engineers to find out the cause which they have failed to do so far. This problem is not operator related since we have experimented with saturating carefully the filament and then leaving the beam on at 120kV until the filament burned out without anyone using the scope during that period. The filament lasted 27 hrs. This problem has started about a year and a half ago. Before that we had unbelievably long filament lifetimes. The record is 1097 hrs! Usually we used to get lifetimes consistently over 300 hrs, with typical time between 500 to 700 hrs. Since the problem developed we have replaced the IGP, the ceramic insulator in the gun, gun chamber O-rings, specimen stage air-lock valve, we have tested different Wehnelt caps, boxes of filaments old and new, the outputs of the power supply have been measured and they are stable and within the specs and nothing seems to make a difference. The Wehnelt cap aperture size and distance is consistently the same as at the time we were getting hundreds of hours of lifetime. Typically the scope is operated at vacuum in the range of 10 to 20 log readings which corresponds to 1x10-7 to 5x10-7 Torr. At the same vacuum levels we used to get very long lifetimes. Any clues or suggestions what could have gone wrong? Krassimir N. Bozhilov bozhilov@ucr.edu May 8

If the electronics are stable (especially the filament drive ... I don't consider 10% anything close to stable, 1-2%/hr is satisfactory), then I would be looking for a vacuum leak in the immediate gun area. You haven't said exactly where you're measuring the vacuum. That can make a big difference, depending upon the vacuum design. One can very easily get pressure differences of a decade or more between sections of the vacuum system even without a significant leak. Have you put a leak detector or RGA on it? Ken Converse kenconverse@qualityimages.biz May 8

Take a good look at the glass/porcelain base of the burnt filaments that lasted less than 30 hrs. Can you positively see deposited (tungsten) material on the base surface around the filament? Additionally - do you have at least an impression, if not positive observation, that emission current somewhat increases on its own at any time during filament life? Irrelevant to arcing. Does not have to go up steadily all the time from installation to burn-out. But at least a few hours of slow steady increase, however small. If any of the above is a 'yes', then I might have an idea. Vitaly Feingold vitalylazar@att.net May 10

The answer to both questions is yes. There is definite deposit of W on the base even for filaments that have lasted about 20 or so hours. I have observed once that the emission current increased quite significantly, from about 8 μM to about 40 μM. After switching off the HT and starting again the emission was normal. I cannot tell if this occurs frequently, since I am not using that TEM very often by myself. I need to talk to users and find out. K. N. Bozhilov <bozhilov@ucr.edu> May 10

AANetNotes 08n4.indd 9 06/22/2008 1:19:04 PM

81:Layout 1 6/26/08 1:56 PM Page 1

Why have 1,000 scientists in 25 countries selected Minus K® vibration isolators?

Because Minus K vibration isolation systems deliver 10x to 100x better performance than high-performance air systems, without air, and for air table prices.

Visit www.minusk.com for more information...



Without Minus K | With Minus K

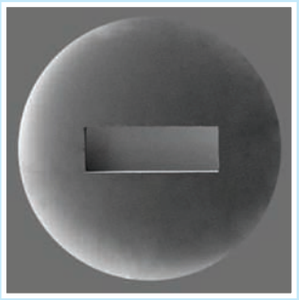
VIBRATION ISOLATION BY:
minus k® TECHNOLOGY

420 S. Hindry Ave., Unit E • Inglewood, CA 90301 USA
Phone: 310-348-9656 • Fax: 310-348-9638
sales@minusk.com • www.minusk.com

PELCO® Silicon Nitride Membranes

Next Generation Si_3N_4 TEM Support Films with many advantages:

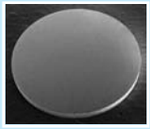
- Durable and chemically inert planar 50nm substrate
- 3.0mm circular frame compatible with standard TEM holders
- EasyGrip™ micro rough edges for ease of handling



- Free from debris - no broken edges
- Large area support film: up to 0.5 x 1.5mm
- Complimented with Aperture Frames and Blank Disks for nanotech experiments



Aperture Frame



Blank Disks

TED PELLA, INC.
Microscopy Products for Science and Industry

800-237-3526 **www.tedpella.com**

NETNOTES

All right, then I suspect the deposit creates an electrical conductance pass between Wehnelt and filament. If you look at the schematic diagram of HT generator, you will see this pass being electrically parallel to gun bias resistors. These resistors are switched back and forth for gun bias control in automatic bias circuit; that is common in modern EM guns. The less resistance - the higher the bias setting- the more current forced from the filament. This deposit may effectively increase the gun bias, with obvious consequences for filament life expectancy. You may prevent this deposit from connecting the circuit, in the following way. Find a piece of copper/brass/bronze thin sheet or thick foil, some 10 mil to 20 mil will do. Actually can be any metal that will not corrode and is easy to solder. Cut a washer from this material. This washer must be soldered on top of filament holding nut, just 2 or 3 points soldering, no durability required. The external diameter of this washer must be little less than the external diameter of the filament holding nut, and the internal diameter must be much smaller, just enough to accommodate filament pins. Make sure of the following: a) distance between filament pins and inner diameter of washer must be not less than 2.5mm, (3mm is good) - do not make it too large, otherwise it will not work; b) washer must not touch filament base - suppose it will bend and come very close to the base, that is OK, but must not touch the base; c) washer does not have to be perfectly even and round, yet (!!!) all must be flat and smooth, with no bumps and sharp points - solder, edges of the washer, etc. Deposit will still form. But the washer will 'cast the shadow' on the outer part of filament base, so the deposit will not close the circuit. The actual reasons for excessive tungsten evaporation/erosion may vary. Perhaps you have bad batch of filaments, which is less likely. Or perhaps your HT generator circuit is outside the specifications which is more likely. Additionally, if my guess was correct, then a filament base with very rough surface may prolong filament life. Bottom line, this method worked for me, on Philips CM series TEMs and it is much preferred to any other remedy as long as it works. Actual configuration of this additional element may vary depending on Wehnelt design for a particular TEM model. Vitaly Feingold vitalylazar@att.net May 10

P.S. A possible alternative - again presuming my guess was correct- a Kimball Physics LaB6 filament might be a solution. It has carbon heater and carbon does not evaporate much at these temperatures. In fact I installed this filament on a CM-10 with same problem a couple of months ago and it works so far without the modification that I described in the previous posting. Too short a time to be certain whether it is a fix or not. Vitaly Feingold vitalylazar@att.net May 10

Vitaly mentioned the Kimball-Physics LaB6: on our heavily used CM12 - the predecessor to the Tecnai 12 - we used and are using Kimball-Physics LaB6 filaments - only three in the last 10 years. The vacuum of the TEM was (very) good, always, and still

is .... I keep my fingers crossed. This means: I am a very satisfied customer ... and I do recommend this type. Reinhard Rachel reinhard.rachel@biologie.uni-regensburg.de May 12

Some Kimball Physics LaB_6 cathodes may be mechanically instable within first 50 or so hours of use, and gun tilt might need repetitive adjustment before the cathode becomes stable. Worst case - cathode may have to be re-centered. However, these cathodes take lots of punishment and still work for years. Leaky/dirty specimen airlock, fast heating/cooling of LaB_6, vacuum accidents, arcing, etc. In other words multi-user environment with little supervision. Vitaly Feingold vitalylazar@att.net May 13

TEM - FFTs in focusing and removing objective astigmatism

I was just wondering, how is a TEM focused using fast Fourier transforms? Also, how do FFTs compare to Fresnel fringes for focusing and removing objective astigmatism at high and low magnifications? Sven Ernst sven.ernst@student.curtin.edu.au Apr 25

FFT from a thin amorphous film contains information of the objective phase contrast transfer function (PCTF). By fitting the 2D intensity distribution in a single FFT image, one can measure the amount of mean defocus and the focus variation as a function of the azimuth angle, i.e. astigmatism. This is how focus and astigmatism are measured using the FFT image. Compared with the Fresnel fringe method, the FFT method is far more accurate at high magnification and high resolution conditions, with a typical accuracy of 1-2nm in both focus and astigmatism measurement. At low magnifications, the Fresnel method is preferred since it is easy to do and the accuracy requirement is not high. Also the FFT image can be used to do coma-free alignment, a must for obtaining HREM images under the right focus condition that can be correctly interpreted using the structural model. At low magnifications, rotation alignment is adequate. Ming Pan mpan@gatan.com Apr 25

FFT from any image contains frequency information (usually the phase information is not used). As such, an angular change in the Fourier domain (ex. 2-D intensity image) can represent astigmatism; and broadening in the Fourier domain represents spread of data. In general, the eye perceives a change in small frequencies as focus changes. Thus minimizing angular features minimizes astigmatism, and minimizing spread mathematically (stochastically) or visually by looking at a 2-D representation of the Fourier domain will improve focus. Andrew Anthony Havics ph2@sprynet.com Apr 26

SEM - low keV imaging

We have a FEI Quanta FEG SEM and would like to optimize it for low keV imaging. I really don't care if my microscope can perform above 2keV. The normal alignment procedure is to start at 30keV and align the top part of the column and then go to 1keV and align the lower part of the column. I am thinking that if we were to align the top part at 2keV and align the bottom part of the column at 1keV that we would be more optimized for 2keV and below. Does anyone think that this is a good idea or are there better ways to get optimized low keV images. R Richard Stallcup rstallcup@zyvex.com May 10

Yes, you are on the right lines for most instruments, but I do not know the FEI FEG too well. The lower the kV that you use to align the instrument, the better it should be at the lower levels. This is standard practice for most W SEM but in that case we often raise the anode to keep the gun fields optimized for best performance. Steve Chapman protrain@emcourses.com May 11

SEM - interference

We have a JEOL 5600LV and we are having an ongoing problem that JEOL say is an 'environmental issue'. We get interference on the images that manifest as bars down the image on the higher scan settings (this is a single solid bar on the right hand side of the image on scan 3, 3 bars on scan 4 across the whole image) These bars do not always seem to vary in their position with changes in KV and WD adjustments. Although the pronounced nature of the bars can be partially reduced by increasing the KV. The effect on the image is was intermittent and now it seems to be permanently present. The lines represent as solid bars running vertically down the screen. It's not caused by vibration. Essentially we want to find out if it is a field, we have had JEOL in to try and track down the field but with no success but they are adamant that there must be one despite being unable to locate it themselves. We don't really want to spend money on an expensive cancellation system if that is not the problem so has anyone out there had experience of: (a) Shielding microscopes cheaply in order to ascertain if it is a field. It doesn't matter if it's really crude it's just for initial diagnostic purposes. (b) Similar problems with ageing microscopes indicating another possible fault? (c) Any situation/equipment that may have produced similar effects. John Mitchels john.mitchels@gmail.com May 13

External magnetic field interference is always worse with lower KV and longer working distance. It usually manifests itself as line to line displacement of the image. There should also be a way to synch or unsynch the raster to 60 cycle to see it get worse. If none of these behaviors are evident, it is probably not an external field. As far as chasing down the source goes, the simple Extech 480823 that you can now get at Amazon.com for $99 http://www.amazon.com/gp/product/B00023RXDC will enable you to find the field and measure it easily. Another thing to look at is very dirty power. I'm not sure how to measure that, but I'm sure your local electrician can. In that case, a UPS or isolation transformer can solve the problem. Of course, the microscopy power supply should have some giant capacitors to do a significant amount of isolation, and maybe JEOL needs to look at that. If your SEM is old, capacitors could easily be not performing properly. John Mardinly a.mardinly@numonyx.com May 14

You say it is an ongoing problem, but give me the impression they were not always there. You also indicate they were intermittent when they first started appearing, and are always present, now. How long ago did they first start to appear? Have you had the system for a while, where it performed nicely, before the current symptom started to appear? You do say "aging microscope" near the bottom. Has there been any new construction, or equipment installations, in the vicinity of your system? Was there a repair, parts replaced, on your system? If so, is there a relationship, time wise? First, to answer your question about shielding, there is no effective way to easily and cheaply block outside fields. Even expensive Active Isolation systems have their limitations. Are these bars directly vertical, or do they angle down across the screen? If the bars look basically the same at 15 kV and 4 mm working distance, as they do at 1 kV and 15 mm working distance, then it is probably from within the

AANetNotes 08n4.indd 11 06/22/2008 1:19:06 PM

system. If JEOL cannot "find", and show you the "environmental" influence, then it is probably not there. You should be able to pick up, and see, a field that is strong enough to influence the beam that much. If the bars are vertical, then I find it difficult to believe an outside field would be that synchronous with the scan of the SEM. I had a JEOL 6400F SEM that had a problem from the start. JEOL had pre-checked the room for fields and vibrations, and had given the room their blessing. After the system arrived, and was set up, there was an intermittent quirk in the image. JEOL could not figure it out, or stop it, so they decided it was from fields outside the system. They could not detect them, or show them to me, but they must be there! After I had relocated the system to a different building, several miles away from the first, to a pretested and approved room, I still had the exact same symptoms. (Just to be clear, my symptoms were different than yours) They thoroughly checked the system again, and then brought in an active field and vibration blocking system, thinking they were going to prove it was the environment, and not the system. They were wrong. If they can't detect, and see the environmental fields, I don't believe they are affecting your system. Darrell Miles milesd@us.ibm.com May 14

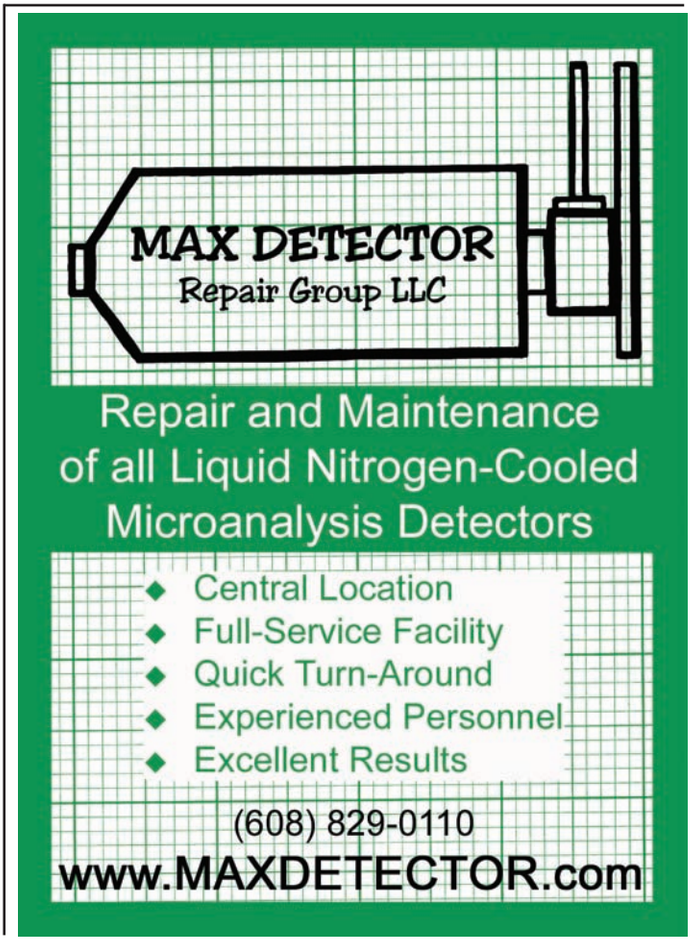
You have clearly carried out some tests for fields but here are more. 1. Long working distance (25-30mm) does the problem become greater? 2. Short working distance (5-7mm) does the problem become less? Or 3. Low kV (5) does the problem become greater? 4. High kV (30) does the problem become less? Each of these series proves the field problem if you have a change. Third test I have rotated a column 45 degrees, the question being is the problem the same or does it change? A change in physical orientation providing a change in the problem indicates it is external as internal (microscope) faults will stay exactly the same. Steve Chapman protrain@emcourses.com May 14

SEM – digital camera

I work with an Hitachi S-570 SEM that is currently setup with a Polaroid film holder, and was previously setup with a 35mm film camera. I am wondering how easily a digital camera could be substituted for the 35mm film camera. If possible, it would be much more affordable then refitting the microscope with a digital system. Sarah Aubut saubut@nrcan.gc.ca Apr 16

The Polaroid back or the 35mm option are still film. They capture line scans as the image is displayed in slow scan on the capture back/port. The problem is that digital cameras are one shot devices--they take a pix of what is there. As such, they do not integrate an image. The final image is not on the record CRT. I can't think of any way to do this digitally unless using a passive or active digital capture system. A digital camera is not going to work, in my opinion. However, if you find a workable solution, please let us know. What is missing is a frame buffer that would store all line scans and present them as a final (total) image as TV which could be frame grabbed as 640x480. But a good record CRT is good for about 4000x3000 lines/inch. Gary Gaugler gary@gaugler.com Apr 16

It is possible to fit a digital camera onto an older SEM. I used a Nikon D70S, focused onto the recording CRT of our Hitachi S-2460N and I took some nice images with the digital camera in the "bulb" mode. That's the key: you must have a digital camera that will "open the shutter" for the entire exposure and close it afterwards. Not many digital cameras have this feature. In operation, I find the image of interest, open the digital camera shutter with a wireless remote trigger, start the SEM slow scan exposure, wait until the SEM slow scan is over, close the digital camera shutter using the wireless remote. These images are as good (noise-wise) as one would capture with conventional film. The resolution is not as good a film, of course. Yes, there are a lot of tradeoffs. It is an inconvenience to operate in this mode--unless you are used to using film. Then, it's nearly the same as shooting conventional film. Once the microscopy is complete, remove the memory card from the camera and download them to your computer. One advantage of this method is that the magnification bar generated by the SEM will be recorded on the digital image (unlike digital capture systems that insert their own). The cost of this system is basically the cost of the digital camera and modification of the existing film camera holder to accept the digital cam ($1,200 total, in our case). Having said this, I must confess that on our other microscope, also an S570, we retrofitted a 4pi digital capture system that we are quite pleased with. On the 2460, that I described above, we only rarely need digital images greater than 1 MB. So, we use the X-ray analysis system to capture images. When we need higher resolution digitals, then we could use the Nikon camera. By the way, an article describing the use of a Canon digital camera to capture images was published in Microscopy Today several years ago. You might check the archives or perhaps the author could give us the citation. John J. Bozzola bozzola@siu.edu Apr 16



AANetNotes 08n4.indd 12 06/22/2008 1:19:06 PM

There are two major considerations when using a digital camera to take slow scan images. I have a background in astronomy, so I'm very familiar with CCD devices and the inherent difficulties with them. I also tried to set up a digital SLR on a Topcon/ISI ABT-SX40. First, I'm going to make a couple of assumptions. I am going to assume that the digital camera is a digital SLR, like the Nikon D70. I am also going to assume that it has a 'bulb' feature, and that it is going to be able to be mounted directly, sans lens, to the photographic system on the SEM. The two major concerns are the alignment of the scan and the size of the chip. The chip is made up of 'buckets' (pixels) which basically count how many photons hit the bucket, and register that as an intensity value on the final photo. These buckets are arranged in a nice x-y pattern. If the scan of the microscope is such that the scan line overlaps two rows, or is at an angle to the x-y orientation of the CCD pixels, you can get a bleed-over effect that causes some distortion in your final image. The Nikon D70 has a pixel size of 8x8 microns, and a resolution of 3000x2000 pixels, so it might not be as obvious an artifact at first, but once you start zooming in, you will see it. This can be corrected, though, given some careful alignment when setting it up. The second major concern is the size of the chip. A 35 mm film negative will record an image in a 36 x 24 mm area. The CCD chip is physically smaller, recording an image in a space of 24 x 16 mm (For a Nikon D70- you can get this measurement off of the specs on your camera). This being said, when you view your images, you have to take into account that you are either not going to get the full image- if you are photographing without any compensating lenses for size, for instance, you might lose the micron bar and information lines at the bottom of the image, for example, or you are going to be off on your measurement calibration if you do correct the optics to capture the full image. Of minor concern is pixel saturation. When the shutter is open for a longer period of time, and a line dwells in a spot for longer than a microsecond, you have the potential of maxing out the intensity resolution of the pixel. This was a problem that we ran into with using CCD cameras on telescopes- a nearby star would be bright enough to "Fill the buckets" of the CCD pixel, which would then overflow into neighboring pixels. CCDs for the most part are more sensitive to light than film, so make sure that the intensity of the photo CRT is set at the lowest possible value to register a satisfactory image, and you won't max out the intensity on the CCD. I hope this helps. I know I seem to go off on the D70, but it's the camera I have, and therefore have the booklet with the specs sitting in front of me. Justin A. Kraft kraftpiano@gmail.com Apr 16

These are important concerns. Yes, I used a digital SLR with a Nikon Micro Nikkor lens that was focused on the recording monitor. When recording the image, I adjusted gamma so that the image was rather flat in appearance (and then did a final adjustment in Photoshop). I included as much of the photo-CRT as possible (including the magnification scale) and only had to minimally crop the final captured image to exclude areas outside of the photo-CRT. I am very pleased with the results, but realize that it is somewhat inconvenient (maybe not even practical) if you have multiple or infrequent users who may not remember all the steps. John J. Bozzola bozzola@siu.edu Apr 17

EDX problems

Today I have the impression that our EDX detector coupled to our Tecnai G20 TEM microscope is just going crazy. The Dead Time (DT) is constantly on 100% when I want to analyze a particle (objective aperture out). I use classical copper grids and I took care not to be near a grid bar while reading. Here is what I did to extend the diagnostic: 1) When I position the beam on a grid bar, the CPS (counts per second) go up to 300 000 and DT 100%, as expected 2) When I target the center of a grid hole with the objective aperture out, I get a count of 30 and DT 100% 3) When I take the specimen holder out and insert the objective aperture, I have a CPS of 5 and a DT of 100% 4) When I take the specimen holder out and take the objective aperture out, I have a CPS of 0 and a DT of 0%, but sometimes it goes suddenly to 100% then come back to 0% (frequency, about every 2 sec) 5) I can retract the detector, in this case I get the same result of point 4) I am a biologist, so I cannot understand much of what is happening, but for me it look like the processor is down. What I wonder is why the counts look correct while the DT is crazy. How can I have a CPS of 5 and a DT of 100%? I never let the Dewar warm up (but there is a protection in this case) and the only thing I did recently is calibrate the instrument (last week). The instrument is from EDAX. I contacted them 2 weeks ago to ask for instructions on how to calibrate it, but still got no answer. So I don't expect much help from their side. Stephane Nizets nizets2@yahoo.com Apr 18

You didn't mention if you tried this test: Set up your normal operating conditions, e.g., objective aperture out, etc. then, turn off the e-beam. If you still get 100% deadtime and various count rates, it could mean that your detector FET, attached to the SI(Li) crystal, is blown. If deadtime and counts go to zero, check the condenser aperture, could someone have pulled out the condenser aperture? That would result in very high beam currents down the column perhaps resulting in enough counts to paralyze your system in the test conditions you presented. As for EDAX, don't give up so soon, contact Steve Mann there, by phone. He's been quite responsive to issues I've had on my EDS systems in the past. Or, give it a rest overnight. Then try again. Possible software glitch? Gilbert Ahlstrand ahlst007@umn.edu Fri Apr 18

A possibility, considering you mentioned a re-calibration. Be certain the low energy end of your spectrum is properly inhibited. This is usually a "threshold" adjustment. Uninhibited noise at the low end (typically below Be/B) will be counted in the DT value. Another possibility, as mentioned is a bad FET pre-amp. Another is poor Dewar vacuum / blown thin window. One thing that "got" me was when I forgot to be certain my IR camera illumination was off (it defaults to ON when the viewing program is executed). The detector can see the IR and goes berserk! Woody White nwwhite@babcock.com Apr 21

High deadtime is a common problem related to the EDS maintenance. Several possibilities for this: 1. Thick ice layer buildup on the window. Consult the manufacture how to remove it. For Oxford INCA, simply run the detector conditioning program (refer to http://www.oxinst.com/wps/wcm/resources/file/ebd6db4f1d7f723/EDS-Hardware-Explained.pdf). This should be done in weeks/months. 2. Detector needs correct re-calibration from time to time (in months/years). If still not working, unlikely your service can be skipped. Zhiping Luo luo@mic.tamu.edu Apr 22

AANetNotes 08n4.indd 13 06/22/2008 1:19:06 PM

Microscopy AND Microanalysis

Table of Contents Preview

Volume 14, Number 4, August 2008

Microanalysis

Electron Diffraction Based Analysis of Phase Fractions and Texture in Nanocrystalline Thin Films; Part I: Principles
János L. Lábár

Estimation of the Reconstruction Parameters for Atom Probe Tomography
Baptiste Gault, Frederic de Geuser, Leigh T. Stephenson, Michael P. Moody, Barrington C. Muddle and Simon P. Ringer

Experimental Method to Determine the Absolute Efficiency Curve of a Wavelength Dispersive Spectrometer
Jorge Trincavelli, Silvina Limandri, Alejo Carreras, and Rita Bonetto

Materials Applications

Gallium Induced Milling of Silicon: A Computational Investigation of Focused Ion Beams
Michael F. Russo Jr., Mostafa Maazouz, Lucille A. Giannuzzi, Clive Chandler, Mark Utlaut, and Barbara J. Garrison

Nondestructive Spectrometric Study on a Radioactive Particle Embedded in a Marine Sediment
Marek Bielewski, Jerome Himbert, Nedialka Niagolova, Gerald Falkenberg, Mats Eriksson, and Maria Betti

Characterization of an Inorganic Cryptomelane Nanomaterial Synthesized by a Novel Process using Transmission Electron Microscopy and X-Ray Diffraction
Longzhou Ma, Thomas Hartmann, Marcos A. Cheney, Nancy R. Birkner, and Pradip K. Bhowmik

Synthesis of Lead Pyrophosphate, $Pb_2P_2O_7$, in Water
Darren A. Lytle, Colin White and Michael R. Schock

Biological Applications

Confocal/TEM Overlay Microscopy: A Simple Method for Correlating Confocal and Electron Microscopy of Cells Expressing GFP/YFP Fusion Proteins
Douglas R. Keene, Sara F. Tufa, Gregory P. Lunstrum, Paul Holden, and William A. Horton

Regulation of Peripheral Spindle Movement and Spindle Rotation During Mouse Oocyte Meiosis: New Perspectives
Jun-Shu Ai, Qiang Wang, Shen Yin, Li-Hong Shi, Bo Xiong, Ying-Chun OuYang, Yi Hou, Da-Yuan Chen, Heide Schatten, and Qing-Yuan Sun

A Novel Technique for Observing the Internal Ultrastructure of Human Chromosomes with Known Karyotype
Mohammad Ghazizadeh, Yoshihiro Sasaki, Tatsuo Oguro, Shigeru Sato, Seiko Egawa, Kyoko Inoue, Akiko Adachi, Hajime Shimizu, and Oichi Kawanami

Electron Digital Imaging Towards High-Resolution Structure Analysis of Biological Macromolecules
Saori Maki-Yonekura and Koji Yonekura

Book Review

Electron Tomography: Methods for Three-Dimensional Visualization of Structures in the Cell, 2nd Edition. Edited by Joachim Frank
Lu Gan

Calendar of Meetings and Courses

Microscopy and Microanalysis website: http://www.journals.cambridge.org/jid_MAM

Indexed in Chemical Abstracts, Current Contents, BIOSIS, and MEDLINE (PubMed)

MSA members receive both *Microscopy Today* and *Microscopy and Microanalysis* FREE!

HUMOR



Dear Abbe

Dear Abbe:

Could you please comment on lectures on "Breaking Abbe's Barrier ...." and similar topics that were presented during the Focus on Microscopy 2008 in Osaka. There's been more of it in the same vein—some of them even suggesting it's about time to start talking about nanoscopy instead of microscopy. Your name was always mentioned with respect, and I would appreciate your point of view on the matter.

Vic from Jena

Dear Vic,

It is so nice to hear from someone from Jena. Do you by chance know Frau Bemisderfer of Swinemünder Straße ? She used to make the most amazing Mohn Strudel and she really enjoyed my Weisswurst. But I digress. Break my barriers you say? Today's youth are so violent! I blame it on telemicroscopy. What is next? Picoscopy? Femtoscopy? Yoctoscopy? This sounds more like one of those unpleasant invasive medical procedures one must endure every year after age 50. Next time you see these nanoscientists ask them "What did one photon say to the other photon?" The answer of course is, "I'm sick and tired of your interference." I'm going to bed now.

Dear Abbe,

We just received authorization to purchase a 300kV, FEG, aberration-corrected, TEM with all the accessories in the catalog. Lucky us! But our vice president wants us to install it under spotlights in a room with floor to ceiling windows off the reception area so he can show it off to visiting VIPs. We explained that it has to be in a private, darkened room. He said "No way!" How do we deal with this?

Funambulistic in East Fishkill

Dear Fun,

I suppose that you already know that administerium is the densest element known to man. With a half-life of 2 to 20 years and being comprised mostly of peons and morons, administerium can spontaneously reorganize resulting in never-ending series of meetings that result in an excess of hot air resulting in twice the number of morons known as "isodopes." When faced with a similar idiotic request I purchased a second TEM of the same make and model. If you buy one without any lenses or electronic components you can get one for a song, and two bottles of inexpensive vodka. Simply install an old fashioned slide projector in the gun assembly and you can display lots of interesting images onto the viewing screen that will easily fool an administrator into thinking that he is witnessing actual science. I included a subliminal picture of me receiving the Nobel prize in Physics and realized a 20% pay raise the following year. These people are easily fooled.

For answers to life's mysteries, please contact Herr Abbe's administrative assistant at jshields@cb.uga.edu.

AA_MAM_08n4.indd 1 06/22/2008 4:45:12 PM

INDEX OF ADVERTISERS

4pi Analysis, Inc (www.4pi.com) 31
Advanced Microscopy Techniques (www.amtimaging.com) 71
Ångstrom Scientific Co (www.angstrom.us) 29
Bruker AXS Microanalysis (www.bruker-axs.com 5
Buehler, LTD. (www.buehler.com) 67
Carl Zeiss SMT, Inc. (smt.zeiss.com) 2
McCrone Group (www.collegeofmicroscopy.com) 27
Diatome (www.emsdiasum.com) 55
Duniway Stockroom Corp. (www.duniway.com) 79
E.A. Fischione, Inc (www.fischione.com) 19
EDAX Inc.(www.edax.com/NEW) 39
El-Mul Electron & Ion Detection Solutions (www.el-mul.com) 75
Electron Microscopy Sciences (www.emsdiasum.com) 37
Ernest F. Fullam (www.fullam.com) 59
Evex Analytical (www.evex.com) 77
FEI Company (www.feic.com) 25
Gatan Inc. (www.gatan.com) 13
Geller MicroAnalytical Lab (www.gellermicro.com) 45
Hitachi High Technologies America (www.hitachi–hhta.com) 16, 17
Hysitron, Inc. (www.hysitron.com) 35
IMAGO - FEI (www.imago.com & www.feic.com) 57
JEOL USA (www.jeol.com) 49, 88
M.E. Taylor Engineering (www.semsupplies.com) 79
Materials Analytical Services (MAS) (www.mastest.com) 45
MAX Detector Repair Group LLC (www.maxdetector.com) 83
McCrone Research Institute (www.mcri.org) 79
Minitool Micro Precision Products (www.minitoolinc.com) 21
minus k TECHNOLOGY (www.minusk.com) 81
Olympus Soft Imaging Solutions Corp (www.soft-imaging.net) 11
Omniprobe, Inc. (www.omniprobe.com) 7
Parallax Research, Inc. (www.parallax-x-ray.com) 21, 47
QuantomiX (www.quantomix.com) 75
Scientific Instruments and Applications (www.sia-cam.com) 59
SII NanoTechnology USA Inc. (www.siintusa.com) 43
South Bay Technology, Inc. (www.southbaytech.com) 73
Ted Pella, Inc. (www.tedpella.com) 41, 51, 81
Tescan USA (www.tescan-usa.com) 23
TGS Technologies (www.tgstechnologies.net) 61
Thermo Scientific (Part of Thermo Fisher Scientific) (www.thermo.com) 87
ULTRA TEC Manufacturing, Inc. (www.ultratecusa.com) 29
XEI Scientific (evactron.com)..... 63
xk, Incorporated (www.xk.com) 53
Employment Ads
Beckman Inst. Univ of Illinois *77*
Tulane University 45
University of Central Florida 9

SUBSCRIPTION REQUESTS/CHANGES

Individuals requesting subscriptions, or wishing to change/correct their current address, are requested to do so via our www site:

http://www.microscopy–today.com

SUBSCRIPTION POLICIES

- Microscopists in Canada, Mexico, and the United States of America are eligible for free subscriptions.
- Microscopy Society of America members receive Microscopy Today as a free member benefit anywhere in the world.
- Non-MSA members, outside North America, may subscribe for $60US per year to cover postage and handling.
- Scanned back issues of MT are available for low-resolution free download on our www site above, after a six-month delay. The entire issues are downloaded—advertisements and all.
- High resolution, CD format, complete volumes are available via airmail for the prices listed below. Note that a volume contains 6 issue for 2002 onwards and 10 issues for 1992 to 2001. Contact editor to order.

Preferred payment is via credit card information when subscribing at the www address. Bank transfer information available from the editor. Checks in US$, payable to "Microscopy Today," to the editor.

MICROSCOPY TODAY Subscription Schedule	***Products***		
	Current Printed Issue	**Back Issue Downloaded After 6-Month Delay**	**Back Issue Volume High Resolution CD**
Anyone in North America	Free	Free Low Resolution	MSA member $30/volume Non-MSA mbr. $45/volume
MSA member outside North America	Free	Free Low Resolution	$45/volume
Non-MSA member, outside North America	$60 /year (6 issues)	Free Low Resolution	$60/volume

AALast_Page.indd 1 06/24/2008 12:11:15 PM



©2008 Thermo Fisher Scientific Inc. All rights reserved.

Get the correct answer up to 100x faster. Really.

Precision and Speed The Thermo Scientific NORAN System 7 speeds you to answers with blazing fast processing at more than 1,000,000 counts per second. Our impeccable accuracy gives you confidence in your results.

Manual or Automatic? In one system you get the ultimate in automation as well as the flexibility to examine your sample manually. You gain the time saving convenience of automatic quantitative mapping and Point & Shoot analysis without sacrificing control.

A Pleasure to Use Included with the powerful spectral and imaging hardware is a suite of software unparalleled in the industry. Just one click to create a report or analyze samples outside the lab with network ready data analysis.

Experience the speed of the NORAN System 7. Sample our demo at www.thermo.com/reallyfast.





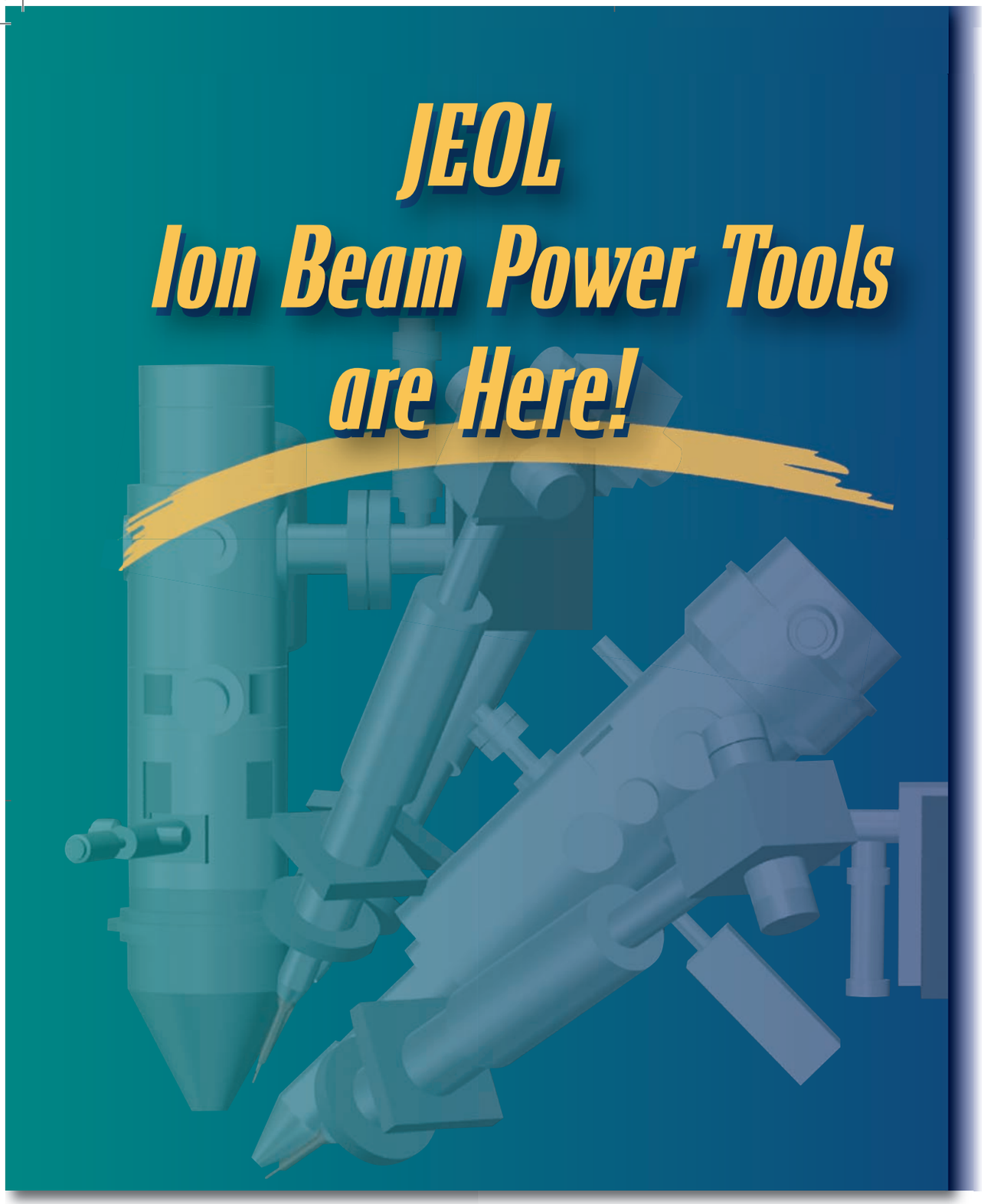
Thermo Scientific NORAN System 7
The optimum combination of detector, analyzer and software for X-ray microanalysis.

Moving science forward

Thermo SCIENTIFIC
Part of Thermo Fisher Scientific

MT Full Page Ad Master.indd 1 06/22/2008 4:54:04 PM

JEOL Ion Beam Power Tools are Here!



JEOL 2008

Seeing is believing!

Out of sight imaging now up close and personal

- *New Thermal FE MultiBeam SEM/FIB*
- *LAB_6 MultiBeam SEM/FIB*
- *Cross Section Polisher sample processing tool*

Visit JEOL at M&M, Booths 1027 and 515.

Another
Extreme Imaging
solution

JEOL

Stability • Productivity • Performance
www.jeolusa.com • salesinfo@jeol.com
978-535-5900